

**Development of evaluation methods for biomass production and lodging in rice  
by digital surface model using unmanned aerial vehicle**

**2022.9**

**Biological Production Science  
United Graduate School of Agricultural Science  
Tokyo University of Agriculture and Technology**

**Peprah Clement Oppong**

**Development of evaluation methods for biomass production and lodging in rice  
by digital surface model using unmanned aerial vehicle**

**A doctoral thesis presented to the United Graduate School, Tokyo University of  
Agriculture and Technology in partial fulfilment of the requirements for the  
award of the degree of Doctor of Philosophy (Agricultural Science)**

**2022.9**

**Peprah Clement Oppong**

This thesis attached hereto, entitled “Development of evaluation methods for biomass production and lodging in rice by digital surface model using unmanned aerial vehicle” is being submitted as a doctoral thesis in partial fulfilment of the requirements for the degree of Doctor of Philosophy (PhD in Agricultural Science) by the United Graduate School of Agricultural Science, Tokyo University of Agriculture and Technology **on June 1<sup>st</sup>, 2022.**

**Board of examiners for thesis review**

Assoc. Prof. Keisuke KATSURA (Academic supervisor)

Prof. Taiichiro OOKAWA (Co-supervisor)

Prof. Yukitsugu TAKAHASHI (Co-supervisor)

Prof. Tsuyoshi OKAYAMA (Examination committee member)

Assoc. Prof. Megumi YAMASHITA (Examination committee member)

Assoc. Prof. Shunsuke ADACHI (Examination committee member)

## **Declaration**

This thesis represents the author's original work for the award of a doctoral degree in Agriculture Science. It contains no materials previously published or materials submitted for acceptance by another University except otherwise duly referenced and acknowledged.

Date.....

Peprah Clement Oppong

## **Abstract**

A digital surface model (DSM) is a 3D structure that represents the reflective surface of an object observed above the earth. It is part of remote sensing (RS) technology used for rapid evaluation of crop status and is less affected by weather, unlike satellite data. DSM can provide 3D canopy height information on the field and has been widely used in assessing relatively taller and heterogeneous canopies compared to homogenous and shorter canopies such as in paddy fields where there is little variation in plant height. However, accurate evaluation of such little variation can potentially model other growth-related traits in rice. Therefore, this study focused on; (1) Using unmanned aerial vehicle (UAV)-based images to develop a DSM to determine plant height in rice varieties, (2) Spatio-temporal monitoring of growth dynamics to estimate biomass increase from canopy height (CH) using DSM, and (3) analyse the feasibility of using a simple and direct assessment of lodging method in a multi-varietal rice field using DSM canopy height by conducting the following studies.

Plant height (PL) is important for phenotyping because it affects aboveground biomass (TDW) increase. However, manual measurement is time-consuming. Hence, UAV DSM to estimate plant height was studied. Three rice cultivars; Nipponbare (japonica), IR64 (indica), and Basmati370 (indica), were cultivated in paddy fields under different fertilizer conditions. RGB images with 80% forward and lateral overlap at an altitude of 30 m were taken above the rice canopies every week and processed. The PL of four hills was manually measured. A canopy surface model (CSM) was developed based on the differences observed between each DSM and the first DSM after transplanting. The average reflectance of eight hills in each plot was used for the calculation of CH using polygons (15 cm x 30 cm). Depending on the growth stage and genotypes, there were large variations in PL (from 0.46 to 1.80 m) and CH (from 0.1 to 1.4 m). CH correlated well with PL ( $R^2 = 0.947$ ) which shows DSM could explain the large variation in PL throughout the growth stages. However, there

was a trend of underestimation, because PL refers to the highest point in an area, whereas DSM considers the average of heights in an area. Nevertheless, DSM can estimate a relatively smaller range of PL, which is useful at every growth stage.

After the usefulness of the DSM was confirmed, a model transfer was done to monitor and estimate other crop growth-related traits like leaf area index (LAI) and TDW to assess the effect of spatial and temporal variations on the model as such information is limited on paddy fields. Materials were the same as in Chapter 2, but the plants were harvested after aerial photography to measure LAI and TDW. Depending on the growth stage and genotypes, there were large variations in LAI (from 1.03 to 7.93 m<sup>2</sup> m<sup>-2</sup>) and TDW (from 64.7 to 1237.2 g m<sup>-2</sup>). The results showed a linear relation between PL and LAI or TDW, so a model was developed from this relationship to estimate LAI or TDW. The estimation accuracy of the model was high for TDW and LAI with large variations among the genotypes. This implies that developing genotype-specific estimation models are necessary.

Lodging, regarded as the displacement of a plant from its upright position or anchorage system, highly affects crop quality and output. However, no simple method for assessing lodging using DSM has been developed. Thus, a simple attempt of the DSM for lodging assessment was evaluated as lodging is related to canopy height. Twenty-four different genotypes were cultivated under the same fertilizer conditions and their angles of inclination were measured during the ripening stage, and their CH was evaluated as in the previous studies. Four lodging estimation methods;  $\Delta PL$  (difference between CH of the target area and PL at heading stage),  $\Delta CH_{max}$  (difference between CH at evaluation time and the maximum CH (at around heading stage) of the target area),  $\Delta CH_{border}$  (difference between CH of border plants and target area), and  $CH_{CV}$  (coefficient of variation of CH among plants hills of target area) were used to assess the canopy structure anomalies. The results showed that  $CH_{CV}$  can be used to detect and quantify lodging with high accuracy ( $R^2 = 0.59$ ). When  $CH_{CV}$  exceeds 0.05, the lodging angle dramatically increased. Hence,  $CH_{CV}$  could be a good indicator

for estimating lodging. In conclusion, the proposed UAV DSM has a great potential to assist in the rapid evaluation of biomass and natural occurrences like lodging. It will be possible to use this technology for future breeding programs in screening and phenotyping rice fields on a large scale. However, the challenge remains with the model improvement to increase the estimation accuracy which needs redress.

## **Dedication**

*This work is dedicated to my wife Mrs Victoria Sylvia Oppong and my lovely daughter Yaa Akyempem Benewaa Oppong-Peprah. Your continuous immense support has brought me this far. Thank You.*

## Acknowledgements

“When all Thy mercies, O my God, my rising soul surveys, transported with the view I’m lost in wonder love and praise”. Grace unending, grace divine, I am forever grateful.

Foremost, I would like to express my sincere gratitude to my academic advisor, whom I also consider a father, Assoc. Prof. Keisuke Katsura, for the training, supervision, and continuous support throughout my graduate studies. His guidance, patience and immense knowledge always helped me during field experiments and the writing of this thesis. You are a great mentor and would forever cherish the time I spent studying under you. Besides my advisor, I would like to thank Prof. Taiichiro Ookawa, and Prof. Yukitsugu Takahashi, my two co-supervisors and Assoc. Prof. Megumi Yamashita for the technical training on how to the Agisoft Metashape professional. Another word of appreciation goes to Assoc. Prof. Onwona-Agyeman Siaw for every piece of advice and other support you provided to make my academic journey easy.

I am also grateful to my wife, Mrs Victoria Sylvia Opong for all the support and wise counsel you have given me until now. You sacrificed a lot for our family by shouldering all the sleepiness nights caring for our beautiful daughter while I was away pursuing this degree. I cannot repay you but with love and care. I cannot forget the support from my father, Nana Kofi Peprah, and my siblings especially Seth Peprah and Isaac Nkansah Opong.

My appreciation also goes to Ms Jeannette Aduhene-Chinbuah for your support throughout my study. Thank you for your words of affirmation and encouragement. I am happy to have you by my side.

I say a big thank you to Katsura lab mates, and a special mention to Tamaoki Yamaguchi Mr Tomoaki, Mr Ryo Sekino, Mr Kyohei Takano, and Mr Koji Matsukawa for all the support you provided for me. The years spent with you have been fun, educative, and challenging as well, but I

am grateful for what we achieved together. And to all my brothers and sisters from my motherland at TUAT, I appreciate your support for giving me a sense of home away from home.

FLOuRISH Fellowship for Support for Pioneering Research also provided financial support for my study, and I am very grateful to the staff and management of the fellowship scheme for your consideration during a time when I was in a dire need of financial support.

Finally, I thank myself for the dedication, perseverance, and hard work I put in to complete this work on time. The saying is true that “what does not break you, cannot destroy you”. This study period was very challenging, but I am happy that I was successful in the end.

## Table of contents

Declaration .....	i
Abstract .....	ii
Dedication .....	v
Acknowledgements .....	vi
Table of contents .....	viii
List of Tables .....	xiii
List of Figures .....	xiv
List of abbreviations.....	xvii
CHAPTER 1 .....	1
Introduction .....	1
<u>1.1.</u> Background of study .....	1
<u>1.1.1.</u> Remote sensing application for agriculture .....	2
1.1.2. UAV-based crop monitoring.....	3
1.1.3. UAV photogrammetric techniques .....	4
1.2 Problem statement and research justification.....	5
1.3. Objectives of study.....	6
1.4. Research hypothesis .....	6
1.5. Structure of this thesis .....	6
CHAPTER 2 .....	8

Development of plant height estimation model by a digital surface model using unmanned aerial vehicle images.....	8
2.1. Introduction.....	8
2.2. Materials and methods.....	11
2.2.1. Experimental site.....	11
2.2.2. Agronomic and management practices.....	12
2.2.3. Rice genotypes and fertilizer application.....	14
2.2.4. Aerial image data acquisition.....	16
2.5. Ground truth data collection.....	18
2.2.6. Generation of the DSM and canopy surface model (CSM).....	19
2.3. Results and discussions.....	22
2.3.1. Variations in manually measured plant length (PL) from field observation.....	23
2.3.2. Relation between the measured PL and DSM_CH.....	24
2.3.3. DSM_CH calculation.....	27
2.4. Conclusion.....	27
CHAPTER 3.....	29
Spatio-temporal estimation of biomass growth in rice using canopy surface model from unmanned aerial vehicle images.....	29
3.1. Introduction.....	29
3.2. Materials and methods.....	31
3.2.1. Experimental site.....	31
3.2.2. Rice genotypes and fertilizer application.....	33

3.2.3. Aerial image acquisition and image processing.....	33
3.2.4. Ground truth data collection. ....	34
3.2.5. Procedures of Spatio-temporal estimation of biomass growth. ....	34
3.3. Results and discussions.....	35
3.3.1. Genotypic variations in leaf area, biomass, and plant length.....	35
3.3.2 Relationship between the measured PL and DSM_CH. ....	38
3.3.3. Biomass modelling and evaluation ....	39
3.3.5. Accuracy Assessment of LAI and TDW estimates and validation.....	42
3.3.5 Temporal changes in time-series estimation.....	47
3.3.6 DSM spatial monitoring.....	49
3.4. Conclusions.....	51
CHAPTER 4 .....	54
Assessing Lodging severity in different rice genotypes using a digital surface model. ....	54
4.1. Introduction.....	54
4.2.2. Rice genotypes and fertilizer application.....	57
4.2.3. Ground truth data collection .....	58
4.2.4. Image collection from the UAV platform.....	60
4.2.5. Generation of orthomosaic images .....	61
4.2.6. CH extraction from DSM.....	61
4.2.7. Lodging assessment and evaluation method.....	62
(4.1).....	66
(4.2).....	66

(4.3).....	66
(4.4).....	66
4.3. Results and discussions.....	66
4.3.1. PL validation.....	66
4.3.2. Lodging and non-lodging comparisons of the height metrics.....	67
Figure 4.7. Lodging assessment among rice genotypes using .....	69
Figure 4.9. Lodging assessment among rice genotypes using .....	71
Figure 4.10 Lodging assessment among rice genotypes using .....	72
Figure 4.11. Comparison of lodging severity among the different rice genotypes using .....	74
4.4. Conclusion .....	75
Chapter 5 .....	76
Summary and conclusions .....	76
5.1 Development of plant height estimation model by a digital surface model using UAV images .....	76
5.2 Spatio-temporal estimation of biomass growth in rice using canopy surface model from UAV images. ....	76
5.3. Assessing Lodging severity in different rice genotypes using the DSM. ....	77
References.....	78
Appendix.....	103
Graphical abstracts .....	103
Chapters two and three.....	103

Publications..... 104

## List of Tables

<b>Table 2.1.</b> Specification of the Inspire 2 DJI (UAV) platform.....	17
<b>Table 2.2.</b> Specifications of the RGB camera (Zenmuse X4S; DJI).....	17
<b>Table 2.3.</b> Parameters of the drone flights and image processing.....	21
<b>Table 3.1</b> Estimation accuracy of LAI and TDW in 2018. ....	44
<b>Table 3.2.</b> Estimation accuracy of LAI and TDW in 2019. ....	46
<b>Table 3.3.</b> Estimation accuracy of LAI and TDW for three rice genotypes in 2019. ....	46
<b>Table 4.1.</b> Information on the different rice genotypes from different locations.....	59

## List of Figures

<b>Figure 2.1.</b> Location of the study site.....	12
<b>Figure 2.2.</b> Rotary levelling (a) and manual levelling (b) of paddy field. ....	13
<b>Figure 2.3.</b> Study field and overview of the plot layout in 2018 .....	14
<b>Figure 2.4.</b> Images of the Genotypes planted in the 2018 growing season.....	15
<b>Figure 2.5</b> The UAV platform used in this study.....	16
<b>Figure 2.7.</b> Examples of photos of 8 hills of 3 genotypes.....	19
<b>Figure 2.8.</b> Generation of a CSM from the DSM.....	21
<b>Figure 2.9.</b> The flowchart of the DSM and orthomosaic image generation from UAV images.....	22
<b>Figure 2.10.</b> Comparison of changes in PL at various days after transplanting (DAT) for three rice genotypes. ....	24
<b>Figure 2.11.</b> Height comparison datasets with canopy surface model for three rice genotypes in 2018. ....	25
<b>Figure 2.12:</b> Comparison between measured plant length (PL) and two types of CHs calculated from the mean CSM values and 97th percentile of CSM. ....	26
<b>Figure 2.13:</b> CH calculation from (a) orthoimage and (b) CSM in a 30 by 30 cm area covering two plants. ....	27
<b>Figure 3.1.</b> Study fields and layout in 2019. ....	32
<b>Figure 3.2.</b> Procedures of Spatio-temporal estimations using canopy surface models.....	35
<b>Figure 3.3.</b> Comparison of seasonal changes in LAI, TDW and PL at various days after transplanting (DAT) for three rice genotypes.....	37
<b>Figure 3.4.</b> Comparison of seasonal relationships between measured PL and estimated DSM_CH in 2018 and 2019.....	38

<b>Figure 3.5.</b> Relationship of (a) LAI and (b) aboveground TDW with measured PL among three rice varieties in 2018 (Rep. 1 & 3).....	41
<b>Figure 3.7.</b> Accuracy assessment of CSM derived estimated (a) LAI and (b) TDW against standard ground-based measurements among three rice varieties in 2018 (Rep. 2)..	43
<b>Figure 3.8.</b> Relationship between the estimated and observed values of (a) LAI and (b) TDW among three rice varieties in 2019 (Rep. 1, 2 & 3).....	45
<b>Figure 3.9.</b> Fourteen weeks of AMeDAS Fuchu weather data during the growing season. ....	48
<b>Figure 3.10.</b> Observed temporal changes of estimated (a) LAI and (b) TDW in (Rep. 2) on various days after transplanting (DAT) in 2018 and 2019. ....	49
<b>Figure 13.</b> Examples of Spatial estimation of LAI in 2019 using the DSM model. ....	52
Figure 14 Example of spatial estimation of TDW in 2019 using the DSM model.....	53
<b>Figure 4.1.</b> Experimental field and layout (2021 growing season). ....	57
<b>Figure 4.2.</b> Sample images of the rice genotypes with different canopy structures.....	58
<b>Figure 4.3.</b> Example of a lodged rice plot (a), and (b) change in the tiller angle of inclination after lodging .....	60
<b>Figure 4.4.</b> Examples of CSM of all acquisition dates until lodging. ....	62
Figure 4.4. A close look at lodged and border non-lodged rice.....	63
<b>Figure 4.5.</b> Modelling with manually measured plant length ( $\Delta PL$ ).....	64
<b>Figure 4.6.</b> Modelling with maximum CH_DSM ( $\Delta CH_{max}$ ). ....	64
<b>Figure 4.7.</b> A schematic diagram of plant height comparison of lodged and non-lodged rice. ....	65
<b>Figure 4.8.</b> Modelling with coefficient variations of CH_DSM ( $CH_{cv}$ ). ....	65
<b>Figure 4.9.</b> Regression of DSM CH compared with in-field measured PL. ....	67
<b>Figure 4.10.</b> Lodging assessment among rice genotypes using $\Delta DSM\_CH_{border}$ .....	69

**Figure 4.11** An example of a CSM image indicating cross-border interference is indicated in red circles. .... 70

**Figure 4.12.** Lodging assessment among rice genotypes using  $\Delta PL$ . .... 71

**Figure 4.13.** Lodging assessment among rice genotypes using  $\Delta DSM\_CH_{max}$ . .... 72

**Figure 4.14.** Comparison of lodging severity among the different rice genotypes using  $DSM\_CH_{cv}$ .  
..... 74

### **List of abbreviations**

2D	Two dimensional
3D	Three dimensional
BAS	Basmati
CGSM	Crop growth simulation models
CH	Canopy height
CSM	Canopy surface model
DAT	Days after transplanting
DEM	Digital elevation model
DSM	Digital surface model
GCP	Ground control points
GIS	Global information system
LAI	Leaf area index
MODIS	Moderate Resolution Imaging Spectroradiometer
N	Nitrogen
NDVI	Normalised differential vegetation index
NIP	Nipponbare
PL	Plant height
RGB	Red Green Blue
RMSE	Root Mean Square Error
RS	Remote Sensing
SAVI	Soil Adjusted Vegetation Index
TDW	Total Dry Weight
TUAT	Tokyo University of Agriculture and Technology
UAV	Unmanned Aerial Vehicle
VI	Vegetation Index
WRC	World Rice Core Collection



## CHAPTER 1

### Introduction.

#### 1.1. Background of the study.

Global food demand continues to rise as a result of some key factors; increasing world population, biofuel consumption and change in consumer preference (Pingali P. 2006; Godfray et al. 2010; Tilman et al. 2011; Foley et al. 2011). According to the FAO report (2017), the world population could reach 10 billion by the year 2050 which will require a 60% - 70%-fold increase in food production (FAO 2019). Given this, many authors have suggested that increasing production rather than expanding arable lands is key to ensuring food security (Phalan, Balmford, et al. 2011; Phalan, Onial, et al. 2011; Green et al. 2005; Tscharntke et al. 2012; Hulme et al. 2013). However, this feat must be realized within the frame of sustainability and environmental protection to ensure minimal effect on biodiversity (Gomiero, Pimentel, and Paoletti 2011).

Rice is an important staple food around the world and its consumption provides about 35% - 60% of the daily required calories of many households (Fageria 2007). Therefore, it is necessary to increase the crop production of rice. Given this challenging issue, there is a need to develop and adopt crop management techniques that use less resource input with high efficiency to improve rice production. The traditional methods of rice growth monitoring rely mainly on time-consuming and labour-intensive manual evaluation in the field which may sometimes be subjective depending on the observer's experience (Cen et al. 2019). This implies that obtaining crop growth status frequently with high precision and accuracy is important to help in the design of the best management methods. To this effect, complex ecological and physiological processes are studied in agroecological research to identify plant genotypes and environmental reactions to crop management options for instance on crop growth. Crop growth simulation models (CGSM) allow for the accurate and timely estimation

of crop growth and development requirements (Ten Berge et al. 1997). Consideration of the spatial variation of crop-growth environmental conditions can improve crop-management practices. In this regard, remote sensing (RS) can be an important tool for meeting the aforementioned requirements because it provides a non-destructive means of providing recurrent information on crop growth status from the local to the regional scale, allowing for the characterization of spatiotemporal variability within a given area (Stafford 2000; Metternicht 2005).

### *1.1.1. Remote sensing application for agriculture.*

Remote Sensing refers to the acquisition of information about an object or phenomenon without contact (Agrios 2004). Satellites and balloons are common remote sensing platforms, and a variety of sensors like optical and near-infrared sensors, as well as RADAR (Radio Detection and Ranging), are fixed on these platforms for remote sensing applications. Remote sensing platforms and sensors have been used for monitoring based on satellite imaging such as Landsat 1 and Ikonos (Seelan et al. 2003; Bauer and Cipra 1973; Mora et al. 2017; Mulla 2013). However, satellite imagery is sometimes not the best option due to the low spatial resolution of acquired images and the limitations of temporal resolutions imposed by the fact that longer revisit times are required. Furthermore, weather conditions, such as clouds, obstructs the use of satellite. Again when using manned aircraft for image data, the cost is usually high, and it's rare to be able to fly multiple times to get more than a few crop images (Tsouros, Bibi, and Sarigiannidis 2019). But recent technological advancements in unmanned aerial vehicles (UAVs) and portable sensors have increased their application in precision agriculture (Zhang and Kovacs 2012a; Verger et al. 2014).

### *1.1.2. UAV-based crop monitoring.*

UAV platforms are equipped with different types of spectroscopic and image sensors, such as Red Green Blue (RGB) sensors, multispectral/hyperspectral imaging sensors, light detection and ranging (LiDAR) and infrared thermal imaging sensors further increasing the base for UAV application. The potential of UAV has been demonstrated in some studies which include measuring plant length (Holman et al. 2016a; Li et al. 2016; K. Watanabe et al. 2017a), biomass (Willkomm, Bolten, and Bareth 2016a), yield (Du and Noguchi 2017), plant density (Jin et al. 2017), and vegetation fraction (Torres-Sánchez et al. 2014) in different crops such as barley (Bendig et al. 2014; Bendig, Yu, et al. 2015), maize (Wang et al. 2016), and soybean (Maimaitijiang et al. 2017). UAV-acquired images usually have higher temporal (e.g., daily acquisitions) and spatial resolutions (e.g., centimetres), necessitating further investigation into the use of high-resolution images in precision agriculture. With regards to high-resolution image data, many studies have examined crop growth parameters like plant length, leaf area index (LAI), and biomass alongside other environmental factors such as nitrogen (N) content, soil water stress, soil surface properties, etc., (Zarco-Tejada, González-Dugo, and Berni 2012; Donoghue et al. 2007; Sullivan, Shaw, and Rickman 2005; López-Lozano et al. 2009; Wan et al. 2020; J. Wu, Wang, and Bauer 2007; Metternicht 2005; Liang 2004).

However, most of the above-mentioned parameters are assessed using vegetation indices (VIs), which are widely used tools in agricultural remote sensing. Specifically, VIs such as the Normalized Difference Vegetation Index (NDVI), the Soil Adjusted Vegetation Index (SAVI), and the GreenNDVI, have been used for quantitative analysis of the aforementioned parameters (Hunt et al. 2005; Lelong et al. 2008; Swain, Jayasuriya, and Salokhe 2007). But a common setback with the use of these VIs in agricultural studies is saturation in the advanced crop growth stage (Haboudane et al. 2004). Additionally, there are concerns of irradiance conditions may affect the results of VIs. For example in Hama et al. (2020) and Zhou et al. (2017), the VIs fluctuates with an increase in the sun's

multitude above the horizon which causes a decrease in VIs (Rahman, Lamb, and Stanley 2015; Cogliati et al. 2015). Furthermore, this effect is also compounded by weather (Ishihara et al. 2015). The spectral information differs depending on the environmental (especially radiation) condition (Rasmussen et al. 2016; Inoue et al. 2016; Yuki, Katsura, and Yamashita 2020).

Another natural occurrence of importance to rice production is lodging because of how it substantially affects rice production. Lodging, regarded as the displacement of a plant from its upright position or anchorage system highly affects crop quality and output (Wei Wu and Ma 2016; Berry et al. 2004; 2003; Foulkes et al. 2011). Timely assessment of lodging would benefit several stakeholders like rice breeders, farmers, and insurance companies, and inform policymakers on farmer incentives and risk management on a large-scale (Liu et al. 2018). Because lodging causes a significant reduction in plant height, DSM could be used to assess lodging. However, no simple method for assessing lodging using DSM has been developed.

### *1.1.3. UAV photogrammetric techniques.*

Photogrammetric techniques are mainly used to construct orthomosaic or digital elevation models (DEMs) to extract 3D information regarding observed vegetation (Tsouros, Bibi, and Sarigiannidis 2019). UAV photogrammetry has facilitated the on-demand generation of high-resolution datasets such as the DSM. DSM represents the ground elevation model consisting of the morphology of the observed objects, such as vegetation and is constructed using surface point cloud data (X. Hu et al. 2021). DSM generated from overlapped aerial images is relatively less affected by the weather and time zone, unlike satellite images except by strong winds and rainfall at the time of the filming. UAVs for image acquisition coupled with structure-from-motion (SfM), provide a robust system capable of creating high-resolution DSMs using less expensive RGB cameras (Javernick, Brasington, and

Caruso 2014; Verhoeven and Vermeulen 2016; Verhoeven 2011; Geipel, Link, and Claupein 2014; Schirrmann et al. 2016).

### *1.2 Problem statement and research justification.*

Plant height is an important agronomic factor for field investigation in crop phenotyping due to its influence on biomass (Boomsma et al. 2010; Salas Fernandez et al. 2009; Yuan et al. 2008; Lübberstedt et al. 1997). DSM can provide 3D plant height information in the field and has been widely used in assessing relatively taller and heterogeneous canopies compared to homogenous and shorter canopies such as in paddy fields where there is little variation in PL (Rueda-Ayala et al. 2019; Zhang et al. 2018). However, accurate evaluation of such little variation has the potential for modelling other growth-related traits in rice (Bendig, Willkomm, et al. 2015; Bendig et al. 2014; Bendig, Yu, et al. 2015; Y. Wang et al. 2019; De Souza et al. 2017; X. Han et al. 2018; Li et al. 2016). In addition, the crop biomass–height relationship is usually specific to different rice genotypes under different crop growth statuses and environments. To date, fewer studies have considered the potential of the DSM approach for evaluating the genotypic differences in plant height among different rice varieties, and there is a dearth of information on paddy fields that requires much attention.

Therefore, this thesis provides the details of a comprehensive study comprising field and laboratory analysis which outlines the feasibility of DSM application in evaluating production and lodging in rice in different rice genotypes. The findings of this study add to the knowledge of remote sensing applications for agriculture to assist all stakeholders in the management decision-making process to increase rice production.

### 1.3. Objectives of the study.

The overall objective of this study was to develop evaluation methods for biomass production and lodging in rice by the digital surface model using an unmanned aerial vehicle. To achieve this objective, the following three specific objectives were set in conjunction with the subsequent chapters of this thesis:

- a. To use UAV-based images to develop a DSM to determine plant height in rice varieties in a paddy field.
- b. To estimate the biomass increase from plant height using DSM by conducting Spatio-temporal monitoring of growth dynamics.
- c. To analyse the feasibility of using a simple and direct assessment of lodging method in a multi-varietal rice field using DSM plant height.

### 1.4. Research hypothesis.

The background and the objectives of this research informed the formulation of the following hypothesis:

1. Significant genotypic differences exist among rice varieties which affect their response to the growth environment.
2. Genotypic and environmental differences affect the development and application of crop growth monitoring and evaluation models.

### 1.5. Structure of this thesis.

This thesis is structured into five chapters.

The first chapter constitutes the general introduction to the research, detailing the background, justification, objectives, and hypothesis. Chapter two focuses on using UAV-based images to develop a DSM to determine plant height in the 2018 growing season. Chapter three focuses on model transfer

and application to monitor and estimate biomass growth in rice in the 2019 growing season. Chapter four further assesses the feasibility of using the DSM to evaluate lodging in rice varieties. Chapter five consists of a summary of the significant outcomes of the research, the conclusion made from the analysis and proposed areas for further study.

## CHAPTER 2

### **Development of plant height estimation model by a digital surface model using unmanned aerial vehicle images.**

#### 2.1. Introduction.

The future of agricultural food production is threatened by a labour shortage that is expected to worsen in the not-too-distant future. However, food demand and consumer preference require that high yields and quality standards are maintained which necessitates the best management practices used throughout the production period. Traditionally cultivation management involves on-site visual appraisal of crops, which is laborious and time-consuming thus prone to many errors. In some cases, the farmer's judgment based on experience may be subjective (Dessart, Barreiro-Hurlé, and Van Bavel 2019). For countries like Japan, the ageing and dwindling labour force in the agriculture sector has become a major social problem, therefore, labour saving and efficiency in cultivation management are pressing issues that need urgent attention. For this reason, Guo et al., (2015) asserted that technological innovations and interventions are eminent to compensate for the physical deficiency in the agricultural labour force. Concurrently, developed techniques must not compromise economically and environmentally sustainable production systems, through increased efficiency of input use and reduced environmental damage (Delgado et al. 2019).

Rice is a major grain crop that feeds over half of the world's population. Rice production and quality have been the subject of many studies (Yuan 2014; Peng et al. 2008; Dan et al. 2016). Precision management, legislation, decision-making, and marketing all benefit from timely and accurate rice monitoring and yield forecasting before harvest (Zhou et al. 2017). Field surveys and destructive sampling at various field scales are common methods for collecting rice ontology information, but they are labour-intensive, complex, and fraught with uncertainty. Furthermore, because rice has a long growth cycle, its yield is affected not only by growth status during the

reproductive phase (booting, heading, and filling), but also during the vegetative phase (seeding, tillering, and jointing), necessitating continuous monitoring of rice growth (Wan et al. 2020).

Plant height is a basic agronomic parameter for field investigation in crop phenotyping and is widely used to assess biomass and potential grain yield (Rueda-Ayala et al. 2019; H. Zhang et al. 2018). Traditionally, plant length (usually from the base to the top-most tip of the plant) has been measured in the field with a meter rule by selecting a few representative plants to represent the canopy. However, this method is time-consuming when it involves large-scale multi-variety trials and can be hampered by severe weather and limited accessibility. As a result, several high-throughput technologies for obtaining three-dimensional (3D) structures under field conditions have been developed (Boomsma et al. 2010; Sankaran et al. 2015). This is because, to characterize phenotypic traits non-destructively and noninvasively for thousands of individual plants with high efficiency and precision, high-throughput phenotyping systems are required (Furbank and Tester 2011; Großkinsky et al. 2015).

Crop growth can now be predicted thanks to advances in remote sensing technology, and satellite-based remote sensing has proven to be extremely accurate. However, satellites' overpass frequency and spatial resolution (>50 cm), which do not correlate well with single rice plants, are limitations for such work (Kawamura et al. 2020; Al-wassai 2013). Single rice plants cannot be identified because they are usually sown in 20 – 25 cm intervals grid (Kawamura et al. 2020). Similarly, ground-based sensing platforms are difficult to transport from one location to another, surface maps are difficult to generate in real-time, and plant parameters of multiple plots cannot be measured at the same time (Sankaran et al. 2015). Also, low resolution, cost, and variable weather conditions limit the ability to obtain timely crop growth information throughout the growth period. Furthermore, many crop yield prediction models can only provide high accuracies at a large scale, such as country, region, or county, but they cannot describe the detailed variations at a small scale,

especially for small farmlands or experimental plots (L. Han et al. 2019; Sulik and Long 2016; Huang et al. 2015).

The increasing availability of UAVs has opened the possibility of increasing image data monitoring frequency and spatial resolution (Shi et al. 2022). For instance, VIs derived from UAV-based images have been proven to be an effective method for predicting crop yields (Zeng et al. 2021). But canopy structure variability at various growth stages is another factor that influences VIs robustness, especially in heterogeneous canopy structures like rice with wide genotypic variations. Laser scanning techniques, such as airborne light detection and ranging (LiDAR), can be used to obtain detailed 3D information on the plant canopy (Hoffmeister et al. 2009; Tilly et al. 2014). Due to the payload limitations of small UAVs and their high relative cost, LiDAR and TLS are not widely available in crop fields, despite their precision (Kawamura et al. 2020). The feasibility of using UAV platforms to estimate plant height and 3D canopy structure in barley, maize, and sugarcane has been demonstrated so far. Conversely, fewer studies have been conducted in relatively shorter canopy crops (Bendig et al. 2014; Berry et al. 2003; Bendig, Willkomm, et al. 2015; K. Watanabe et al. 2017b; X. Han et al. 2018) because of smaller distinctions in plant height possibly leading to lower accuracy.

Therefore, in this study, UAV digital surface model (DSM) was used to estimate plant height in a relatively shorter crop, rice, using different genotypes throughout the growth period in the paddy field. Canopy height (DSM\_CH) obtained by extracted crop surface models (CSM) from successive DSMs were validated by ground measured data and explained by linear regression models. The established relationships could serve as the basis for modelling other crop growth-related traits.

## 2.2. Materials and methods.

### 2.2.1. *Experimental site.*

A field experiment was conducted in 2018 in a paddy field containing alluvial clay loamy soil, on the farm belonging to the Field Museum Honmachi, Tokyo University of Agriculture and Technology, Honmachi, Fuchu-shi, Tokyo (35° 39' 57" N, 139° 28' 16" E, 49 m above sea level). The total land area measures approximately 3.39 ha and consists of 13 rice paddy plots with a total area of 2.4 ha (Figure 2.1). The climatic conditions of this area are mild and generally warm, with a mean annual temperature and precipitation of 15 °C/59 °F and 1530 mm, respectively (Japan Meteorological Agency n.d.). The experimental area measured 45 m × 15 m and was arranged in a randomized complete split-plot block design, with three replicates each, with fertilizer treatment as the main plots and rice varieties as sub-plots (Figure 2.3). The dominant soil at this site is grey lowland, alluvial loamy soil which is the typical soil of paddy fields in Japan. The site has been in continuous rice cultivation for over 30 years with little off-season fallow period in between growing seasons. Based on a report that industrial effluents polluted the water supply from the Fuchu irrigation to this farm in the 1970s, groundwater from a depth of about 150 m now supplies water for irrigation to the farm ever since (Tatsumi, Kuwabara, and Motobayashi 2019; Aoyama et al. 2010; H. Watanabe et al. 2007; Okazaki and Saito 1989).

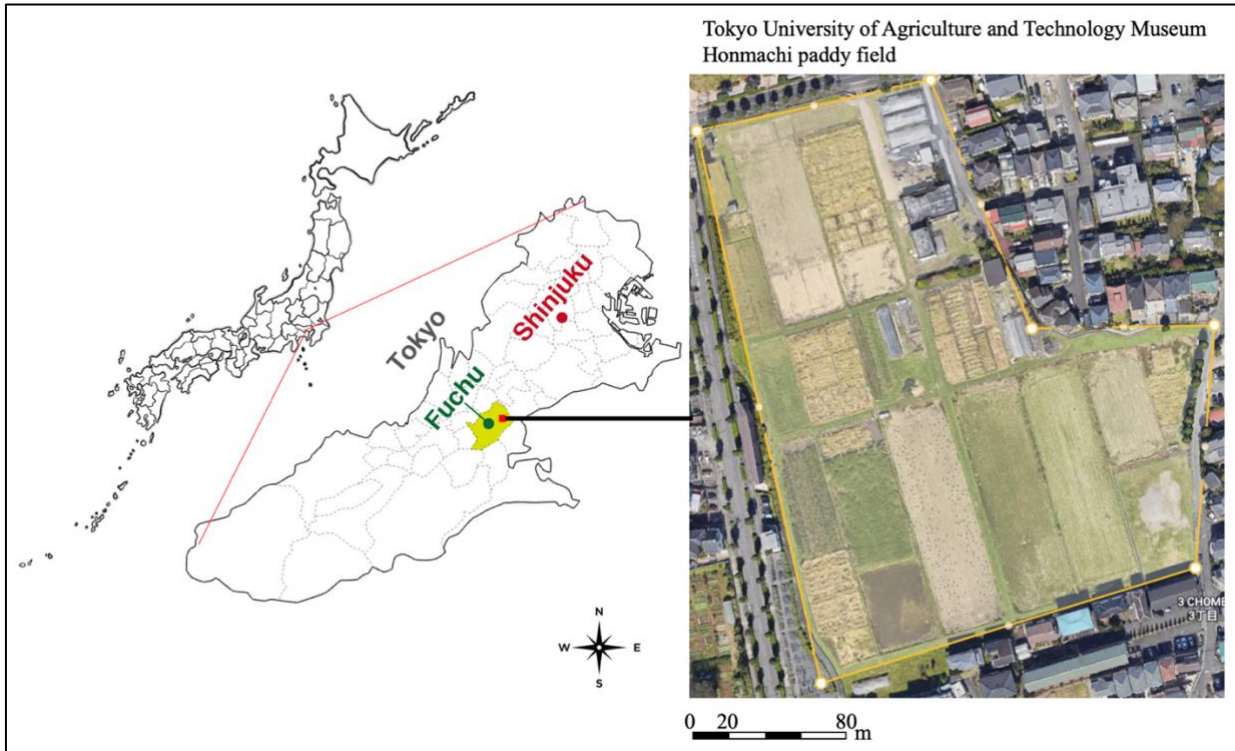


**Figure 2.1.** Location of the study site at Fuchu Honmachi, Tokyo

### 2.2.2. Agronomic and management practices.

The field was irrigated with groundwater from the pump station at the paddy field. The water flows to the research field by underground pipes connected to the pump station, which allows for full and independent control of water levels appropriately. Following the general paddy field preparation and water ponding, the paddy soil was paddled by several passes of a rotary tiller under a few centimetre ponding water conditions (Figure 2.2). Submerged field condition was normally maintained for most of the growing season. Hand-picking of weeds was done when necessary to reduce competition for available nutrients with crops. Herbicides are normally applied in the first and third weeks after transplanting using 350g granules herbicide containing Imazosulfuron 0.9%, Pyrazlonil 2.0%, and Brombutide 9.0%. Before transplanting, water was introduced into the paddy to a level of 0.01-0.02 m above the soil surface. All other standard agronomic practices were observed, and plant protection measures were taken as required.

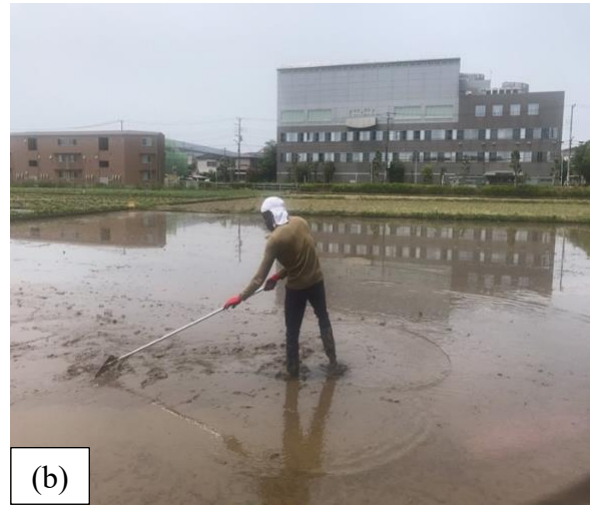


**Figure 2.2.** Rotary levelling (a) and manual levelling (b) of paddy field.



**Figure 2.3.** Study field and overview of the plot layout in 2018.

### 2.2.3. Rice genotypes and fertilizer application.

Three rice genotypes; Nipponbare (Japonica), IR64 (Indica), and Basmati370 (Indica) were planted based on their wide genotypic variability. Nipponbare is the first japonica cultivar in the world whose genome sequence has been sequenced in 2004 and was used as a representative of the japonica varieties (Matsumoto et al. 2005). IR64 is the most widely cultivated indica variety in the world and was used as a representative of indica varieties (Mackill and Khush 2018). Basmati370 is a traditional indica variety of aromatic rice with relatively less genetic improvement (Cosmas Mojulat et al. 2017). It was used in this study because the traditional (less genetically improved) varieties tend to show vigorous vegetative growth, and the plant morphological traits are very different from the improved varieties such as Nipponbare and IR64 (Shaobing Peng and Khush 2003). Seedlings at the fourth leaf

stage were transplanted at a hill spacing of 15 cm x 30 cm with one seedling per hill. The transplanting date was May 30, 2018. N fertilizer was applied in three splits. Fertilization in 2018 was divided into no fertilization (0N), low fertilization (Low) (basal: 3 g m<sup>-2</sup>, and topdressing 3 g m<sup>-2</sup>) and high fertilization (High) areas (basal: 3 g m<sup>-2</sup>, and topdressing 3 g m<sup>-2</sup> x 6 times). Phosphorous pentoxide (P<sub>2</sub>O<sub>5</sub>) and potassium oxide (K<sub>2</sub>O) were also applied at a ratio of 10:10 g m<sup>-2</sup> as the basal dose for each plot (17.5% P and 60% K concentrations, respectively).

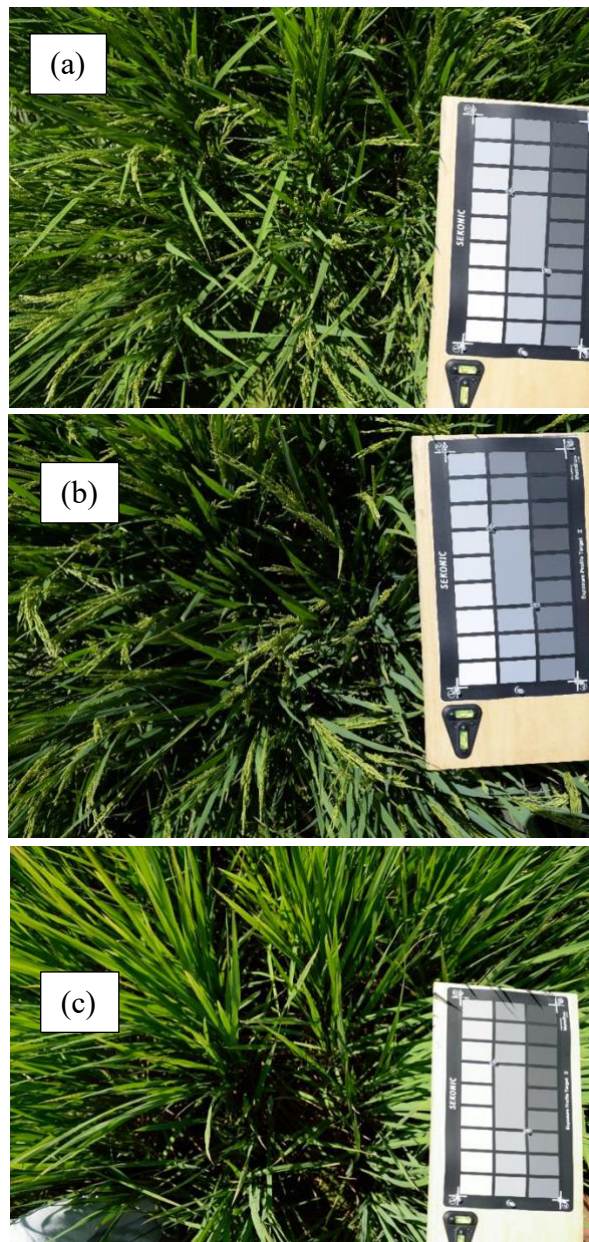


**Figure 2.4.** Images of the Genotypes planted in the 2018 growing season (a: Nipponbare, b: IR64, C: Basmati370).

#### 2.2.4. Aerial image data acquisition.

Ground control points (GCPs) were established in the experimental field using the total station and auto level by conducting traverse surveying and levelling. The coordinates of the GCPs were referred to in the Japan Geodetic Datum 2011 / Plane Rectangular Coordinate System zone 9 as a map projection, and the GCPs were set at the four corners of each field (Figure 2.3). Later, the GCPs were identified in the ortho mosaicked images for geo-referencing and height calibration.

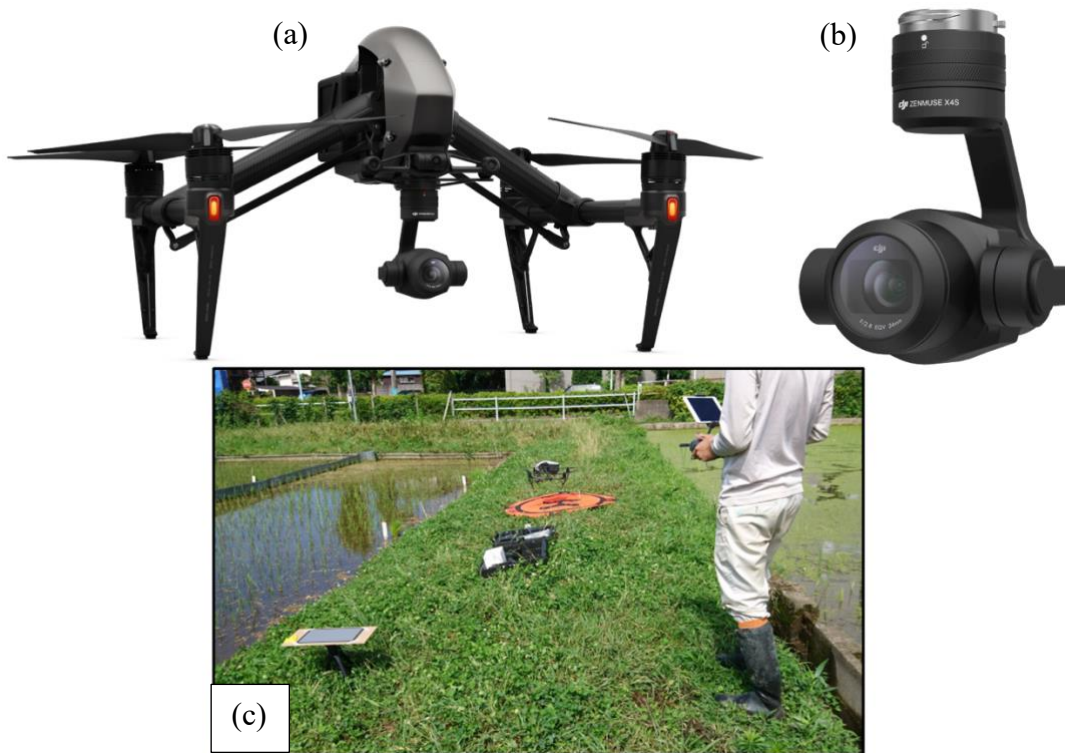


**Figure 2.5** The UAV platform used in this study: (a) Inspire 2 DJI UAV (b) RGB camera (Zenmuse X4S; DJI) (c) The UAV in the take-off position.

Sets of overlapped images of the fields were taken using a UAV (Inspire 2; DJI) equipped with an RGB camera (Zenmuse X4S; DJI) with 20 megapixels ( $5472 \times 3648$  resolution). The UAV flights were set to an autonomous flight plan using the ‘double grid’ mission in Pix4Dcapture. The flight altitude was fixed at 30 m above the rice canopy with a forward and lateral overlap rate of 85%.

Approximately 160 images were acquired during each flight campaign, and the flight survey was performed at two-week intervals in 2018 (eight flights). In the event of rain or strong winds, the shooting time and dates were altered accordingly. Due to the predominant flooded conditions in the paddy field at the early stages, it was better to take the UAV images at a time when the sun altitude was not high.

**Table 2.1.** Specification of the Inspire 2 DJI (UAV) platform.

Item	Specification
Maximum take-off weight	4,250 g
Maximum rotation speed	Pitch: 300 ° / s, Yaw: 150 ° / s
Speed (Max)	94 km h <sup>-1</sup>
Wind pressure resistance	10 m s <sup>-1</sup>
Gimbal accuracy	± 0.01 °
Battery (standard)	4280 mAh
Obstacle detection range	0 - 5 m
Image processing system	CineCore 2.1

**Table 2.2.** Specifications of the RGB camera (Zenmuse X4S; DJI).

Item	Specification
Size	125 x 100 x 80 mm
Weight	253 g
Sensor	CMOS, 1 "
Lens	F / 2.8-11, 8.8 mm (35 mm equivalent: 24 mm)
Viewing angle	84 °

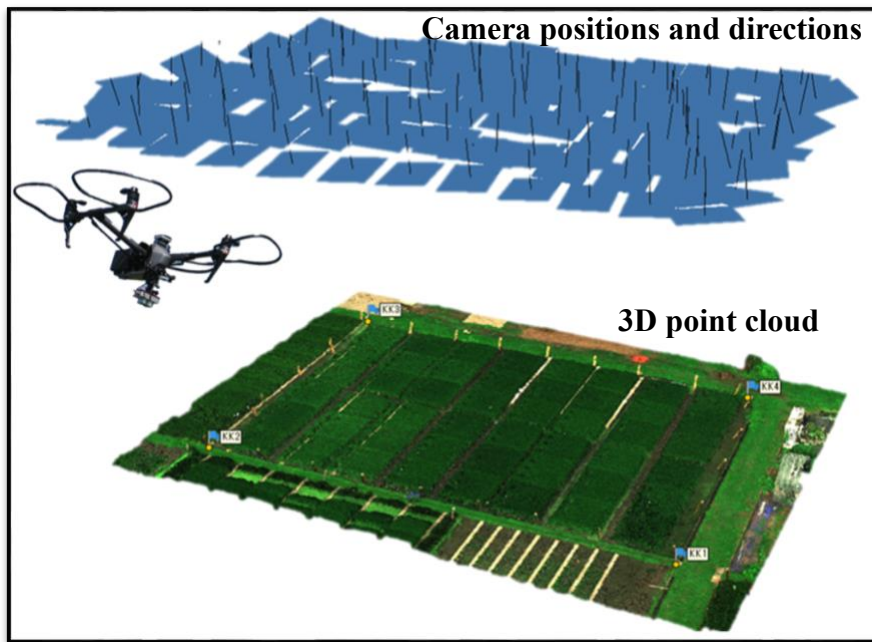


**Figure 2.6.** UAV flight trajectory of the flight mode.

#### *.2.5. Ground truth data collection.*

Plant length was measured from a 60 cm x 60 cm area that covers four standard hills from each plot. Figure 2.7 shows an example of images of three genotypes taken on July 3<sup>rd</sup> and 27<sup>th</sup>, and the area of the photos almost corresponds to the sampling area covering eight hills per plot. A total of 12 hills were sampled in 2018 per each sampling date. Plant length was obtained by straightening the plants one at a time and measuring the four hills from the ground surface level to the tip of the rice plant. The plant length was measured simultaneously along with the DSM\_CH on each UAV survey Day.

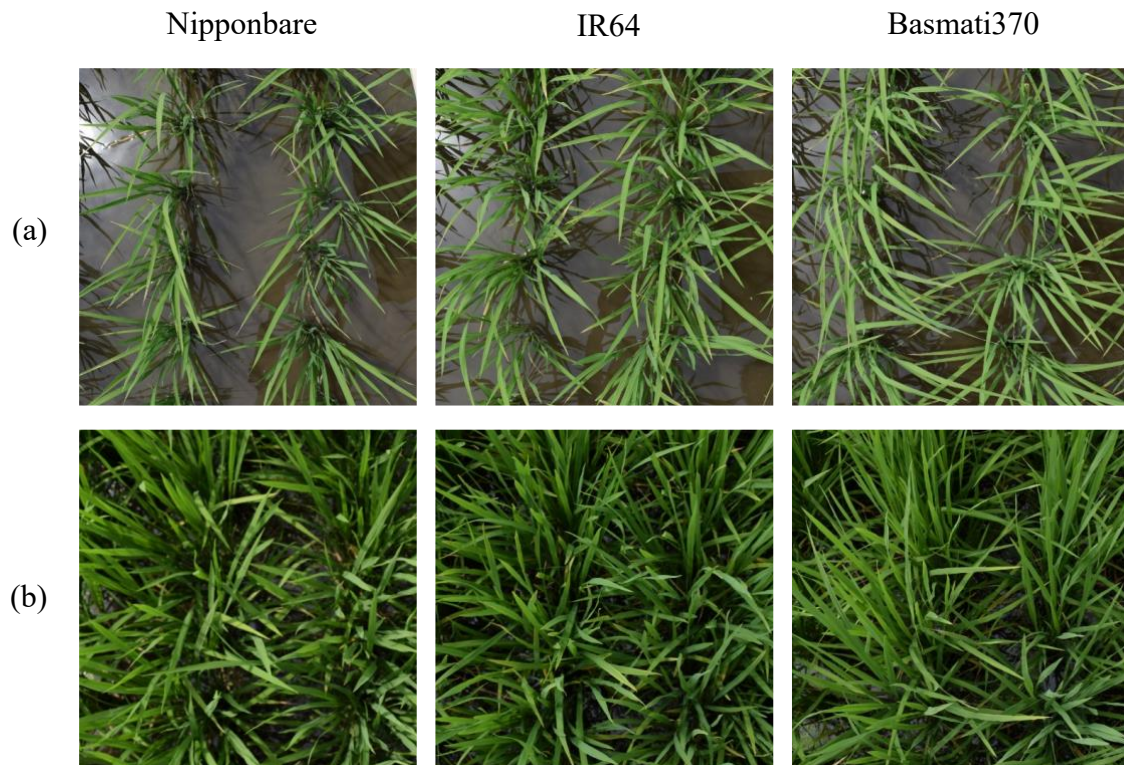


**Figure 2.7.** Examples of photos of 8 hills of 3 genotypes (Nipponbare, IR64 and Basmati370) with medium fertilization in replication 2 that were taken on (a) July 3rd and (b) July 27th in 2018.

#### 2.2.6. Generation of the DSM and canopy surface model (CSM).

The Agisoft Metashape Professional (ver. 1.5.1) was used to generate a 3D point cloud, ortho-mosaic images, and DSMs by processing the UAV-acquired images. As outlined by Gindraux et al., (2017), this approach supports the simultaneous processing of overlapped images using the geometric constraints of camera positions. Hereafter, the DSM is also referred to as the canopy surface model (CSM) because it reflects the crop surface. The process of generation of DSM and ortho mosaic images as explained by Yamaguchi et al. (Yamaguchi et al. 2020) was used in this study as shown in Figure 2.9.

First, tie points were automatically identified from the overlapped aerial images; then the tie points were used to calibrate the camera parameters such as the focal length of the lens, principal point positioning, and radial and tangential distortions. The parameters of external orientation (camera position and tilting angle) were estimated using the detected tie points and the four installed GCPs, and a dense point cloud was generated. This processing was performed to achieve a GCP accuracy within 1 pixel. A DSM and an ortho mosaic with a spatial resolution of approximately 9 mm/pixel were developed. The standard deviations of the z-coordinate (elevation) at the two checkpoints were examined from the generated time-series DSMs and were  $\pm 8.4$  mm and  $\pm 18.4$  mm in 2018.

From this, it was confirmed that the DSM generated using the minimum number of 4 GCPs required for photogrammetry showed sufficiently robust and stable in the use of the analysis of crop height. Using the DSM, CSM was calculated from the difference between the DSM of each observation day ( $DSM_n$ ) and the first DSM after transplanting ( $DSM_{1st}$ ) as seen in figure 2.8 (van Iersel et al. 2018).  $DSM_{1st}$  can be regarded as almost flat inside the paddy field and is defined as the reference plane to generate CSMs. At this time, since the paddy is flooded, the influence of the refraction of water may be included in the z-coordinate, but this was a systematic error and was not corrected. The value of the CSM was defined as the  $DSM\_CH$ . This relation is mathematically expressed as

$$CSM_n = DSM_n - DSM_{1st} \quad (2.1)$$

where  $n$  represents the observation dates.

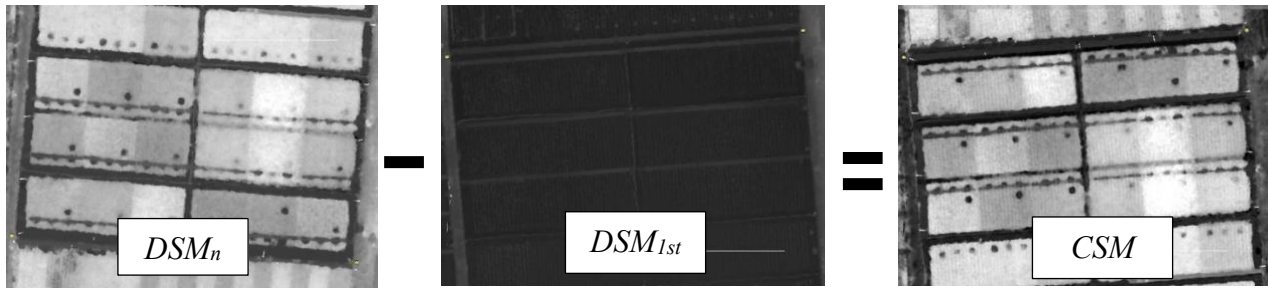


**Figure 2.8.** Generation of a CSM from the DSM.

**Table 2.3.** Parameters of the drone flights and image processing.

Process	Parameter	Setting
Drone flight	Altitude (m)	30 m
	Overlap	Forward 85% and lateral 85%
	Number of GCPs	4
	Coordinate system	JGD2011/Japan Plane Rectangular CS IX (EPSG:6677)
Camera alignment	Accuracy	Highest
	Adaptive camera model fitting	No
Build point clouds	Quality	Ultra-high
	Depth filtering	Mild
Build texture	Mapping mode	Generic
	Blending mode	Mosaic
Orthomosaic	Blending mode	Mosaic
	Surface	DEM

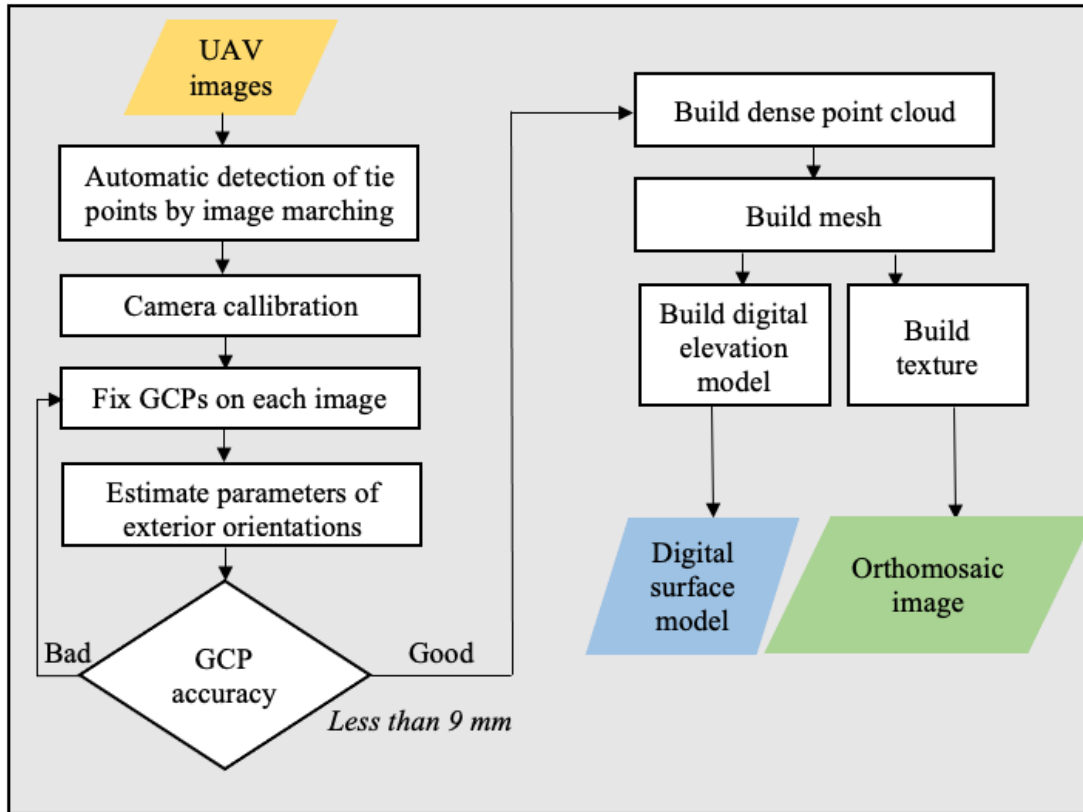


**Figure 2.9.** The flowchart of the DSM and orthomosaic image generation from UAV images.

### 2.3. Results and discussions.

This study analysed the potential of UAV-based DSM to estimate plant height, with an emphasis on developing estimation models to predict plant height of three rice varieties grown under varying environmental conditions. The results demonstrated the feasibility of using DSM-derived CH to predict plant height in rice genotypes. The approach used is uncomplicated, practicable, and can achieve timeliness compared to the conventional destructive sampling method. Although the droopy nature of rice leaves makes it difficult to measure accurately using UAVs in the field, the high correlation with the ground truth data shows a high degree of accuracy in using this technology.

### *2.3.1. Variations in manually measured plant length (PL) from field observation.*

A growth survey was conducted on three rice genotypes between July 3<sup>rd</sup> and August 27<sup>th</sup>. The results showed significant large variations in PL (from 0.46 m to 1.8 m) which were influenced by the genotype and the growth stage (Figure 2.10). Basmati370 attained the highest PL under both growth conditions. This is principally due to the tall nature of traditional Basmati varieties even under reduced nitrogen conditions (Bhattacharjee, Singhal, and Kulkarni 2002). Even though manual measurement of plant length tends to be accurate, however, manual measurement on a large scale has been a thorny issue (Tilly et al. 2014; Bendig et al. 2014). In literature, the problem of determining the representative mean of the PL of a field plot has also been addressed (Bendig et al. 2014). Therefore, it is beneficial to use the DSM for rapid and accurate estimation of PL in the field to save time and energy.

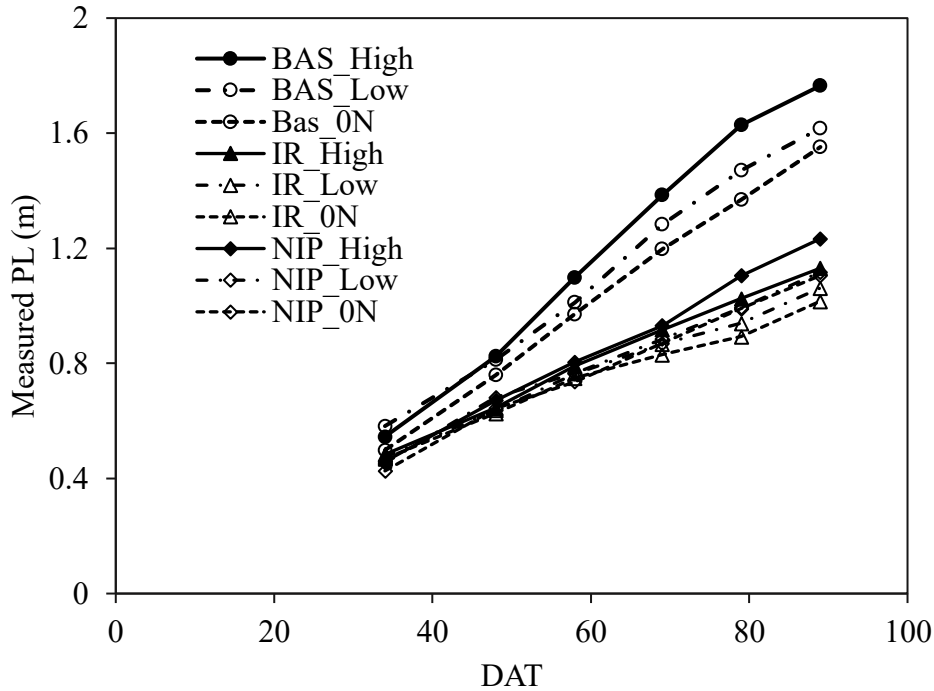


**Figure 2.10.** Comparison of changes in PL at various days after transplanting (DAT) for three rice genotypes: Basmati370 (Circles), IR64 (Triangles), and Nipponbare (Squares) under high fertilization (solid lines, filled) and Low fertilization (long broken lines, unfilled) and no fertilization (short broken lines, unfilled) conditions.

### 2.3.2. Relation between the measured PL and DSM<sub>CH</sub>.

A large variation was observed in CH (from 0.1m to 1.4 m) based on the growth stage and the genotypes. Generally, CH is relatively lower than PL because of (1) the droopy nature of fully matured rice leaves, (2) CH represents the entire canopy surface of the average height of several leaves including those in the lower position and is not necessarily the highest point of the plant when measured from the field (Bendig et al. 2014; Zhang et al. 2020), and (3) the wind may bend plants and generate false parallax, which can make the DSM height estimate method more difficult (Chu et al. 2018). Regarding the DSM<sub>CH</sub>, numerous measuring points exist within a pixel including lower

point areas within the pixel, therefore, a mean difference of about 0.3 m between PL and DSM\_CH is quite reasonable.

After the detailed processing of the 3D image as described in the previous section, the following spatial and temporal variations and patterns within each CSM and between different CSMs can be obtained as seen in figure 2.11. The increase in CH could be calculated from the height differences between successive CSMs using the maps obtained, as shown in Figure 2.11. Plant growth across the three dates accurately reflected changes in crop coverage and CH, which implies that plant growth is observable using DSM. In the early growth stages, a homogeneous canopy growth pattern was observed, which changed in the later growth stages. The results of the recorded CSMs indicate the suitability of the model developed to estimate CH with a high spatial resolution (approximately 9 mm) and accuracy as opposed to the spaceborne remote sensing approach (Koppe et al. 2012; Lopez-Sanchez et al. 2011; Ribbes and Letoan 1999).

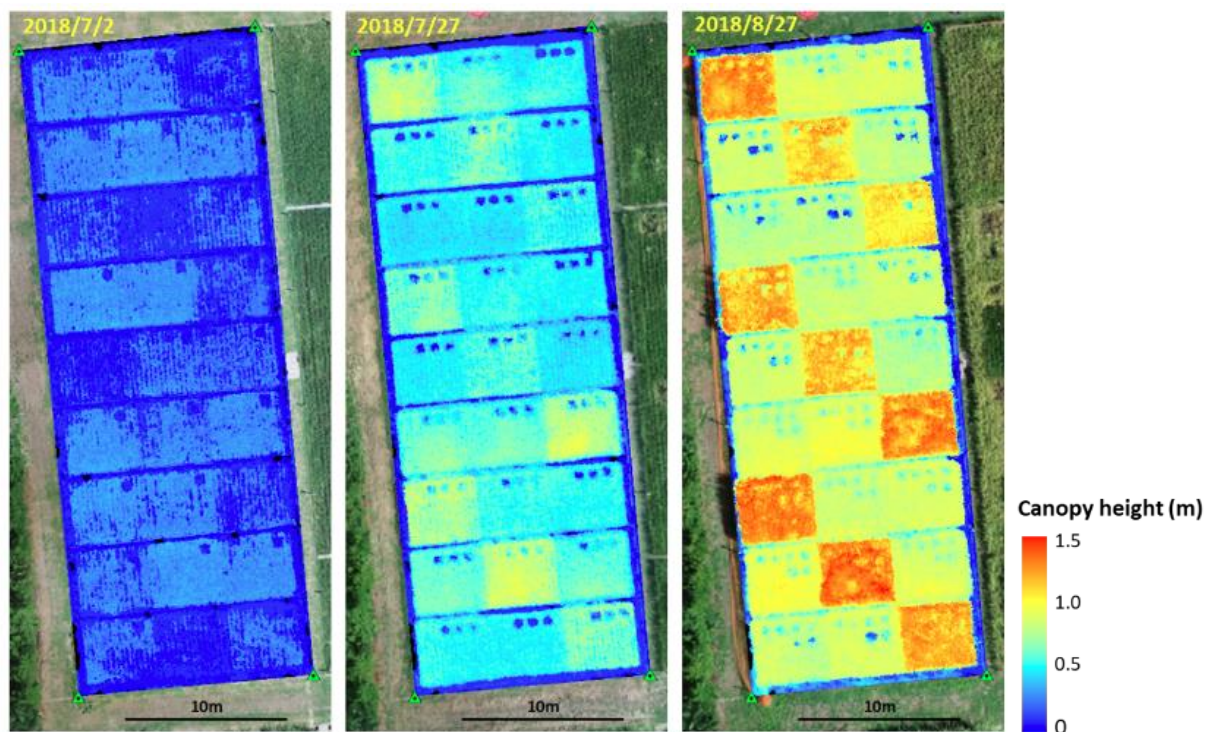


**Figure 2.11.** Height comparison datasets with canopy surface model for three rice genotypes in 2018.

In Figure 2.12, two types of CH calculated from  $CSM_n$  using the values at the 97<sup>th</sup> percentile (Kawamura et al. 2020) and the mean values of a 60 cm x 60 cm area that covers four hills are presented. As seen in figure 2.12, the two types of CH strongly correlate with PL, and the determination coefficient ( $R^2 = 0.947$ ) of the mean CSM shows a little higher than the 97<sup>th</sup> percentile ( $R^2 = 0.937$ ). This shows that DSM could explain the large variation in PL throughout the growth stages. However, there was a tendency for underestimation.

Also, the RMSE of the mean CH and the 97<sup>th</sup> percentile of CSM were 0.067 m and 0.074 m respectively. From these results, a complicated method is not required to derive representative CH in this case, and it implies that plant height can be estimated simply using the mean of CSM with higher accuracy.

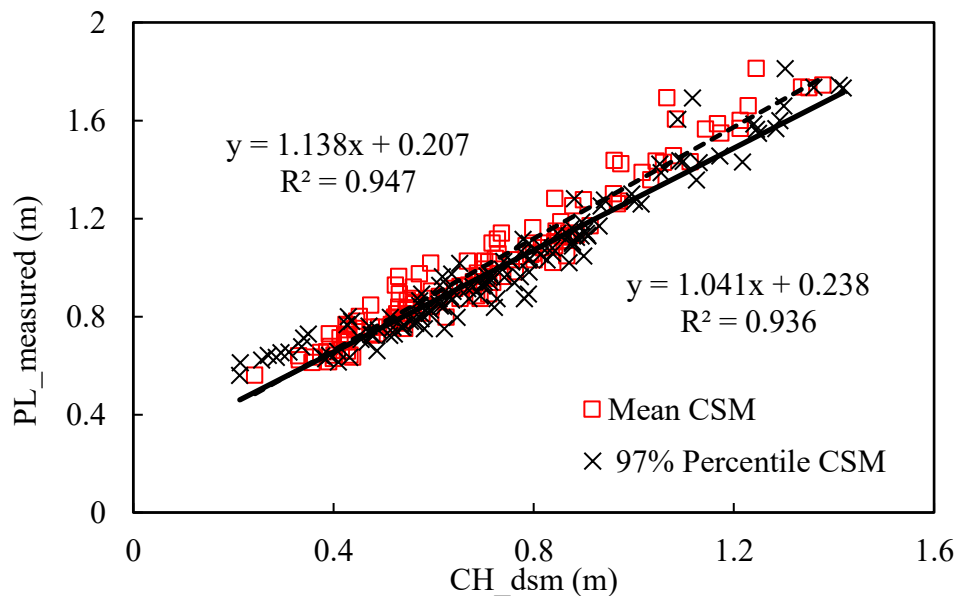


**Figure 2.12:** Comparison between measured plant length (PL) and two types of CHs calculated from the mean CSM values (red squares) and 97th percentile of CSM (black cross signs).

### 2.3.3. DSM\_CH calculation.

Variations in pixel units make it difficult to estimate crop growth accurately. Therefore, as shown in figure 2.13, ortho-mosaic and CSM images were developed, and the entire field was divided into polygons of 30 cm × 30 cm square meshes (2 plants) from which the mean value of the PL of each mesh was used as the representative value.

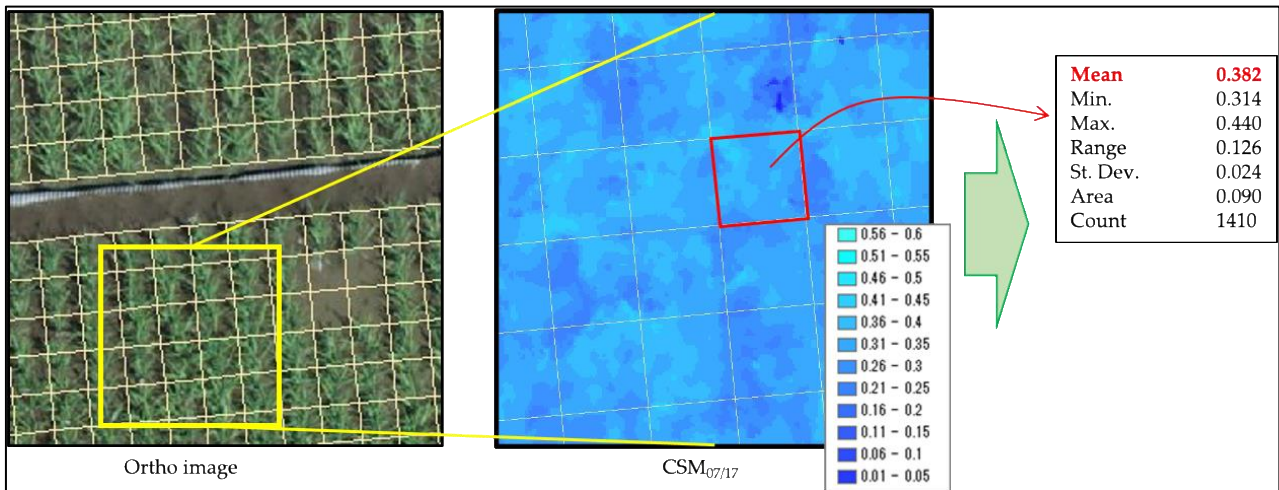


**Figure 2.13:** CH calculation from (a) orthoimage and (b) CSM in a 30 by 30 cm area (yellow square) covering two plants.

### 2.4. Conclusion.

This study used DSM to determine CH from UAV aerial images. The results showed significant variations in PL among the rice genotypes from 1.8 m in Basmati370 to 0.46 m in Nipponbare depending on the growth stage. CH correlated well with PL ( $R^2 = 0.947$ , root-mean-square error (RMSE) = 0.067 m) with large variation (from 0.1m to 1.4 m) depending on the genotype and growth stage. However, there was a tendency for underestimation in CH due to a composite of factors. Nonetheless, the ability of DSM to estimate such a wide range of CH is beneficial in assessing crop growth status, especially at the early growth stages where plant height is relatively low. These results proved the potential of DSM for deriving PL, which can be used for modelling other important

crop growth-related traits. Furthermore, since DSM was used in this study, the influence of weather was relatively minimal. The results outlined in this study require further investigation in different environmental conditions over multiple years to ascertain its transferability, because several other factors that influence model development and application were not investigated in this study.

## **CHAPTER 3.**

### **Spatio-temporal estimation of biomass growth in rice using canopy surface model from unmanned aerial vehicle images.**

#### 3.1. Introduction.

Obtaining knowledge about the dynamics of plant biomass is an essential part of precision agriculture, as such information aids in the management decision-making, risk assessment, and the design of labour-saving and efficient technologies that can compensate for the physical deficiency in the agricultural labour force (Guo, Wen, and Zhu 2015; Gil-Docampo et al. 2020; Tang et al. 2020). Biomass estimation has been widely explored due to its direct relation to crop yield commonly by farmers' expert knowledge through destructive sampling which is not timely and labour efficient. The consequences thereof lead to lower productivity (Li et al. 2015; Jimenez-Berni et al. 2018)

Alternatively, the potential of satellite-based remote sensing for crop management has been widely studied by MacDonald (1983). However, satellite imaging is hindered by coarse resolution, cloud cover, and fixed-timing image acquisition, which may not synchronize with some specific phenological phases (Matese et al. 2015; Cen et al. 2019). In addition, information on sufficient resolution and apt revisit frequency for precisely mapping smallholder farm units has been a challenge until the influx of UAVs (Hegarty-Craver et al. 2020). The low cost, high flexibility, simple handling, and high spatial resolution of UAVs enable their application in many fields of research including biology, forestry, and hydrology (Burkart et al. 2018; Candiago et al. 2015; C. Zhang and Kovacs 2012b; George et al. 2013; Zhou et al. 2017; Bendig, Yu, et al. 2015; Debell et al. 2015; Anderson and Gaston 2013; Rasmussen et al. 2016). Recent studies based on VIs extracted from the images captured by relatively inexpensive UAV-based digital and multispectral cameras have been used to examine many options for crop growth indices (Honkavaara et al. 2013; Lee and Lee 2013). However, it has been established that the normalized difference vegetation index (NDVI), widely used in remote

sensing, saturates the index values as the growth stage progresses, affecting its sensitivity to genetic and environmental conditions in the acquisition of high-resolution data (Lee and Lee 2013; Christopher et al. 2016). Also, spectral information is affected by various factors, including plant morphology, soil background, and the shooting environment (Rasmussen et al. 2016; Inoue et al. 2016; Tanaka, Katsura, and Yamashita 2020)

The emergence of UAV photogrammetry has facilitated the on-demand generation of high-resolution datasets such as the DSM (Hoffmeister et al. 2009). Comparatively, DSM generated from UAV photogrammetry offers advantages such as easy handling of the UAV platform, the likelihood of adapting sensors, user-friendly data evaluation tools, accessibility of difficult terrains and low cost, over terrestrial platforms or the light detection and ranging (LiDAR) (Fischer et al. 2016; Barrand et al. 2009; Baltsavias et al. 2001). Unlike satellite imagery, the DSM generated from overlapped aerial images is relatively less affected by the weather and time zone, except by strong winds and rainfall at the time of the filming. The spike in the use of UAVs for image acquisition proceeded simultaneously with the onset of a novel photogrammetric technique known as structure-from-motion (SfM), which together with multi-view stereo (MVS) provides a robust system capable of creating high-resolution DSMs using less expensive cameras (Javernick, Brasington, and Caruso 2014; Verhoeven 2011; Geipel, Link, and Claupein 2014; Schirrmann et al. 2016).

DSMs have been used extensively in agriculture for monitoring important traits such as plant height, yield, and biomass estimation in major crops such as maize, rice, barley, potato, and even perennial grasses such as *Miscanthus giganteus* (Bendig et al. 2014; Papadavid 2011; Verhoeven and Vermeulen 2016; Freeman et al. 2007; Sharma et al. 2016). However, little information is known of studies conducted on rice paddy fields and their particularities, highlighting significant varietal differences among genotypes. Additionally, the factors that constrain the location of control points (unlike dry land), could lead to potential correlation errors in SfM due to water reflections. Although,

investigations into several other factors that affect DSMs from UAV photogrammetries such as image quality, the layout of the Ground Control Point (GCPs), and flight altitude among others have been carried out (Rock, Ries, and Udelhoven 2012; Tahar et al. n.d.; Nouwakpo, Weltz, and McGwire 2016). Nonetheless, the analysis of time-series dynamic processes of various allometry and phenology mechanisms and their relationship with a different environment in rice has not been well studied. For these reasons, rigorous efforts to redress these information gaps are needed.

Unquestionably, previous works have made significant contributions to improving the feasibility of DSM application in agriculture by outlining various prospects, methodologies, challenges, and mitigation strategies. However, lapses in the available information for estimating crop growth under various environmental conditions using DSM require significant attention, especially in a homogeneous canopy like rice fields. Hence, in this study, UAV photogrammetry was used to assess the time-series aerial growth dynamics of different paddy rice varieties cultivated under different conditions to improve the estimation of biomass growth from CH using the DSM. Obtaining such data is a good step toward designing precise phenological calendars that are variety specific to feed crop estimation models. Linear regression models based on the DSM and extrapolated from overlapped RGB images were developed to estimate crop growth. From the estimated LAI and crop biomass results, the differences in the planting year and growth conditions were revealed using DSM instead of VIs, especially under various conditions, with high Spatio-temporal resolution.

## 3.2. Materials and methods.

### 3.2.1. *Experimental site.*

Two field experiments were conducted during the summers of 2018 and 2019 as shown in Figure 3.1 (hereafter referred to as Area 1 and Area 2, respectively) in a paddy field containing alluvial clay loamy soil, on the farm belonging to the Field Museum Honmachi, Tokyo University of

Agriculture and Technology, Honmachi, Fuchu-shi, Tokyo (35° 39' 57" N, 139° 28' 16" E, 49 m above sea level).



**Area 1 (2018)**

**Area 2 (2019)**

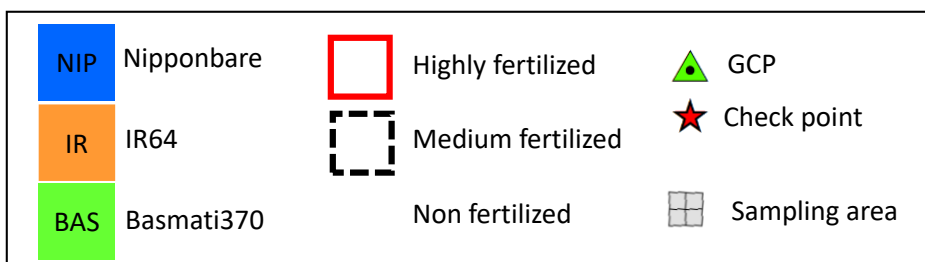


**Figure 3.1.** Study fields and layout in 2019.

The climatic conditions of this area are mild and generally warm, with a mean annual temperature and precipitation of 15 °C/59 °F and 1530 mm, respectively (“Japan Meteorological Agency, n.d.). Areas 1 and 2 measured 45 m × 15 m and 15 m × 27 m, respectively, and were arranged in a randomized complete split-plot block design, with three replicates each, with fertilizer treatment as the main plots and rice varieties as sub-plots.

### *3.2.2. Rice genotypes and fertilizer application.*

Three rice cultivars—Nipponbare (Japonica), IR64 (Indica), and Basmati370 (Indica) were used based on their wide genotypic variability. The reasons for their selections have been thoroughly discussed in the 2018 experiment. Seedlings at the fourth leaf stage were transplanted at a hill spacing of 15 cm x 30 cm with one seedling per hill. The transplanting dates were May 30, 2018, in Area 1, and May 22, 2019, in Area 2. Nitrogen fertilizer was applied in three and two splits in 2018 and 2019, respectively. Fertilization in 2018 was divided into no fertilization (0N), low fertilization (Low) (basal: 3 g m<sup>-2</sup>, and topdressing 3 g m<sup>-2</sup>) and high fertilization (High) areas (basal: 3 g m<sup>-2</sup>, and topdressing 3 g m<sup>-2</sup> x 6 times). For 2019, the plots were divided into non-fertilized (0N) and fertilized (+N) areas (basal: 2 g m<sup>-2</sup>, and topdressing: 2 g m<sup>-2</sup> × 6 times). Phosphorous pentoxide (P<sub>2</sub>O<sub>5</sub>) and potassium oxide (K<sub>2</sub>O) were also applied at a ratio of 10:10 gm<sup>-2</sup> as the basal dose for each plot (17.5% P and 60% K concentrations, respectively).

### *3.2.3. Aerial image acquisition and image processing.*

The detailed information about aerial imaging was mentioned in the second chapter of this thesis which is the 2018 experiment. However, the UAV flight campaign was adjusted to weekly intervals making eleven flights in total. For time-series monitoring, the aerial survey was done weekly in 2019 to acquire more detailed phenological changes in rice growth. All other precautionary measures were observed to ensure a successful UAV campaign throughout the study period. The standard deviations

of the z-coordinate (elevation) at the two checkpoints (Figure 3.1) were examined from the generated time-series DSMs and  $\pm 4.9$  mm and  $\pm 4.5$  mm in 2019.

#### *3.2.4. Ground truth data collection.*

Plants were harvested from a 60 cm x 60 cm area that covers eight standard hills from each plot (Figure 3.1). The total number of samples was 189 and 108 for up to 89 and 87 days after transplanting in 2018 and 2019, respectively to examine aboveground biomass (TDW), leaf area index (LAI) and PL. A total of 27 and 18 plots were sampled in 2018 and 2019 respectively per each sampling date. The above-ground parts of the plants such as leaf blades and stem plus leaf sheaths were retained, while the roots were discarded. PL was obtained by straightening the plants one at a time and measuring the height from the ground surface level to the tip of the rice plant. The PL was measured simultaneously along with the CH on each UAV survey Day. Leaf area was obtained by measuring randomly sampled leaves using an automatic leaf area meter (AAM-9A; Hayashi Denko, Japan) with a conveyer belt assembly. After determination of leaf area, the plant organs were oven-dried at 80 °C for 72 h to attain a constant dry weight, after which their dry weights were measured and LAI on a ground area basis was calculated.

#### *3.2.5. Procedures of Spatio-temporal estimation of biomass growth.*

Using CSM and ground truth data collected in 2018 and 2019, models were developed to estimate LAI and TDW from CH with PL and tried to estimate LAI and TDW spatially and temporally. Figure 3.2 shows the flowchart of spatio-temporal estimation of biomass growth using the CSM. First, the method of calculating CSM in 2018 to derive the relations with PL was examined. In addition, the relations between PL and LAI/TDW were derived, and from these relation formulas, LAI and TDW estimation models using CH as the variable were derived and evaluated. Furthermore, these models

were applied to CH in 2019 to estimate and evaluate LAI/TDW and estimated LAI and TDW spatially and temporally.

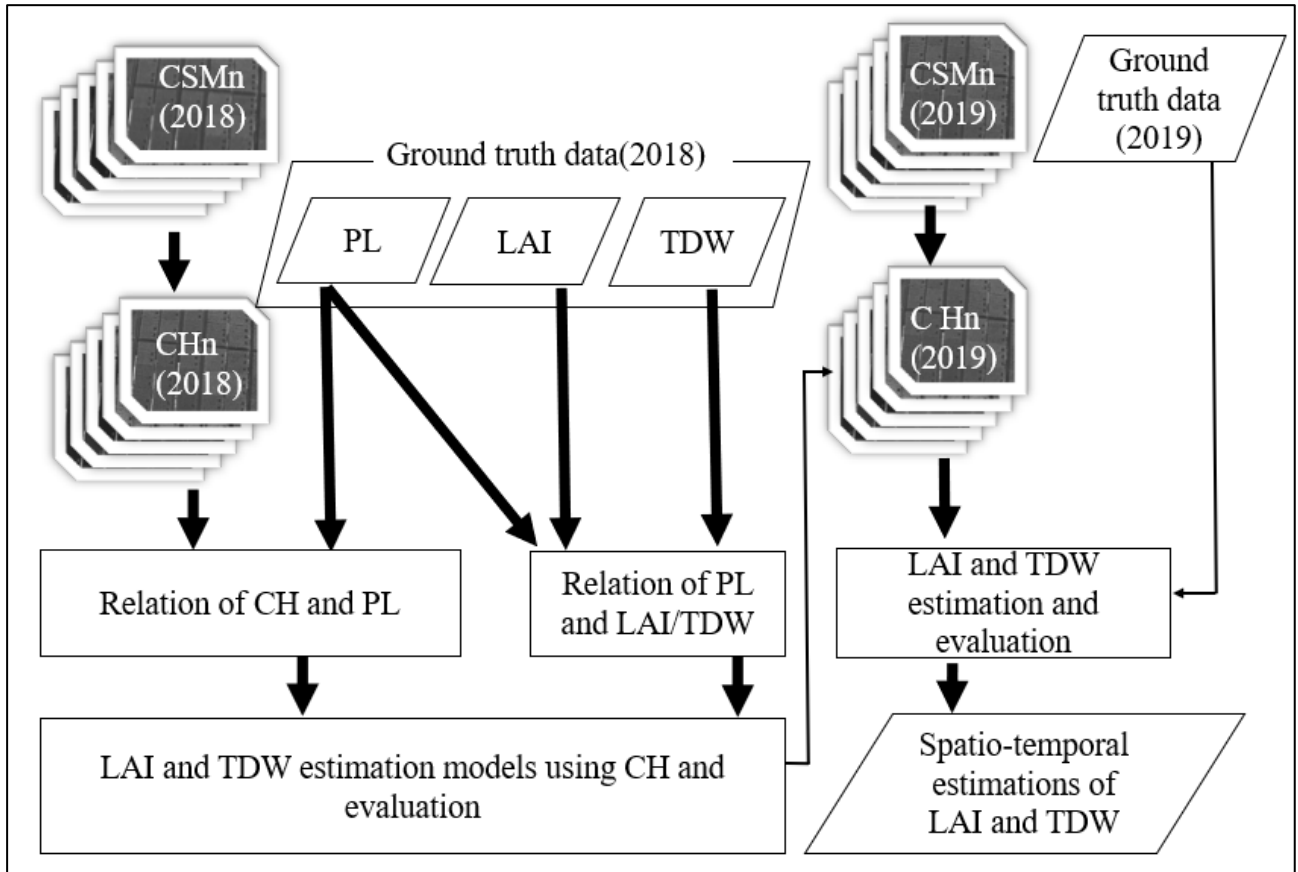


**Figure 3.2.** Procedures of Spatio-temporal estimations using canopy surface models.

### 3.3. Results and discussions.

#### 3.3.1. Genotypic variations in leaf area, biomass, and plant length.

Biomass production and harvest index determine rice productivity (Yoshida Souichi 1981). However, it is widely acknowledged that following the Green revolution, there is less room to increase the harvest index (Laza et al. 2015) and realizing higher rice yield will largely depend on increasing biomass production (S Peng et al. 1999). The agronomic parameters investigated in this

study yielded similar per-unit area values over the growth period as seen in Figure 3.3a-f compared to other previous studies (Fageria 2007; Yoshida et al. 2007; Njinju et al. 2018). The results presented in Figure 3.3 shows large variations in manually measured LAI, TDW and PL depending on the genotype, growth stage and growth condition. First, the largest LAI range was observed in Basmati370 (from 8.8 – 9.4 m<sup>2</sup> m<sup>-2</sup>) in the two growing seasons. Conversely, Nipponbare and IR64 achieved nearly the same LAI increase with little variation between them. The LAI range for Nipponbare and IR64 was relatively lower (from 7.1-7.5 m<sup>2</sup> m<sup>-2</sup>). The results show that genotypic differences affect LAI development. LAI increased almost linearly, especially under nitrogen fertilization conditions until after heading, in all varieties (Figure 3.3a and 3.3d), and this result agrees with Yoshida and Horie (2010), who emphasized the importance of fertilizer application in enhancing LAI growth. A similar trend was observed in PL with Basmati370 achieving the highest PL (from 177 – 180 cm) in 2018 and 2019 respectively compared to Nipponbare and IR64 (from 120 to 123 cm) in both growing seasons. TDW was relatively higher in 2018 than in 2019 (Figure 3.3b and e). TDW reached approximately 1334 g m<sup>-2</sup> and 1242 g m<sup>-2</sup> in Nipponbare and IR64 in 2018 and 2019 respectively compared to lower TDW recorded in Basnati370 (from 1144 – 1238 g m<sup>-2</sup>) in 2018 and 2019 respectively which confirms the effects of genotypic differences (Semchenko and Zobel 2005). Since water level condition was the same for the growing seasons, the difference in biomass may be attributed to the significant variation in daylight hours between the two seasons. The significant drop in TDW production could be explained by the intercepted solar radiation as determined by total incident radiation during rice ontogeny and the possible radiation intercepted by the radiation canopy (Yoshida et al. 2007). As it can be seen from Figure 3.9, there was a significant drop in the daylight hours which affected the radiation and absorption by plants for dry matter production emphasizing the importance of light intensity Photosynthetic-related biomass compounds

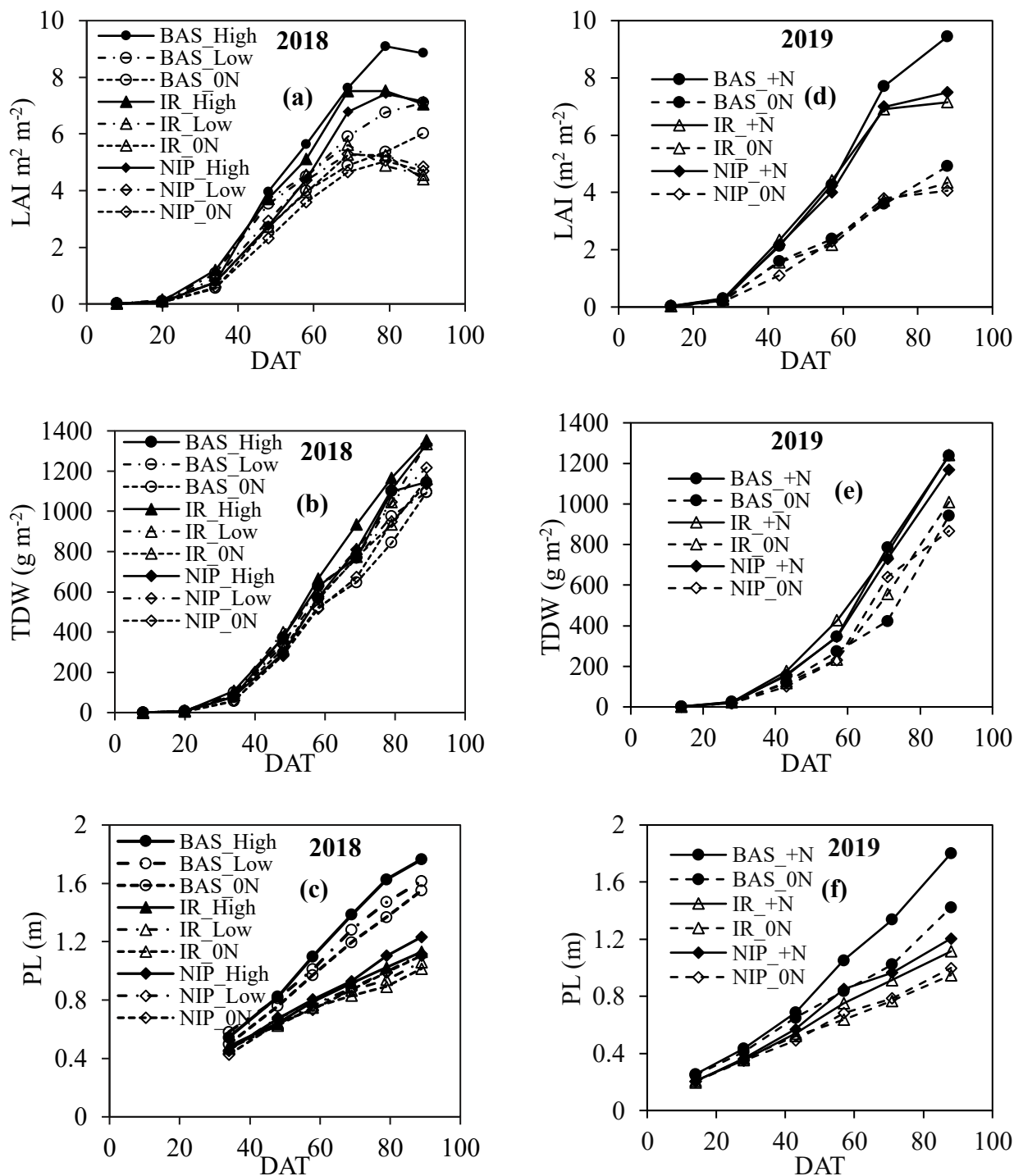


**Figure 3.3.** Comparison of seasonal changes in LAI, TDW and PL at various days after transplanting (DAT) for three rice genotypes: Basmati370 (Circles), IR64 (Triangles), and Nipponbare (Squares) under high fertilization (solid lines, filled) and Low fertilization (long broken lines, unfilled) and no fertilization (short broken lines, unfilled) conditions.

(Xu, Ibrahim, and Harvey 2016). This is mainly because, at lower irradiance, the rate of photosynthesis depends mainly on the light interception capacity (Pearcy and Sims 1994).

Additionally, Nitrogen fertilization plays a pivotal role in rice growth because of its involvement in physiological processes such as LAI development and biomass growth. The data collected exhibited large variations in each parameter, as described above, and plant height could be obtained throughout the growth period.

### 3.3.2 Relationship between the measured PL and DSM\_CH.

The model accurately estimated DSM\_CH in agreement with the conventional meter rule measurement method of PL ( $R^2$  0.904) in 2019 as shown in Figure 3.5. The strong linear correlations between the predicted and measured datasets of 2019 indicate a high accuracy in the model application. When deriving the estimation formula of LAI and TDW from CH, the relational formula of PL and CH in 2018 ( $y=1.1384x + 0.207$ ) was used.

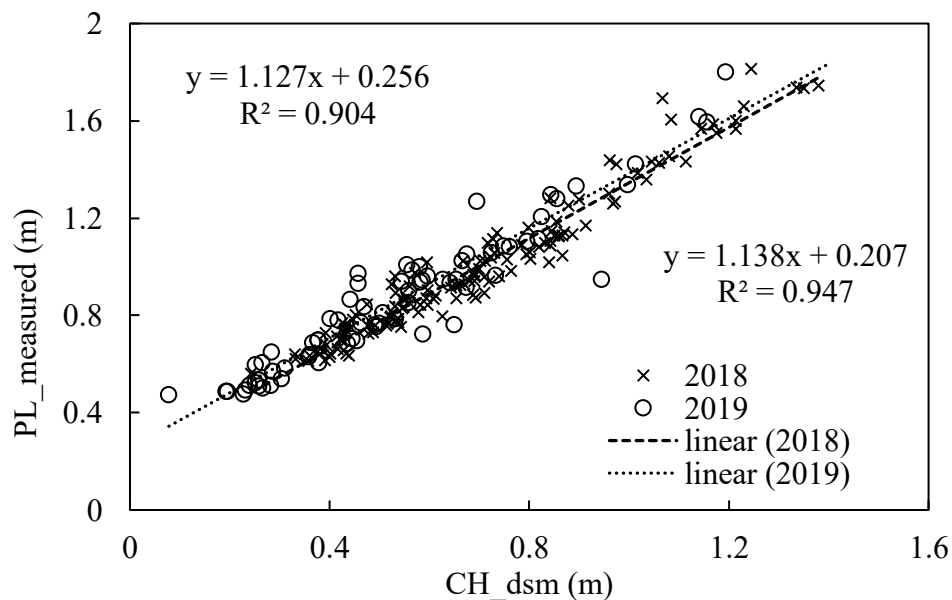


**Figure 3.4.** Comparison of seasonal relationships between measured PL and estimated DSM\_CH in 2018 (cross sign) and 2019 (unfilled circles).

Even though constraints such as underestimation by DSM exist as reported, the results showed enhanced accuracy compared to that of earlier reported models (Yamaguchi et al. 2020; van Iersel et al. 2018). The result thus shows that the model using DSM with RGB images could provide an alternative to the methods of using a multispectral camera and vegetation indices to estimate plant height.

### *3.3.3. Biomass modelling and evaluation.*

From the previous dataset in 2018, the dataset was further divided into two; datasets of replications 1 and 3 were for the model calibration ( $n = 48$ ) and replication 2 was used for the model validation ( $n = 24$ ). A linear regression model was then developed to compare the measured PL with LAI and TDW and was evaluated using their coefficient of determination values (Figure 3.5). The calibration data for LAI yielded  $R^2$  values of 0.886 and 0.764 for Basmati370, and Nipponbare and IR64 combined respectively (Figure 3.6a). Aboveground shoot biomass recorded a high  $R^2$  value of 0.961 in Basmati370 (Figure 3.6b). A similar correlation between biomass and PL has been previously reported by (Ehlert, Adamek, and Horn 2009; Willkomm, Bolten, and Bareth 2016b; Aasen et al. 2015). The effect of nitrogen fertilizer application on the relationship between PL and LAI/TDW was not significant in this study (Figure 3.6), so it was regarded as negligible because the same regression lines could be developed for the parameters. From the observed linear relationship between the PL and DSM\_CH, and the relationship of PL with LAI and TDW, a model for estimating LAI and TDW from the CH was developed using the two types of relational expressions expressed below:

### Nipponbare & IR64

$$LAI_{nipir} = 9.15CH - 0.66 \quad (3.2)$$

$$TDW_{nipir} = 2071.3CH - 412.8 \quad (3.3)$$

### Basmati370

$$LAI_{bas} = 7.21CH - 0.83 \quad (3.3)$$

$$TDW_{bas} = 1030.7CH - 201.6 \quad (3.4)$$

Basmati370 had different relational expressions compared to the other genotypes; therefore, different models were built for Basmati370 and the other two genotypes using ArcMap. Relatively, Basmati370 is less genetically improved than the other two genotypes used in this study, and generally, less genetically improved rice varieties tend to have higher N requirements and become taller compared to genetically improved rice varieties. Therefore, to establish a method for estimating the biomass growth of rice under various cultivation controls, it is necessary to have knowledge of different genotypes and develop different models to fit the different models as the results of this trial have proven that large variation exists in growth-related parameters among different rice genotypes and also plants response to the growing environment.

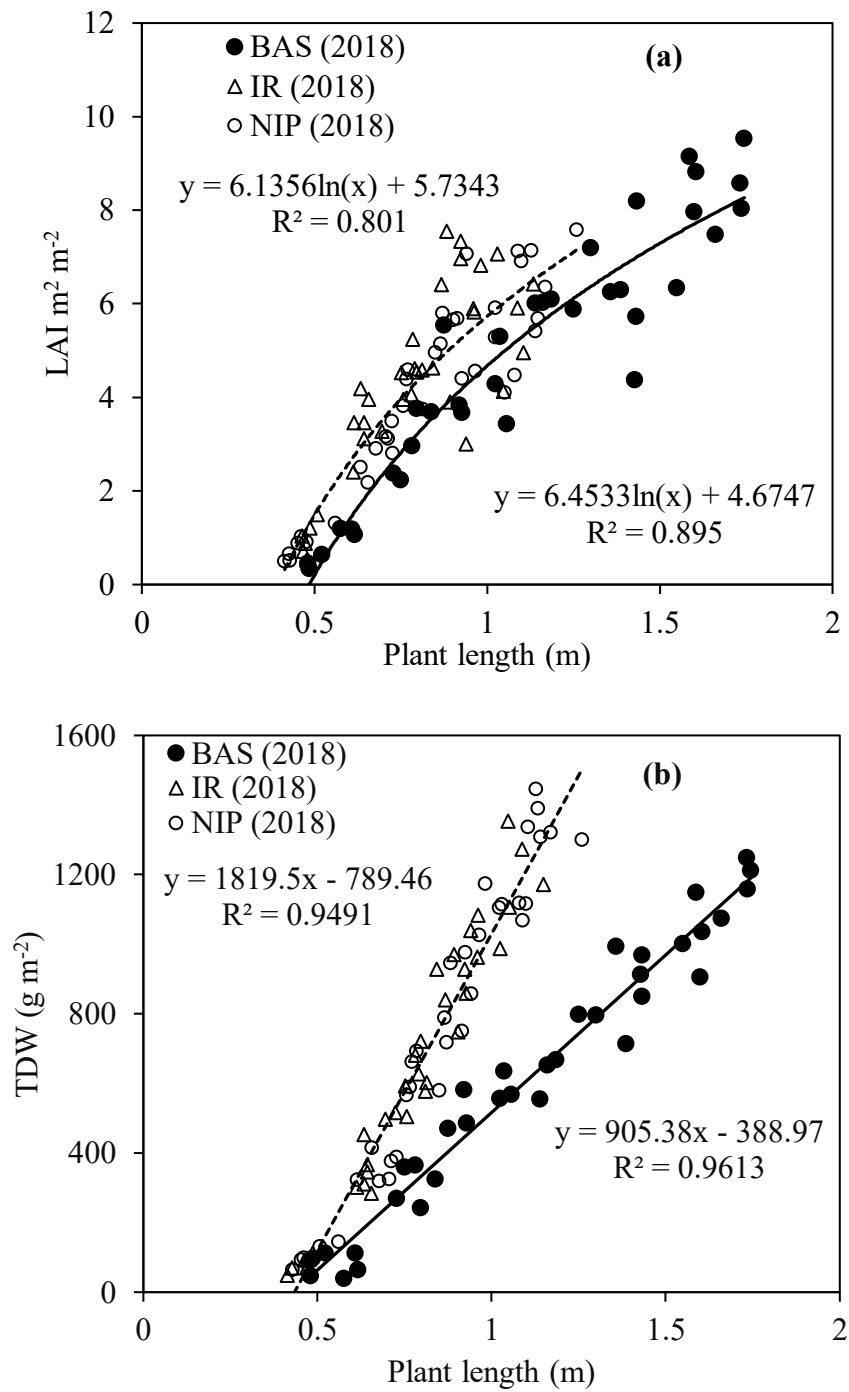


**Figure 3.5.** Relationship of (a) LAI and (b) aboveground TDW with measured PL among three rice varieties: Basmati (filled circles), IR64 (unfilled triangles), and Nipponabare (unfilled circles) in 2018 (Rep. 1 & 3). Solid line (Basmati trendline); Broken line (IR64 and Nipponabare trendline).

### 3.3.5. Accuracy Assessment of LAI and TDW estimates and validation.

The derived model from the validation dataset was used to estimate LAI and TDW as shown in Figure 3.7, and the results were compared with the measured values considering their strong relationship with PL. The correlation between measured and estimated values was high in

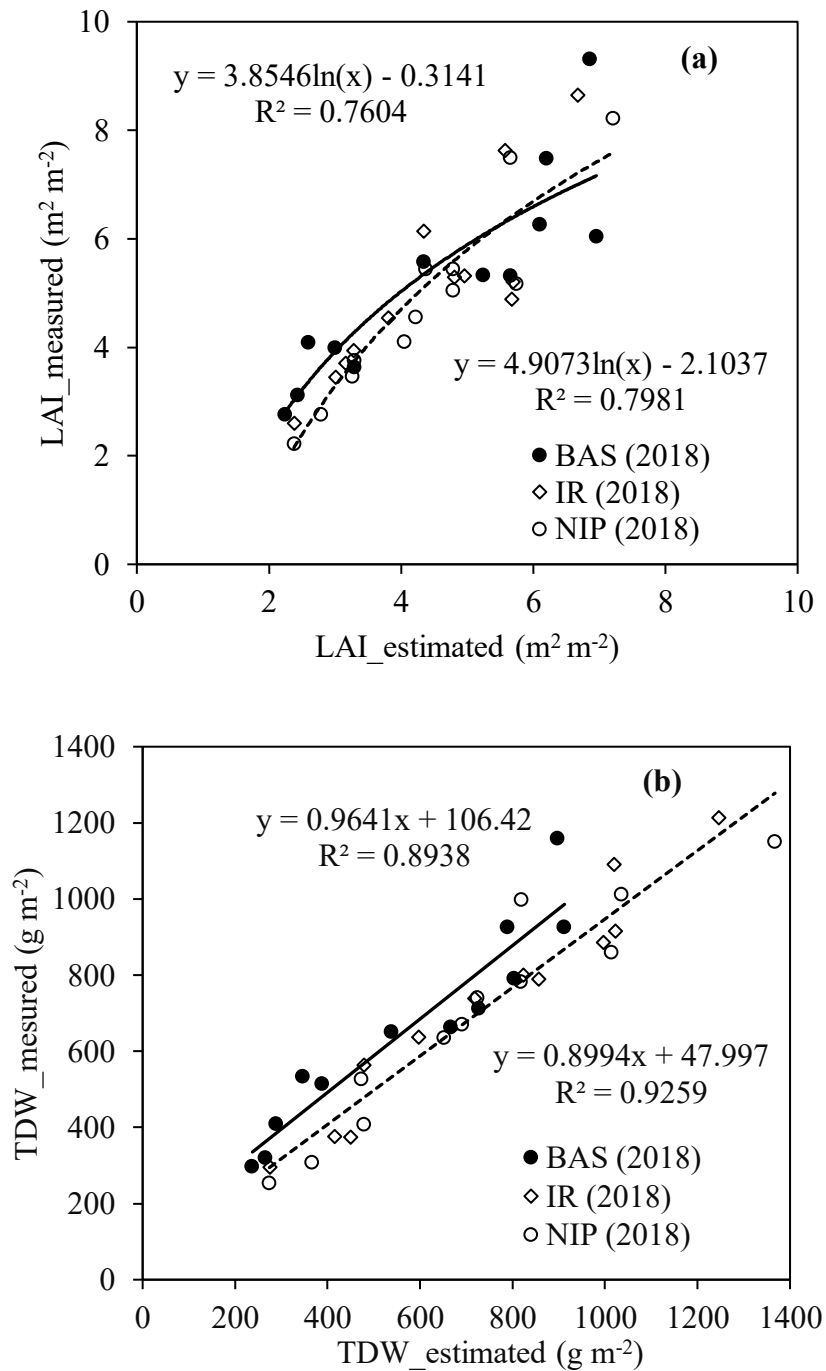


**Figure 3.7.** Accuracy assessment of CSM derived estimated (a) LAI and (b) TDW against standard ground-based measurements among three rice varieties. Basmati (filled circles), IR64 (unfilled triangles), and Nipponbare (unfilled circles) in 2018 (Rep. 2). Solid line (Basmati trendline); Broken line (IR64 and Nipponbare trendline). BAS: n=12, NIP & IR: n=24.

TDW ( $R^2$  between 0.894 and 0.926) as compared to LAI ( $R^2$  between 0.780 and 0.814). In rice canopies, where leaves overlap during canopy closure, leaf area estimation could be hindered as segregation of individual tillers and leaf blades become difficult, which could result in underestimation (Fang et al. 2014). Again, the scattering of values increased with the progress in vegetative growth, especially in LAI.

The aerial survey campaign was suspended on August 27 because of strong winds from a typhoon that resulted in the lodging of some plots; thus, subsequent surveys became challenging. Therefore, the CSMs up to August 17 were used for the estimation. The influence of lodging on the development of different genotypes could be a major limiting factor in the application of the CSM (Bendig et al. 2014). Table 3.1 shows the estimation accuracy of the LAI and TDW on the validation dataset that was set in 2018. The root mean square error (RMSE) of LAI was approximately  $1.0 \text{ m}^2 \text{ m}^{-2}$  for all varieties. The RMSE of TDW was approximately  $119 \text{ g m}^{-2}$  and  $84 \text{ g m}^{-2}$  for Basmati370 and the other two varieties, respectively. The relative RMSE of estimating LAI and TDW was approximately 18% to 20% and 12% to 18%, respectively, for all genotypes. The results indicated the ability of PL derived from the DSM approach to predict crop growth.

**Table 3.1** Estimation accuracy of LAI and TDW in 2018 (Rep. 2).

	LAI (m <sup>2</sup> m <sup>-2</sup> )		TDW (g m <sup>-2</sup> )	
	BAS	IR& NIP	BAS	IR & NIP
<b>Mean</b>	5.24	4.96	657.8	708.5
<b>Mean error</b>	-0.67	-0.55	-85.9	25.9
<b>RMSE</b>	1.09	0.93	119.0	84.4
<b>Relative RMSE (%)</b>	20.8	18.8	18.1	11.9

BAS, n=12; NIP and IR, n=24.

In 2019, the regression model derived from the validation dataset of 2018 was applied and evaluated based on the relationship between the measured and predicted values of LAI and biomass (Figure 3.8). As shown in Figure 3.8a, the prediction of aboveground dry biomass had the highest R<sup>2</sup> value (0.937) in Basmati370 with an RMSE of 0.76 (Table 3.1). Compared to 2018, the LAI distribution was slightly smaller in 2019 (R<sup>2</sup> = 0.894 to 0.866 (Figure 3.8b) in Basmati370 and the two other genotypes. However, the values tended to be more scattered toward the estimated LAI and TDW compared to the measured values. This is the result of bad weather conditions experienced in the early stages of the growing season, which had adverse effects on the plants. Reduced sunshine or daylight negatively affected the slope of the relationship between PL and TDW and LAI. This event led to an underestimating of the growth parameters in 2019.

The estimation accuracy of the model applied in 2019 showed that there was an improvement in LAI, as shown in Table 3.2. Even though there was a reduction in the mean, which decreased from approximately 5.0 in 2018 to approximately 3.7 in 2019, the RMSE improved from 1.0 in 2018 to approximately 0.8 in 2019, with little variation between the years. As mentioned earlier, this result seems to suggest that the estimation results of 2018 tend to be underestimated. Regarding the accuracy

of TDW estimation in 2019, a significant mean reduction from 657.8 g m<sup>-2</sup> in 2018 to 472.6 g m<sup>-2</sup> was observed in Basmati 370 (Table 3.2).

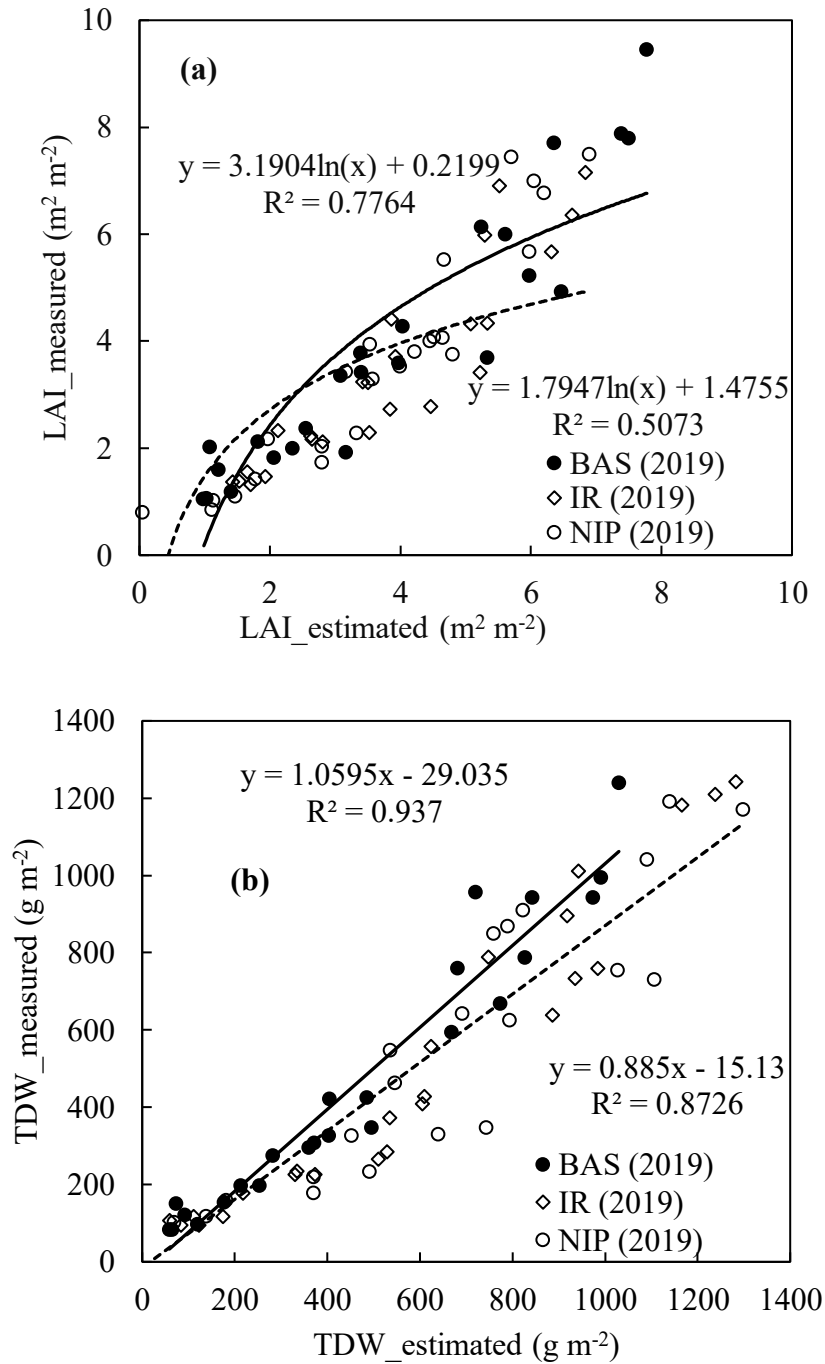


**Figure 3.8.** Relationship between the estimated and observed values of (a) LAI and (b) TDW among three rice varieties in 2019. Basmati (filled circles), IR64 (unfilled triangles), and Nipponabare

(unfilled circles) in 2018 (Rep. 2). Solid line (Basmati trendline); Broken line (IR64 and Nipponbare trendline). (Rep. 1, 2 & 3). BAS: n=24, NIP & IR: n=48.

The RMSE of Nipponbare and IR64 in 2019 ( $161.5 \text{ g m}^{-2}$ ) was approximately twice that of 2018 ( $84.4 \text{ g m}^{-2}$ ), indicating a large variance between the two seasons. The relative RMSE increased from 18.1% in 2018 to 18.7% in Basmati370 in 2019 (Table 3.3). In 2018, 12 samples were used to evaluate the accuracy compared to the 24 samples used in 2019. Because the number of samples was large, the model fitted well with the variation, which was evaluated to be relatively small as the accuracy was improved.

**Table 3.2.** Estimation accuracy of LAI and TDW in 2019 (Rep. 1, 2 & 3).

	LAI ( $\text{m}^2 \text{ m}^{-2}$ )	TDW ( $\text{g m}^{-2}$ )
Mean	3.66	442.9
Mean error	0.13	55.3
RMSE	0.76	141.4
relative RMSE (%)	20.8	28.7

**Table 3.3.** Estimation accuracy of LAI and TDW for three rice genotypes in 2019 (Rep. 1, 2 & 3).

	LAI ( $\text{m}^2 \text{ m}^{-2}$ )		TDW ( $\text{g m}^{-2}$ )	
	BAS	NIP & IR	BAS	NIP & IR
Mean	3.93	3.53	472.6	503.0
Mean error	-0.04	0.22	0.9	82.5
RMSE	0.79	0.75	88.3	161.5
relative RMSE (%)	20.1	21.2	18.7	32.1

BAS: n=24, NIP & IR: n=48

Cloudy weather conditions caused about an 80% reduction in the average daylight, which reduced from approximately 7.9 h in 2018 to 1.5 hours in 2019 as shown in (Figure 3.9). This period coincided with the time in which CH could be estimated from CSM Under cloudy weather conditions, which results in reduced solar radiation, plants tend to elongate more rather than increase their net biomass weight, and several studies assert this assumption (Pierson, Mack, and Black 1990; Song and Jin 2020; T. Zhang, Huang, and Yang 2013). This implies that as the environment changes, there may be a need to modify the model to fit the environment.

### *3.3.5 Temporal changes in time-series estimation.*

By changing the survey frequency from bi-weekly intervals in 2018 to weekly intervals in 2019, our approach could gather a multi-temporal dataset that provided detailed changes in LAI and biomass growth dynamics under field as shown in Figure 3.10. LAI development increased sharply between June 20 and July 10 after which a steadier growth pattern was observed. A similar tendency was observed in biomass increase but the increase was prominent in Nipponbare and IR64 under +N conditions. The weekly observation revealed the detailed growth pattern of the genotypes relative to the growth environment which may not have been revealed by prolonged intervals between monitoring periods. This approach helps in real-time monitoring of crop growth at important phenological stages essential for precision agriculture (Hansen and Schjoerring 2003), in contrast to single-date measurements, which may hinder growth dynamics monitoring in real-time (Kawamura et al. 2020). In addition, the hassle of in situ destructive growth evaluation was eliminated (Jay et al. 2015). Biomass production in rice is very important for yield formation, and it was pointed out that its importance changes dynamically depending on the growth stage (Takai et al. 2006). Therefore, the ability to monitor growth on a fine temporal scale can be used to predict yield with high accuracy.

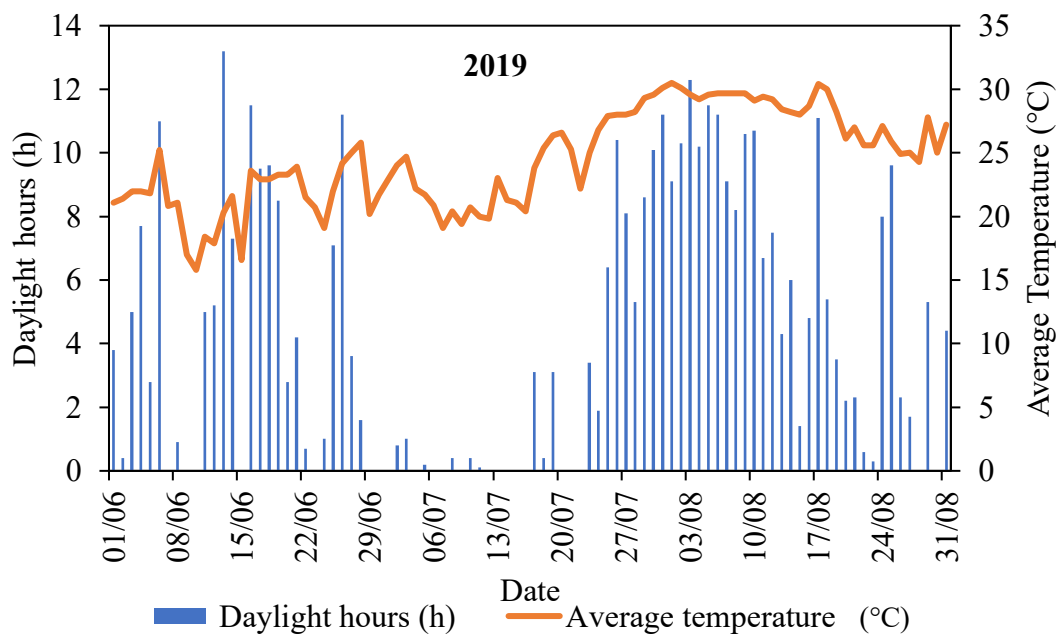
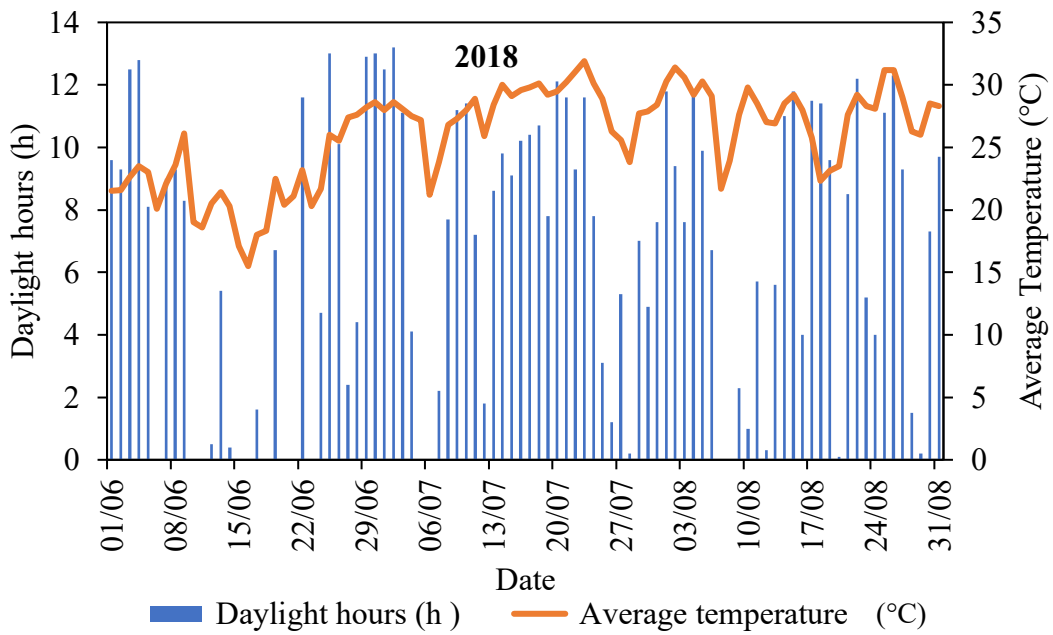


**Figure 3.9.** Fourteen weeks of AMeDAS Fuchu weather data during the growing season.

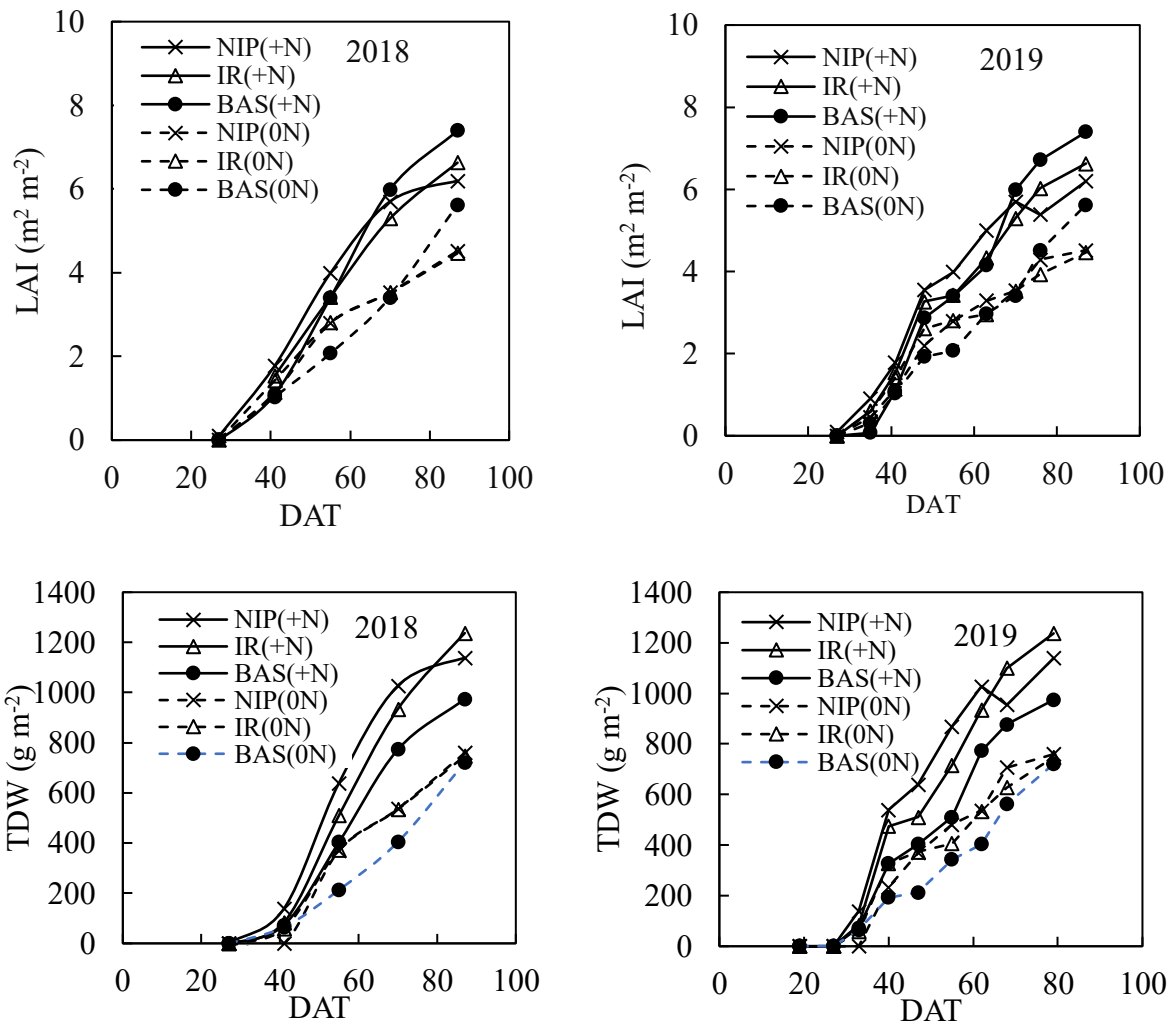


**Figure 3.10.** Observed temporal changes of estimated (a) LAI and (b) TDW in (Rep. 2) on various days after transplanting (DAT) in 2018 and 2019.

### 3.3.6 DSM spatial monitoring.

For farmers and researchers alike, information on within-field variations and discrepancies in crop status and edaphic factors is beneficial for making management decisions (Maes and Steppe 2019). In this regard, UAV-based DSM offers clear advantages over conventional manual practices in addition to providing reliable estimates of CHs from mean CSM, as seen in this study. Such time-saving and real-time monitoring of spatial variations within the field (Figures 3.11 and 3.12) can also provide cost-effective and site-specific information for important farm operations, such as fertilizer

and pesticide application (Portz, Molin, and Jasper 2012; Dammer and Wartenberg 2007; Shanahan et al. 2008). The spatial estimation showed a uniform growth pattern in LAI and TDW at the initial growth stages; however, detailed genotypic differences were evident at the advanced growth stages, with fertilized areas showing more prominent growth. Based on these results, it can be inferred that a good correlation between the variables translates into areas with high CH (greener areas), indicating high LAI and aboveground biomass. Thus, this technology can be used to evaluate rice growth spatially. In addition, the technology can be applied not only to precision agriculture technologies, such as site-specific fertilization but also for accurate prediction of growth dynamics in the entire field. The key limitations of the models developed in this study were the effects of weather and genotypic differences between varieties. When the model was applied in 2019, a tendency of overestimation due to reduced sunshine hours during the initial stages of the growing season was observed. As the bad weather persisted, the relationship between PL, LAI, and TDW was affected. Therefore, further investigation is required to understand the variations in the measured and estimated values and to improve the robustness of the model because the genotypes, environmental conditions, and parameters investigated in this study were limited.

### 3.4. Conclusions.

Rice genotypes with wide genotypic variations were cultivated under N fertilization conditions, and CSM developed from UAV RGB images by linear regression models was used to estimate growth and other leaf area development. The estimation accuracy of the model was found to be high, with relative RMSEs of 20.8% and 28.7% for LAI and TDW, respectively. Depending on the growth stage and genotypes, there were large variations in LAI (from 1.03 to 7.93 m<sup>2</sup> m<sup>-2</sup>) and TDW (from 64.7 to 1237.2 g m<sup>-2</sup>). The results showed a linear relation between PL and LAI or TDW, so a model was developed from this relationship to estimate LAI or TDW. The estimation accuracy of the model was high for TDW and LAI with large variations among the genotypes. This implies that developing genotype-specific estimation models are necessary. Also, by altering the survey frequency, it was determined that it is possible to perform time-series biomass estimation using this model. Furthermore, since DSM was used in this study, the influence of weather was relatively small and stable, and easy weekly observations could be made. However, the model developed was limited by the differences in varieties and the growing environment. The results outlined in this study require further investigation in different environmental conditions over multiple years to ascertain its transferability, because several other factors that influence model development and application were not investigated in this study. Furthermore, the spatial resolution of the data can also influence the results obtained, especially in the earlier stages of the growth cycle. By comparing the results under different environmental conditions or planting seasons, the effect of weather variables such as sunshine, temperature, and cloud cover on the application of the model could be explained.

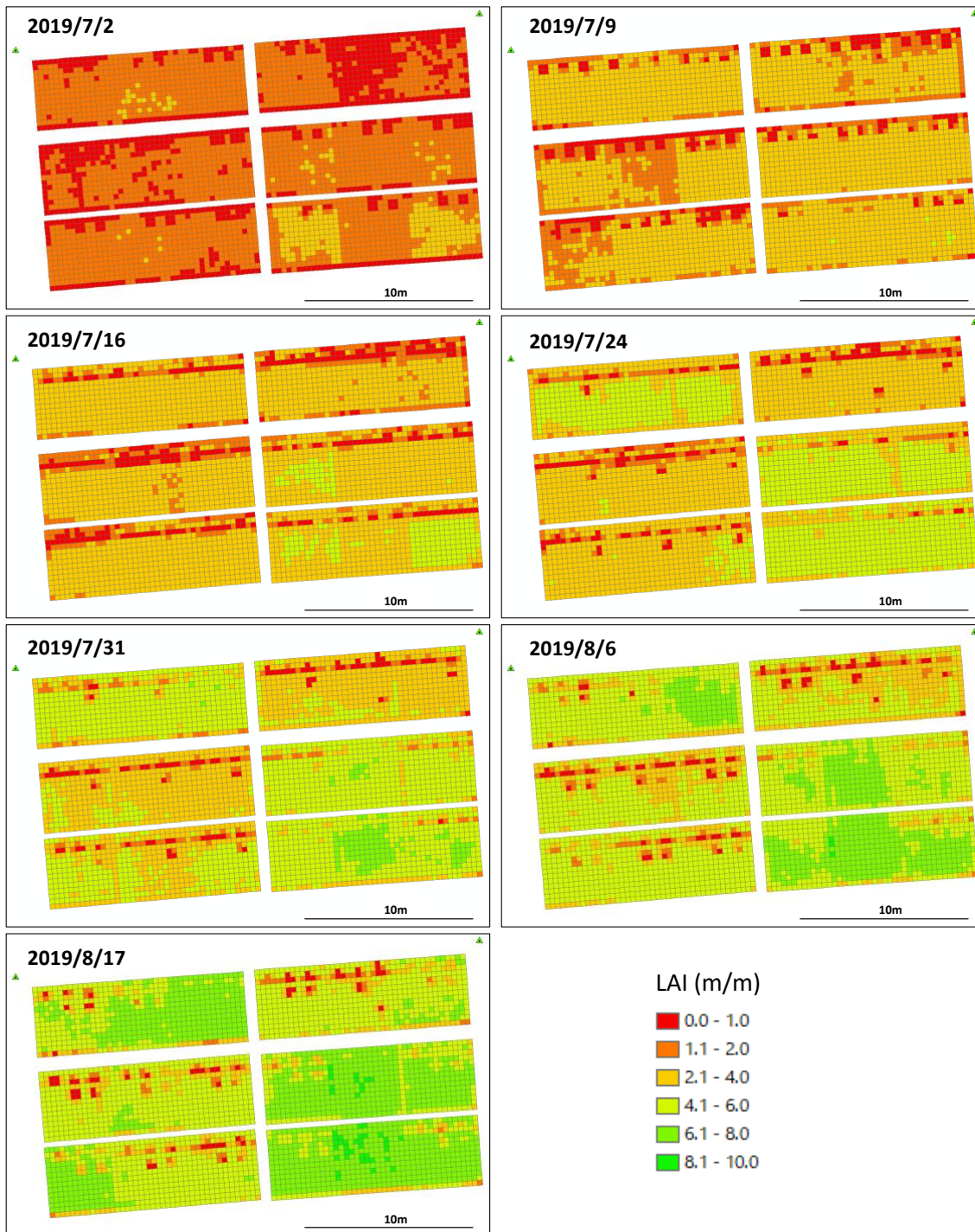


**Figure 3.11.** Examples of Spatial estimation of LAI in 2019 using the DSM model (greener areas represent higher LAI).

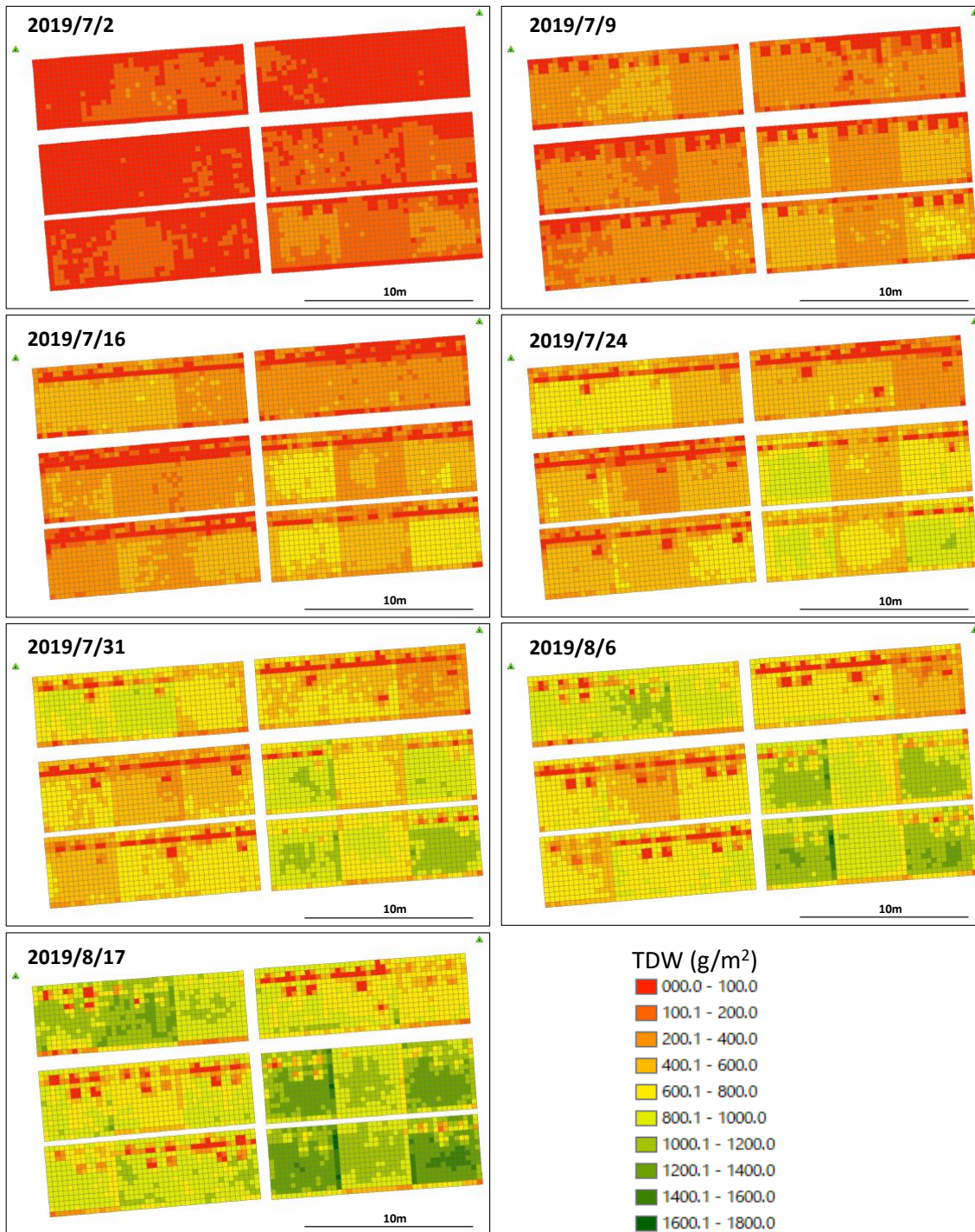


**Figure 3.12.** Example of spatial estimation of TDW in 2019 using the DSM model (greener areas represent higher biomass growth).

## CHAPTER 4

### **Assessing Lodging severity in different rice genotypes using a digital surface model.**

#### 4.1. Introduction.

Rice, wheat, and maize are the three most important food crops in the world, with rice ranking third in terms of production (Su et al. 2022). The importance of rice production for food security cannot be overemphasized because it is a staple meal for more than half of the world's population, providing more than 20% of their daily calories (Muthayya et al. 2014; Dhillon et al. 2018). Lodging is a frequent physiologic problem that impairs crops' output and quality throughout the middle stages of their growth cycle. It is a major yield-limiting factor for staple cereal crops such as wheat, rice, barley, maize and oats (Islam et al. 2007; W. Wu and Ma 2004). Aside from the physical destruction, it also reduces grain quality (Norberg, Mason, and Lowry 1988; Setter, Laureles, and Mazaredo 1997). Rice lodging as explained by Pinthus (1974) is defined as the displacement of crop stems from their upright posture (stem lodging) or the collapse of the root-soil anchoring system (root lodging). Strong winds or heavy rain/hail cause it, and inappropriate crop management methods like excessive N treatments or high planting density worsen it (Quang et al.2004).

Rice lodging is influenced by rice types, cultivation methods, field management, disease, and insect pests. During the growing phase, rice types with extremely long internodes, elongated plants, bent leaves, and rice with huge panicles are prone to lodging (Plaza-Wuthrich et al. 2016). Obtaining information such as the location and size of rice lodging sites quickly and accurately is critical for lodging disaster assessment, yield loss assessment, agricultural disaster insurance, and post-disaster management. Manual lodging assessment methods are not only time-consuming, labour-intensive, and inefficient, but it is also space constrained. Also, especially when thousands of plots are being screened in a breeding program, making repeatable surveys difficult (Duan et al. 2017; P. Hu et al. 2018; Sun et al. 2019; Shu et al. 2020). In some cases, secondary damages are induced during the in-

situ assessment (Han et al. 2018). Crop lodging assessment has become common in recent years thanks to advances in remote sensing technologies. However, satellite remote sensing cannot identify lodging information correctly in real-time due to geographical and temporal resolution limitations. Satellite remote sensing is challenging to satisfy the demands for rice lodging monitoring at a precise time and location. Furthermore, weather conditions have a significant impact on the satellite imaging (Weiss, Jacob, and Duveiller 2020).

The UAV platform offers minimal risk, and excellent flexibility while flying even in cloudy conditions and is ideal for crop lodging monitoring and analysis (Ampatzidis et al. 2019). The plant height differences between the lodging area and the non-lodging area of rice are significantly larger ( $\sim >20$  cm) in some cases (Yang et al. 2017). Given this, much attention has been given to height data derived from UAV image-generated DSMs because studies have proven that height data possess a beneficial contribution to classification and have the potential to improve classification accuracy in phenotyping rice varieties (Kuria et al. 2014; Tamminga et al. 2015). For instance, Murakami et al. (2012), employed crop height obtained from a computerized canopy model as a measure of lodging stage in buckwheat, with lower values indicating severe lodging. Chapman et al. (2014) also used a digital elevation model (DEM) to compute the average height of lodged and non-lodged crops and used a height threshold (50 cm, based on pixel height variation) to detect lodged regions. Such significant delineation of 10–70% of the lodged region using these approaches appears to validate the usefulness of employing height information for lodging assessment. Conversely, a major drawback of using spectral indices for lodging assessment is that the changes in variability may be caused by composite factors.

To date, recognition of lodging in rice fields still has low accuracy and lacks real-time performance. There is a dearth of statistics related to lodging on a local, regional, or global scale unlike crop yield (Chauhan et al. 2019). Heterogenous distribution of lodging affects the accuracy of

estimation, especially in rice fields (Patel et al. 2006; Schaepman et al. 2009). Therefore, it is important to provide quantitative estimates of the lodging stage which is vital for mid-season interventions. This study developed a novel approach to identify and assess lodging in rice genotypes based on DSM\_CH variations in the rice field to establish a UAV imagery-based crop lodging estimation method. The approach of this study is simple and provides theoretical and practical support for accurate rice lodging monitoring.

## 4.2. Materials and methods.

### 4.2.1. Experimental site.

A field experiment was conducted at a paddy field in the Field Museum Honmachi, Tokyo University of Agriculture and Technology, Honmachi, Fuchu-shi, Tokyo (35.41 N and 139.29 E) in 2021. The experimental field measured 45 m × 15 m, arranged in a randomized complete design in two replicates (Figure 4.1).

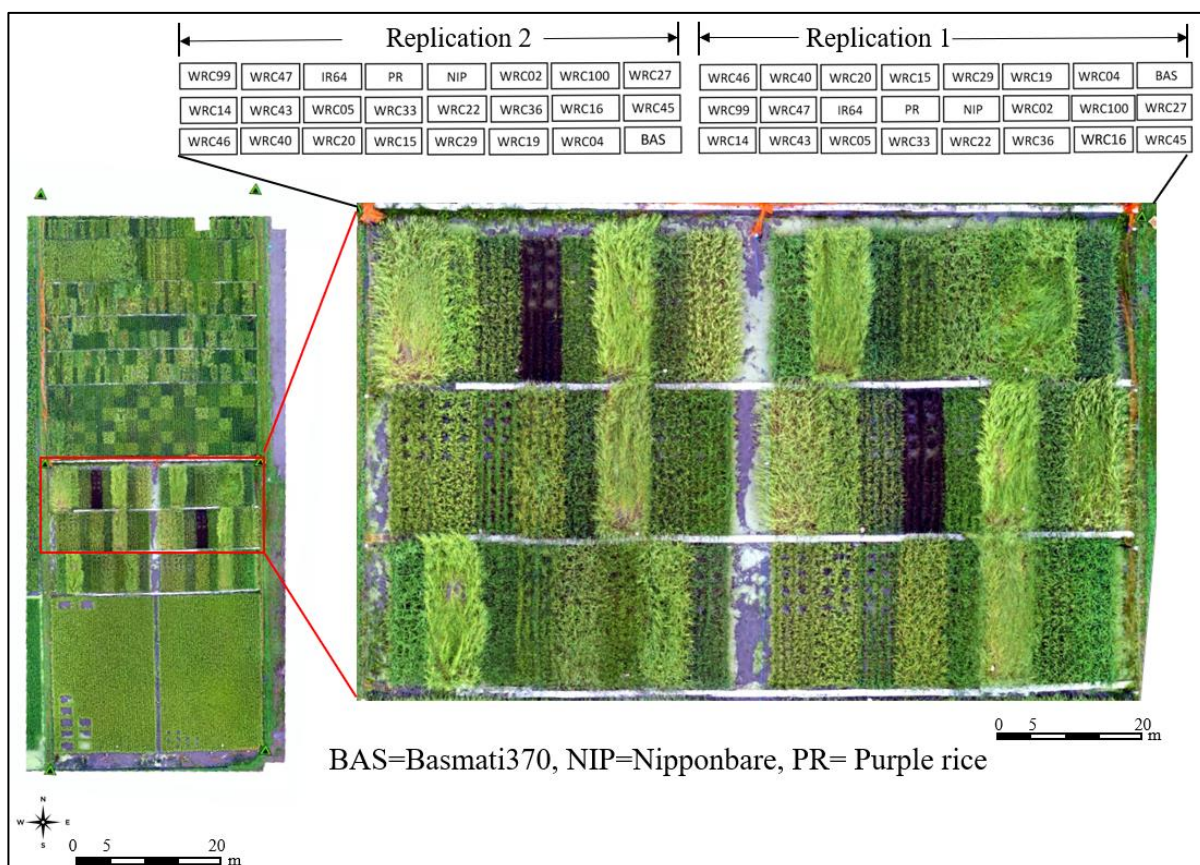


**Figure 4.1.** Experimental field and layout (2021 growing season).

#### 4.2.2. Rice genotypes and fertilizer application.

In this research, to verify the differences between as many genotypes as possible, 24 rice genotypes were selected. The genotypes were obtained from the Agricultural Bioresource Gene Bank of the National Institute of Agriculture and Innovation, Japan collection that collects genetically diverse varieties. Detailed information on the genotypes is presented in Table 4.1. The genotypes were cultivated under the same N fertilization whereby 2 g m<sup>-2</sup> was applied as a basal on May 23. In addition, 10 g m<sup>-2</sup> of P<sub>2</sub>O<sub>5</sub> and K<sub>2</sub>O were applied as a basal on May 15. Transplanting was carried out on May 20 with a planting density of 22.2 hills m<sup>-2</sup> (30 cm × 15 cm) with one plant per hill.

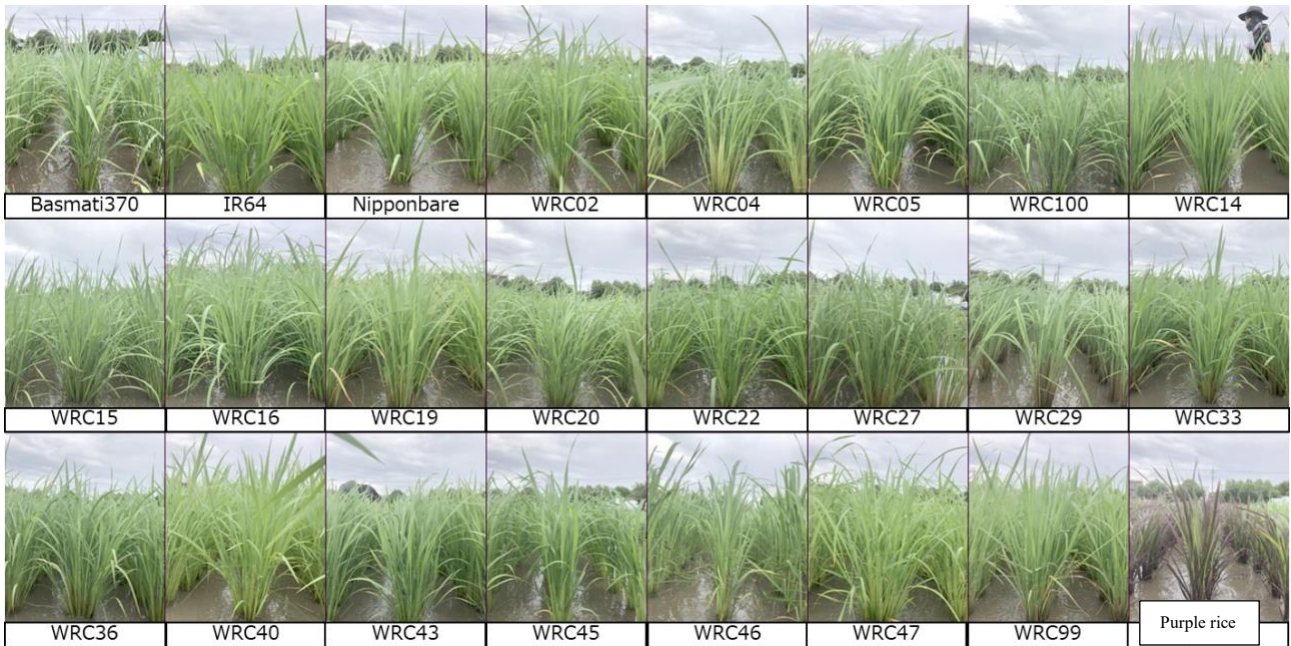


**Figure 4.2.** Sample images of the rice genotypes with different canopy structures.

#### 4.2.3. Ground truth data collection.

The PL in this study was measured as the vertical distance from the ground level to the apex of the plant using a measuring ruler on a per-plot basis. Although using a ruler is debatable and may also introduce inaccuracy issues and tediousness, it is still considered a standard and still acceptable in field trials (F. Holman et al. 2016; Willkomm, Bolten, and Bareth 2016a; Murakami, Yui, and Amaha 2012a). The above survey was conducted every week from the date of transplanting to the date of heading. Four plants from each plot were selected for PL and their tiller angle of inclination were measured.

**Table 4.1.** Information on the different rice genotypes from different locations

Variety name	ID	Origin	Variety type
Nipponbare	WRC 01	Japan	Japonica
Kasalath	WRC 02	India	Indica
Jena 035	WRC 04	Nepal	Indica
Naba	WRC 05	India	Indica
IR 58	WRC 14	Philippines	Indica
CO 13	WRC 15	India	Indica
Vary Futsi	WRC 16	Madagascar	Indica
Deng Pao Zhai	WRC 19	China	Indica
Tadukan	WRC 20	Philippines	Indica
Calotoc	WRC 22	Philippines	-
Nepal 8	WRC 27	Nepal	Indica
Kalo Dhan	WRC 29	Nepal	Indica
Surjamukhi	WRC 33	India	Indica
Ratul	WRC 36	India	Indica
Nepal 555	WRC 40	India	Indica
Dianyu 1	WRC 43	China	Japonica
Ma Sho	WRC 45	Myanmar	Japonica (tropical)
Khao Nok	WRC 46	Laos	Japonica (tropical)
Jaguary	WRC 47	Brazil	Japonica (tropical)
Hong Cheuh Zai	WRC 99	China	Indica
Vandaran	WRC100	Sri Lanka	Indica
IR 64		Philippines	Indica
Basmati 370		India	Indica
Purple rice		Japan	Japonica

WRC; world rice core collection.

For each plot, the angle of inclination was measured directly using a slant gauge application on a smartphone. The angle of inclination from the vertical was then derived for each subplot based on the measurements shown in Figure 4.3b.

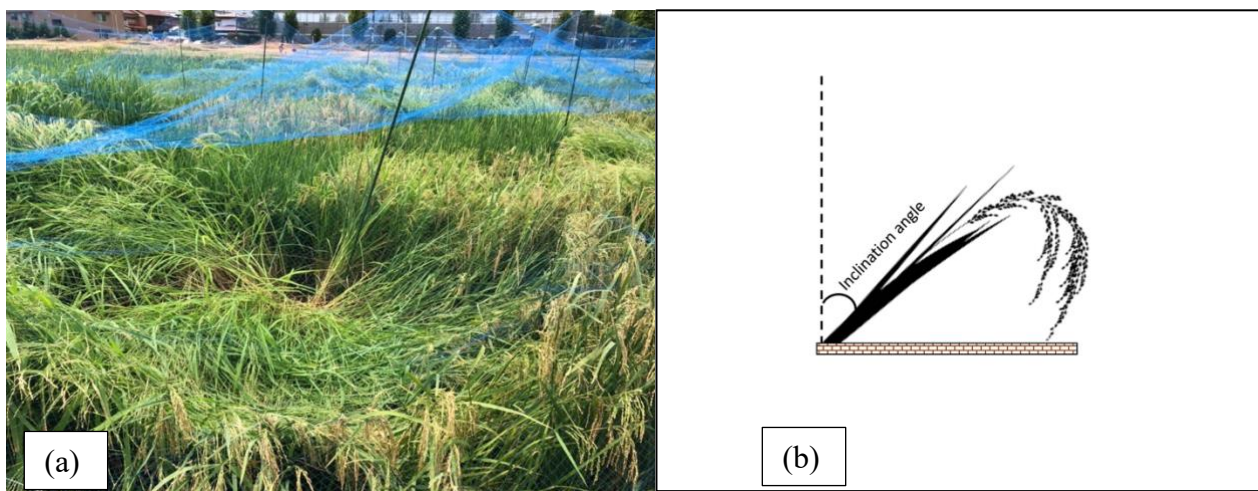


**Figure 4.3.** Example of a lodged rice plot (a), and (b) change in the tiller angle of inclination after lodging.

#### 4.2.4. Image collection from the UAV platform.

The rice field trial was frequently observed by a UAV platform equipped with an RGB camera with four reference points set up at the corners of the experimental field using a flight planning application (Atlas Flight, Micasense; Pix4D capture, Pix4D). The forward and lateral overlaps were set at 80% at an altitude of 20 m. Routine flight surveys were conducted from transplanting to physiological maturity stage with the flight frequency targeted every week and adjusted based on the prevailing weather conditions. A minimum cruise speed of 3 m/s was desired. It must be noted that the lodging method proposed in this experiment depended on the canopy's 3D structural information (height) and not necessarily on the rice spectral features' response to the lodging analysed.

#### 4.2.5. Generation of orthomosaic images

Closed traverse surveying was used to obtain the coordinates of the reference points installed at the four corners of the field, and these four points were used as ground control points using the Japan Geodetic System 2011 Plane Cartesian Coordinate System 9 was used as a map projection method (GCPs). Each ortho-mosaic image was created using 5-band multispectral images captured by the UAV. Camera calibration (correction of the lens focal length, principal point position, and radial and tangential distortion) was performed with the tie points, which were automatically detected from the overlapping area between aerial images. After that, the detected tie points and four installed GCPs were used to estimate external orientation parameters (camera position and tilting angle), and as well as the creation of the 3D model GCPs were processed to within one-pixel accuracy. Each of the 3D models was used to generate 2D orthomosaic images of 5-band multispectral cameras with a resolution of 9 mm.

#### 4.2.6. CH extraction from DSM

The 3D point cloud contains estimated height information of the canopy. As described in the previous chapter, CSM was derived by subtracting the underlying ground model ( $DSM_{1st}$ ) from the DSM of the different phenological growth stages ( $DSM_n$ ), and absolute heights could be extracted. The height difference between the two enables the assessment of the CH. The Zonal Statistics as Table tool in ArcGIS was used to calculate statistical information about each pixel area as well as average plot heights. Thus, absolute PL and growth dynamics were calculated between acquisition dates (Willkomm, Bolten, and Bareth 2016; Norman Wilke et al. 2019b; N. Wilke et al. 2019a).

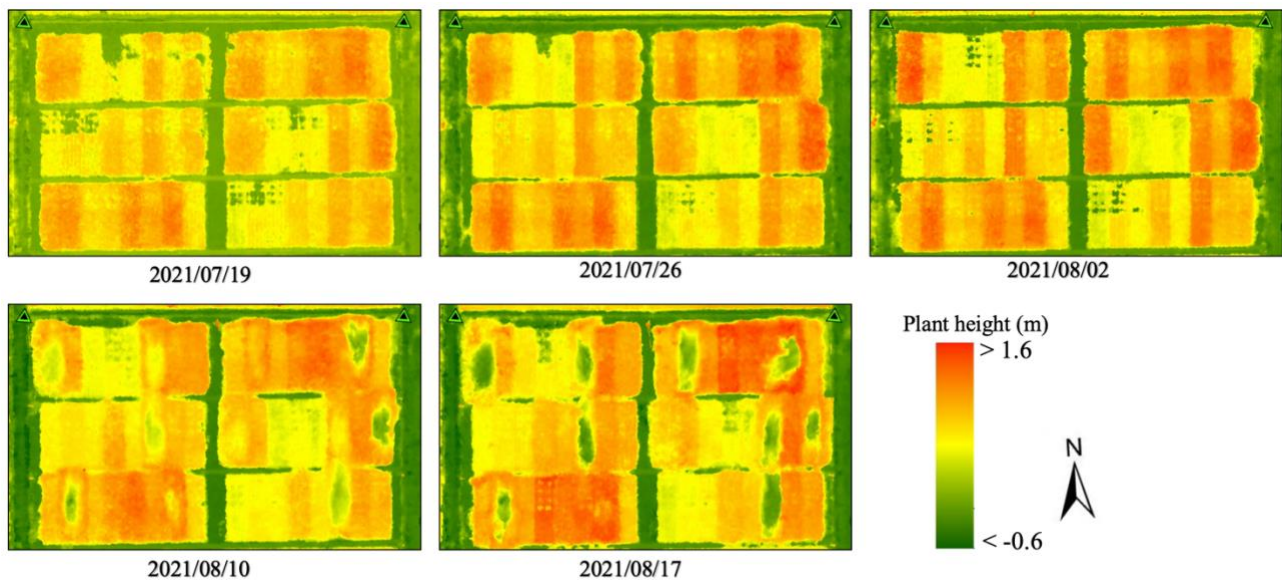


**Figure 4.4.** Examples of CSM of all acquisition dates until lodging.

#### 4.2.7. Lodging assessment and evaluation method

When compared to non-lodged areas, lodging severity is thought to be linked to a canopy structural anomaly (Chu et al. 2017). In this experiment, two main canopy architectures were set and compared for CH evaluation: (1) the target area, the lodged area within the plot. The height of the lodged area was considered as a constant variable on either a canopy scale which consisted of 3\*6 plants or one central line of 6 plants, and (2) the border plants used as a control variable. The border plant was used as a control variable because generally border plants were not lodged easily as seen in Figure 4.4. A quick observation revealed the lodged rice has a relatively lower height than the healthy rice in Figure 4.4. By obtaining PL or CH, it will be possible to estimate or assess the degree of lodging on the backdrop that lodging causes a significant reduction in height.

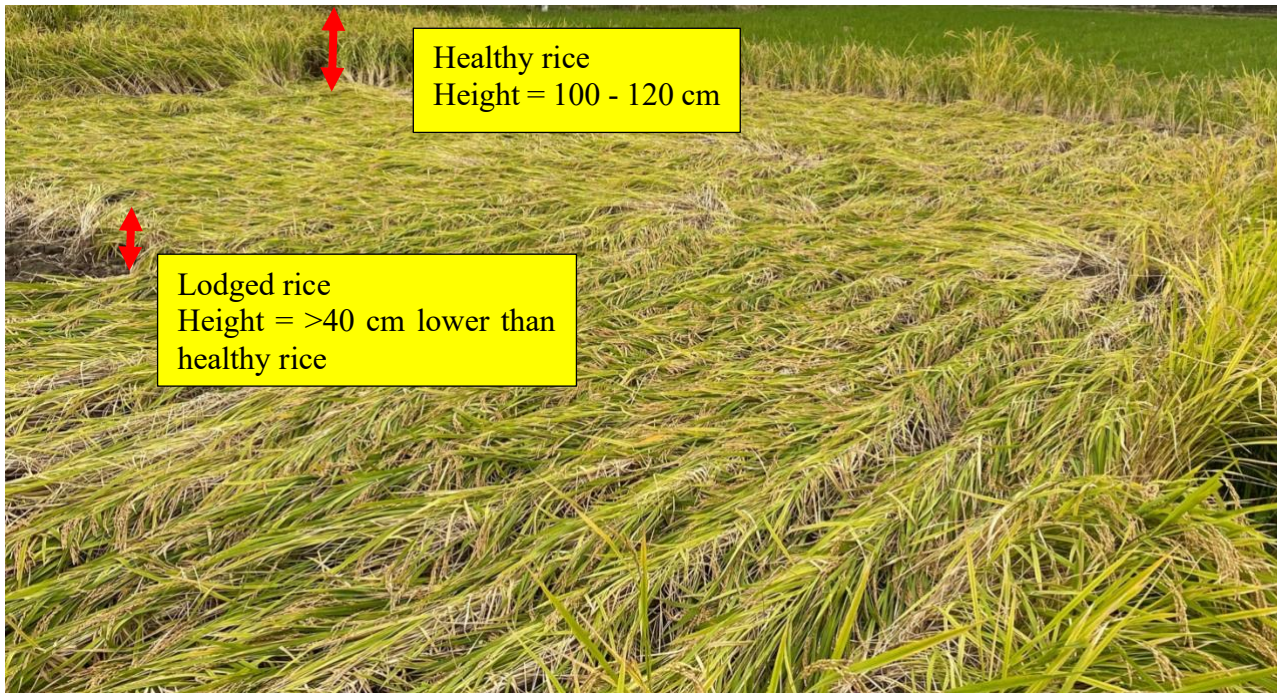
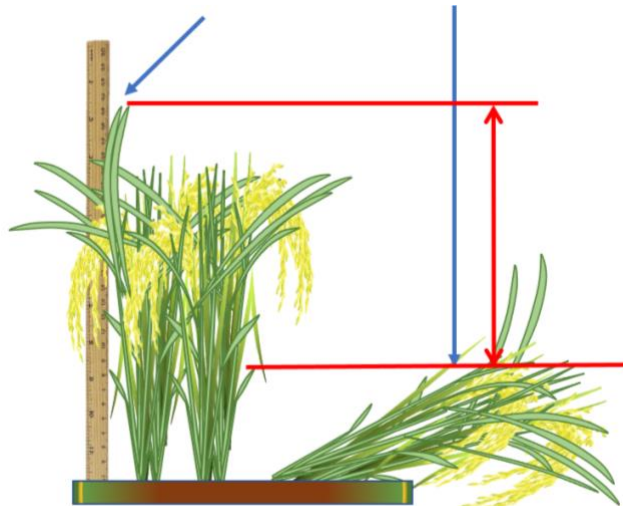


Figure 4.4. A close look at lodged and border non-lodged rice.

By using the orthomosaic CSM height calculation method outlined in the previous section, height metrics differences such as  $\Delta PL$ ,  $\Delta DSM\_CH_{max}$ ,  $\Delta DSM\_CH_{border}$  and  $DSM\_CH_{cv}$  associated with the CH of the lodged and non-lodged plots were calculated and compared with their tiller inclination angles. Among these height metrics,  $\Delta PL$  represents the difference in ground measured PL and CH of the target area at heading by using the maximum plant length as depicted in figure 4.5.



**Figure 4.5.** Modelling with manually measured plant length ( $\Delta PL$ ).

$\Delta DSM\_CH_{max}$  difference between CH at evaluation time and the maximum CH (at around heading stage) of the target area by comparing successive CSMs as shown in figure 4.6.

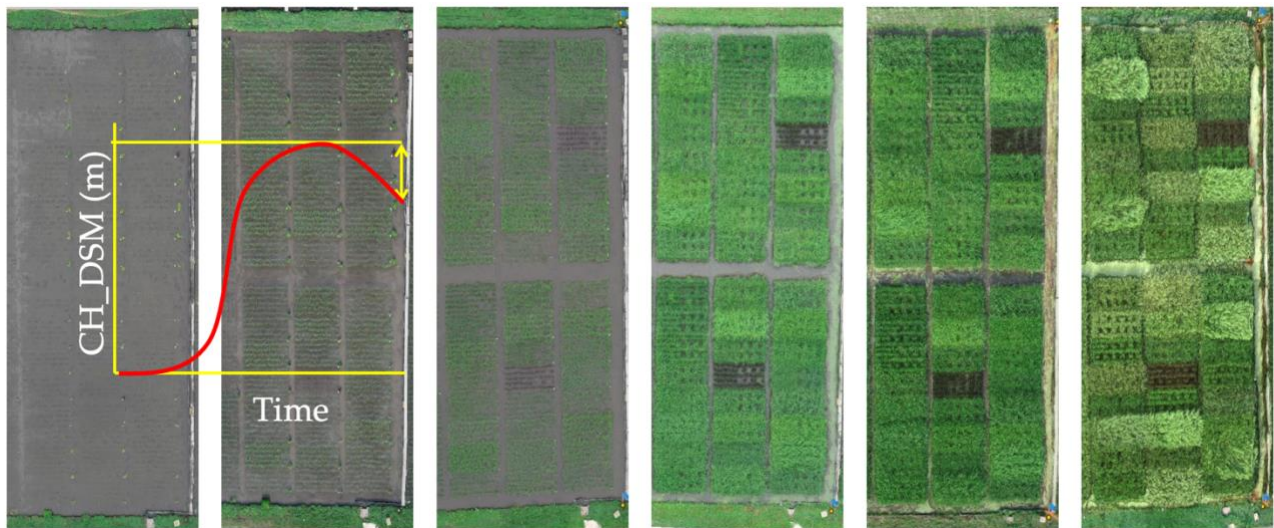


**Figure 4.6.** Modelling with maximum  $CH\_DSM$  ( $\Delta CH_{max}$ ).

$\Delta CH_{border}$  represents the difference CH of the target area and the border plants of each polygon as seen in figure 4.7.

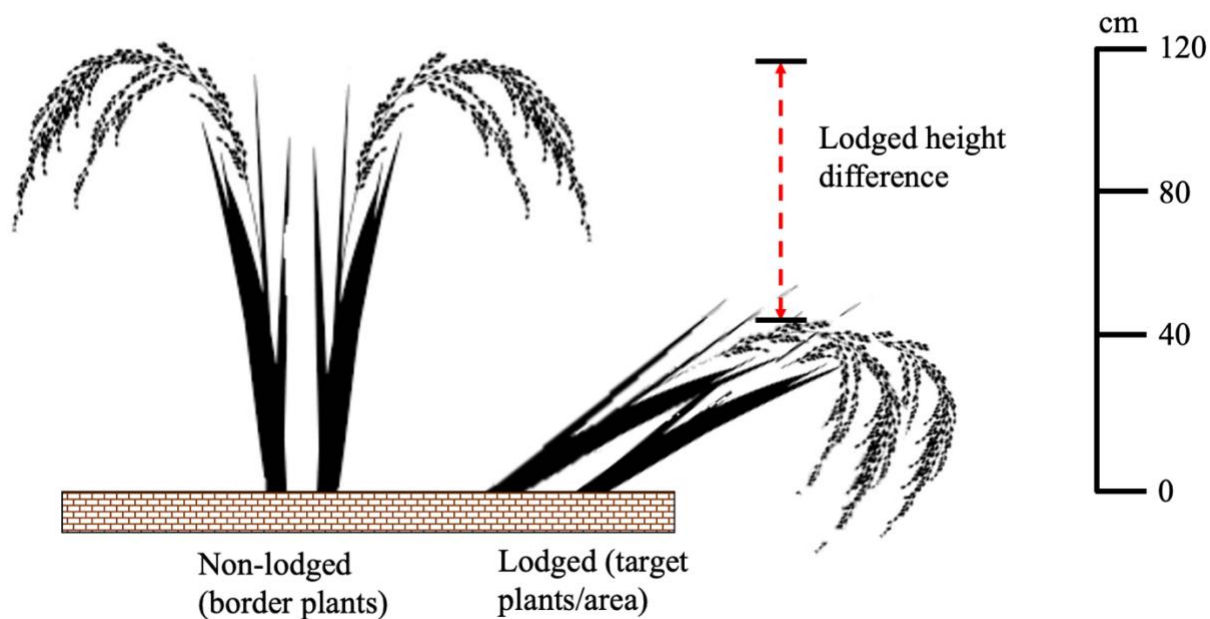


**Figure 4.7.** A schematic diagram of plant height comparison of lodged and non-lodged rice.

CHcv has been widely used for evaluating CH variation and is expressed as the ratio of CHstd to CHmean. In this study, DSM\_CHcv is the coefficient of variation of CH among all plant hills of the target area as seen in figure 4.8.

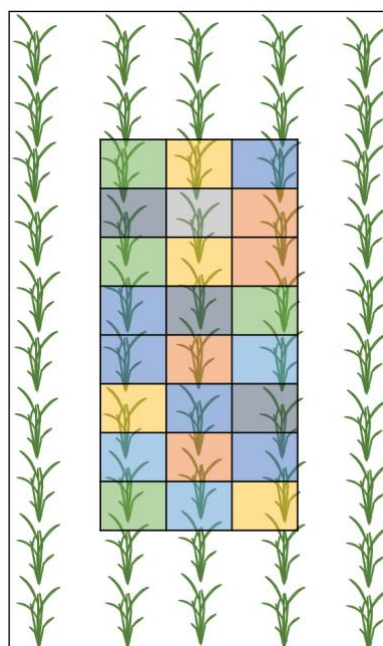


**Figure 4.8.** Modelling with coefficient variations of CH\_DSM (CHcv).

It must be noted that in this experiment, the angle of inclination of the healthy and non-lodged hills was assumed as 90° perpendicular to the ground. The height metrics are mathematically expressed as follows.

$$\Delta PL = PL_{heading} - CH_{target} \quad (4.1)$$

$$\Delta DSM\_CH_{max} = CH_{\sim heading} - CH_{target} \quad (4.2)$$

$$\Delta DSM\_CH_{border} = CH_{bd} - CH_{target} \quad (4.3)$$

$$DSM\_CH_{cv} = \frac{CH_{std}}{CH_{mean}} \quad (4.4)$$

Where *cv* represents the coefficient of variation, *std* represents the standard deviation, “ $\sim$ ” represents data taken around the heading stage, and *bd* represents border plants.

### 4.3. Results and discussions.

#### 4.3.1. PL validation.

In-field measurements of PL were taken for each acquisition date to verify the calculated CHs of all CSMs. Four sample hills were chosen per plot to use a ruler to measure PL. The results were compared to the mean CSM raster values of the sample points. Figure 4.9 presents the validation results. The calculated CSM height correlated very well with the ground measured PL ( $R^2 = 0.73$ , RMSE = 0.002) but the accuracy was lower compared to the results obtained in the previous chapter. The reason for the underestimation is because figure 4.9 represents data taken at the ripening when there is a drastic structural change in the canopy structure as plants begin to bend due to the upper canopy weight added on by grain filling. However, the DSM could obtain a relatively accurate CH as seen in the previous experiments. The linear regression model's y-intercept is around + 0.134 cm,

indicating that CH values from DSM are generally lower than in-field measurements. This implies an underestimation of CH by DSM. Another possible reason as reported by Takeda et al. (2010), the DSM may record a lower foliage layer (most visible layer) than the plant tip, especially in clustered canopies.

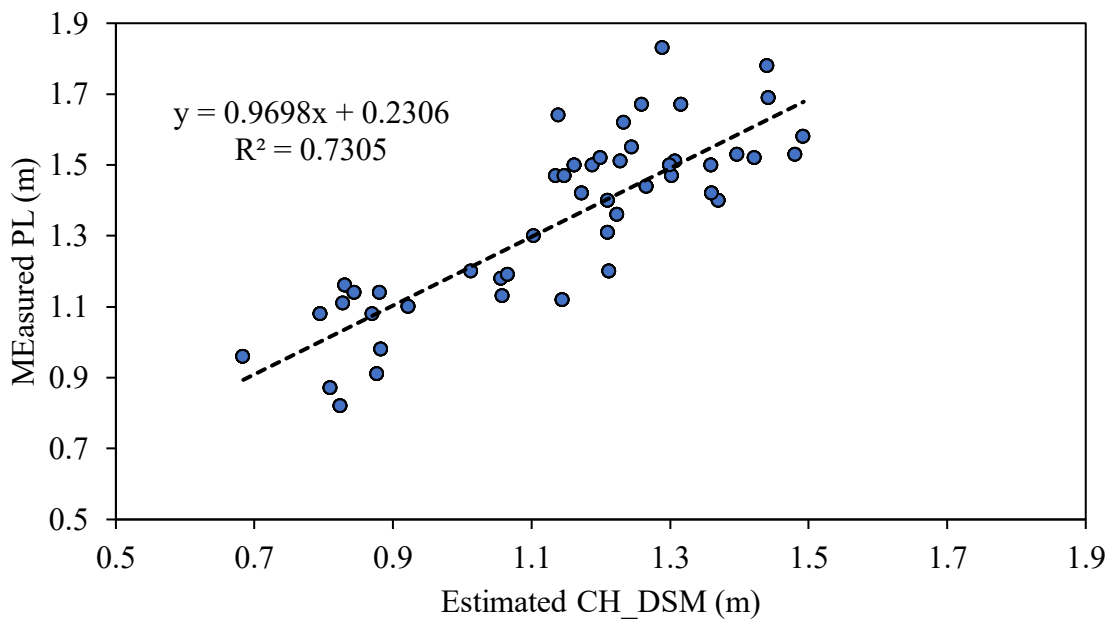


**Figure 4.9.** Regression of DSM CH compared with in-field measured PL.

#### 4.3.2. Lodging and non-lodging comparisons of the height metrics

Lodging was severely affected by canopy structure variations, and the height evaluation over lodged and non-lodged varieties over the growing season is presented in Figure 4.4. To identify the ideal metric for quantitative assessment of lodging four different height metrics ( $\Delta$ DSM\_CHborder,  $\Delta$ PL,  $\Delta$ DSM\_CHmax, and DSM\_CHcv) were compared to the reference measurement of the lodged

height of the target area. First, the difference in height between the lodged target area and the non-lodged border plants known as the  $\Delta\text{DSM\_CHborder}$  metric was used to assess lodging as explained in Figure 4.7. The UAV lodging ratio derived by  $\Delta\text{DSM\_CHborder}$  achieved the lowest accuracy ( $R^2 = 0.406$ ) and a low amount of scattering. Although, this approach looks simple as a set of image data at any point in time is sufficient for assessing the height difference between the border plant and the target area, there was however some difficulty in estimating the height of the border plants due to border effects of adjacent plants as seen Figure 4.11. Additionally, background noise from bare soil in the border regions also affects the estimation of the height of the non-lodged border plants. It also became clear that the lodging ratio of non-lodged varieties (0 inclination angle) was too large for most of the genotypes resulting in a possible overestimation of lodging. Alternatively, assessing the lodging degree at an earlier growth stage whereby cross border effect of the adjacent plot may be minimal may improve the estimation by this metric (Chu et al. 2017), however, this is outside the extent of discussion in this study.

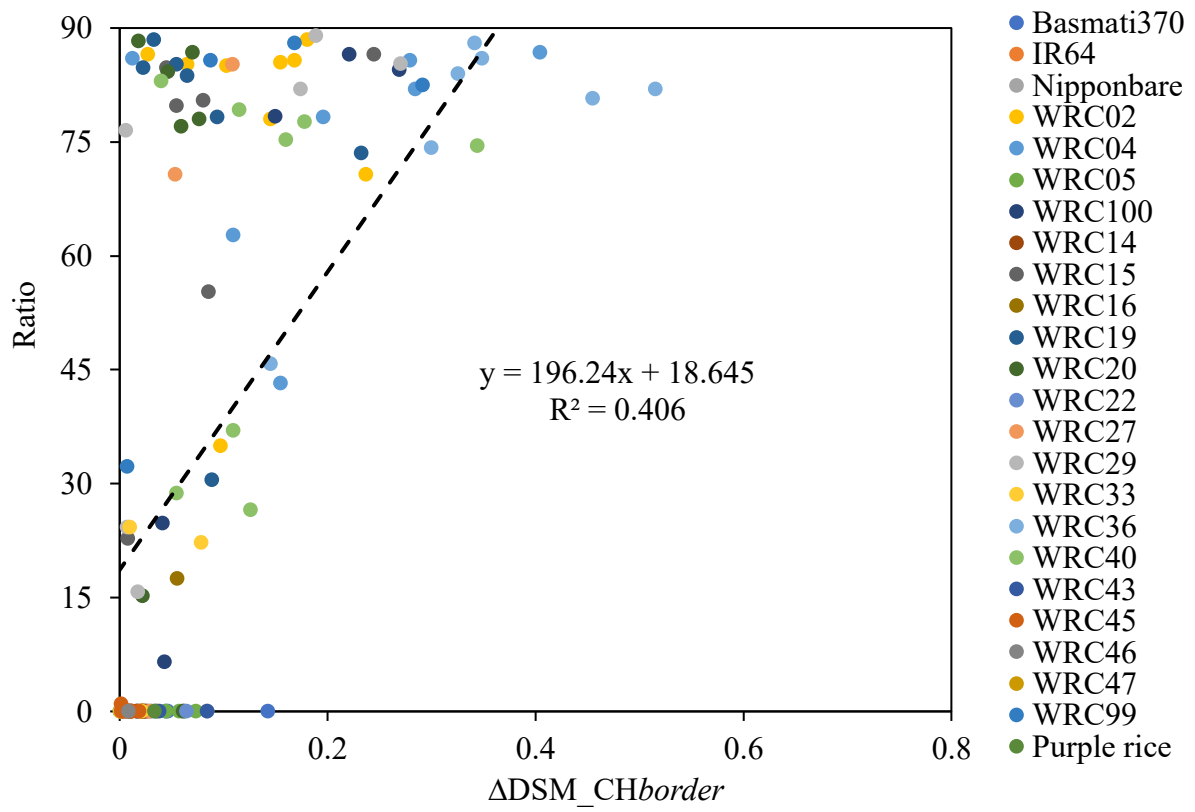


**Figure 4.10.** Lodging assessment among rice genotypes using  $\Delta\text{DSM\_CHborder}$



**Figure 4.11** An example of a CSM image indicating cross-border interference is indicated in red circles.

Furthermore, The UAV lodging ratio derived from the change in measured maximum PL at heading and the target area had a high correlation ( $R^2 = 0.629$ ) (Figure 4.12). However, manually collecting lodging data requires considerable effort, time and energy and the relationship varies depending on the canopy structure. Compared to CH of the UAV-based derived from the DSM which provides information on the spatial height distribution of a continuous canopy and contains height information of numerous single plants (Aasen et al. 2015), the PL only represent height information of single plants covering a very limited area measured with a ruler in the field at a specific location which is not feasible for large scale assessment of lodging.

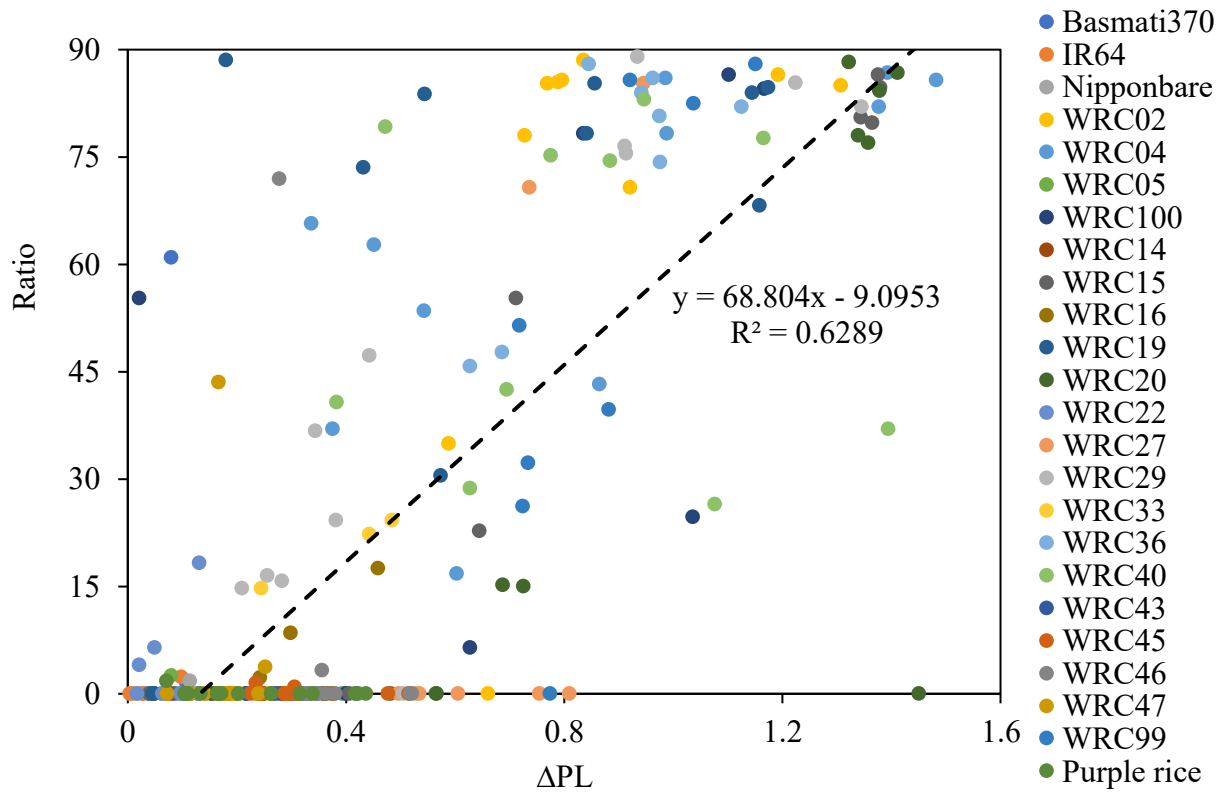


**Figure 4.12.** Lodging assessment among rice genotypes using  $\Delta PL$ .

To further avoid setting threshold and subjective decisions, the maximum CH ( $\Delta DSM\_CH_{max}$ ) was calculated up to around the heading stage and compared to the CH of the target area for all the genotypes which required multiple surveys or periodic shooting to develop multiple DSMs.  $\Delta DSM\_CH_{max}$  had relatively high lodging assessment estimation accuracy ( $R^2 = 583$ ) as shown in Figure 4.13. However, as already established, the canopy structure limits the method, especially after the ripening stage. In cases where large variation in CH exists, lower-grown canopy areas that were not necessarily lodged may be partly defined as lodged resulting in an overestimation (Wilke et al. 2019). For this reason, Wilke et al. (2019) propose using differentiated  $\Delta DSM\_CH_{max}$  in areas with large CH variations caused by soil background noise or fertilizer conditions.

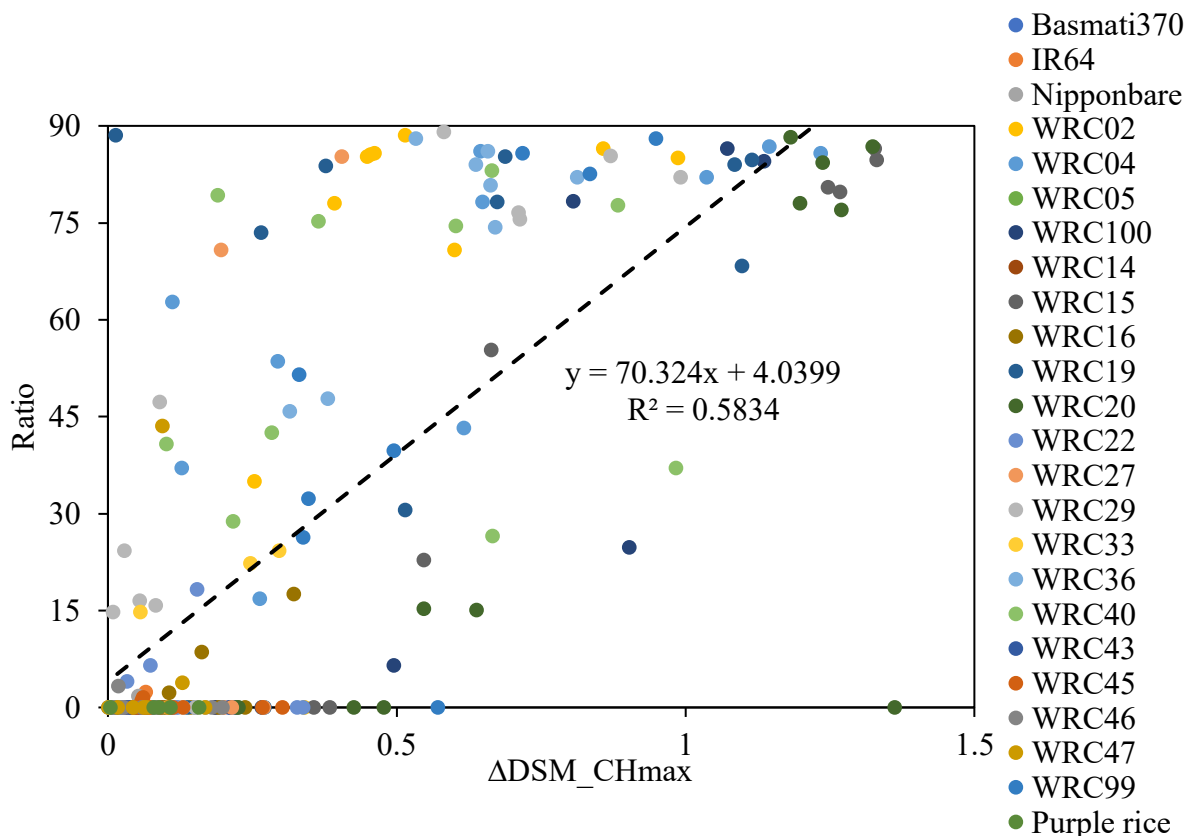


**Figure 4.13.** Lodging assessment among rice genotypes using  $\Delta\text{DSM\_CHmax}$ .

There was a high correlation between the ratio and the  $\text{DSM\_CHcv}$  which increased as the ratio also increased ( $R^2 = 0.58$ ) as seen in Figure 4.14. At a threshold of about 0.05  $\text{CHcv}$ , the corresponding variety was considered as lodged. This is because at  $< 0.05 \text{ CHcv}$ , the plant may not have necessarily lodged but the DSM may consider it lodged due to the reduced height caused by the droopy canopy structure. These results support the effectiveness of  $\text{CHcv}$ , as a point cloud metric for describing height variation, as reported by Li et al. (2014) and Næsset et al. (2013).

Generally speaking, it would be desirable to be able to evaluate the overthrow of plants even at the onset of lodging, but in this case, it appears that only 0 and 1, i.e., whether the plant is overthrown or not, could be evaluated.

One reason for this is that the  $\text{CHcv}$  can be large even when there is no overturning at all (Inclination angle = 0). In addition, the degree of lodging was measured at the base of the stem, but there are cases

where the stem is lodged even if the base is not inclined. Thus, the assessment of lodging in itself is difficult, but these results could estimate lodging quantitatively with some level of accuracy.

Compared to the other forms of metrics that were proposed in this study, the  $CH_{cv}$  was relatively less contaminated by background noise which resulted in either underestimation or overestimation of the proposed metric as seen in figures 4.10, 4.12 and 4.13. The reasons for the overestimates could be that the (1) evaluation was susceptible to ground observational errors. More specifically, some plants that had no inclination angles were mathematically estimated as lodging in the method especially in the  $\Delta CH_{max}$  and  $\Delta PL$  as seen in Figures 4.12 and 4.13. At advanced growth stages, plants may fail to form a closed canopy structure in the point cloud which can lead to a reduced height estimation (Murakami, Yui, and Amaha 2012b; F. H. Holman et al. 2016b; Willkomm, Bolten, and Bareth 2016a) and overestimate lodging. This implies that, for evaluation methods like  $\Delta CH_{border}$  and  $\Delta CH_{max}$  that require multiple surveys, the evaluation accuracy will be affected at advanced growth stages. As observed in the previous chapter the relationship between CH and PL is not 1:1, but relatively higher for PL as was observed in the  $\Delta PL$  metric. (2) it was also observed that leaves from lodged adjacent plots extended into non-lodged plots leading to misinterpretation by DSM of these plots as lodged and thus deceived the lodging assessment method as reported earlier by (Chu et al. 2017). The  $CH_{cv}$  was regarded as the best metric for detection and evaluation of lodging in this study for reasons such as (1) does not require multiple observations of the rice field and that at any point in time, a single observation data is sufficient for lodging evaluation, thereby reducing

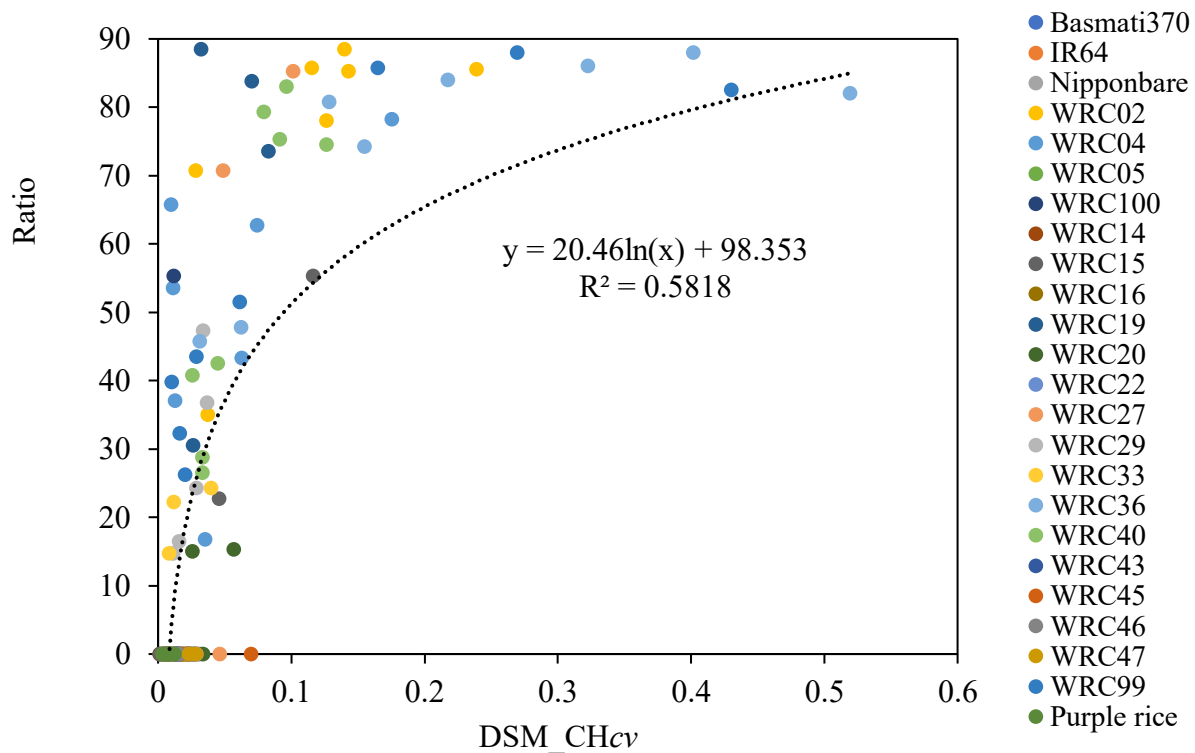


**Figure 4.14.** Comparison of lodging severity among the different rice genotypes using DSM\_CHcv.

timeliness of obtaining crop status information in the field, and (2) it was less affected by the background noise. As explained by the inverse relation with *CHmean* in equation 4.4, *CHmean* in each polygon usually decreases as the lodging rate increases, thus lodged polygons tend to produce higher *CHstd* than non-lodged polygons.

Although the metrics used in this study have the potential as a direct and simple lodging assessment and evaluation technique, especially *CHcv*, the challenge remains with accurate CH estimation of lodged and non-lodged plots by the DSM. For example, the actual CH of non-lodged rice canopies may likely be lower than the threshold set in *CHcv* caused by composite factors, genotype, topography, and management type among others. Such defects can cause misrepresentation and miscalculation in large-scale field trials. Therefore, further examination of large-scale field trials is needed to better evaluate and improve the performance of the method

#### 4.4. Conclusion.

Simplified quantitative metrics and evaluation techniques have been combined to form a UAV-based method for lodging assessment and evaluation in rice. An accuracy assessment proved that the DSM PL estimation is reliable and correlates well with ground-measured data ( $R^2 = 0.63$ ). The lodging assessment and assessment metrics used in this study could evaluate lodging in two distinct canopy structures with high accuracy levels, especially  $CH_{cv}$  which was less affected by background noise and cross border effect. This implies that DSM  $CH_{cv}$  ( $R^2 = 0.58$ ) estimated lodging compared favourably to ground-based assessment in terms of noise reduction and decreased timeliness of field operations.

The proposed central line canopy structure in this study has the potential to assist phenotyping in breeding programs whereby numerous genotypes may be planted in strips. Lodging assessment on such fine-scale in-between strips of breeding lines can assist in rapid assessment. However, more exploration is needed to finetune the proposed metrics to improve the accuracy of the DSM model.

## Chapter 5

### Summary and conclusions.

#### 5.1 Development of plant height estimation model by a digital surface model using UAV images.

The feasibility of estimating PL by using the DSM was evaluated in a paddy field cultivated with rice varieties with different genetic backgrounds under different fertilizer conditions. The results showed large genotypic variations in PL and CH throughout the growth stages with a PL range between 1.80 m, and 0.46 m, for Basmati 370, and Nipponbare, respectively. CH also ranged between 1.10 m and 0.33 for Basmati37 and Nipponbare and IR64 respectively. CH correlated well with PL ( $R^2 = 0.947$ ) which signifies DSM could explain the large variation in PL throughout the growth stages. However, there was a trend of underestimation mainly because, PL refers to the highest point in an area, whereas DSM considers the average of heights in an area. Therefore, since the DSM could measure a relatively smaller range of PL, it will be useful for plant height estimation even at the early growth stage when height variations are relatively smaller.

#### 5.2 Spatio-temporal estimation of biomass growth in rice using canopy surface model from UAV images.

In this contribution, Spatio-temporal monitoring of growth dynamics to estimate TDW increase from CH using DSM was evaluated. The results of this study revealed the following assertions. LAI and TDW could be estimated from DSM with high accuracy. The mean estimations of TDW and LAI were  $442.9 \text{ g m}^{-2}$  and  $3.66 \text{ m}^2 \text{ m}^{-2}$  with  $\text{RMSE} = 141.4 \text{ g m}^{-2}$  and  $0.76 \text{ m}^2 \text{ m}^{-2}$  respectively. Here, significant genotypic differences in the estimation by the model were also observed. Additionally, by adjusting the observation time from biweekly to weekly, the time-series growth variations in TDW and LAI could be revealed. Information on such Spatio-temporal variations helps to understand the growth pattern and make the necessary changes in input management when necessary. DSM can also be used for site-specific management (Schellberg et al. 2008; N. Zhang, Wang, and Wang 2002).

### 5.3. Assessing Lodging severity in different rice genotypes using the DSM.

A simple lodging assessment using DSM PL was developed and evaluated among 24 rice genotypes under the same fertilizer condition. The approach mainly considered two canopy structures between lodged and non-lodged areas on a pilot basis and measured again the ratio. Thus, a simple DSM approach for lodging assessment was evaluated. Four PL estimation lodging assessment methods ( $\Delta PL$ ,  $\Delta CH_{max}$ ,  $\Delta CH_{border}$  and  $\Delta CH_{CV}$ ) were used to assess the canopy structure anomaly. The results showed a high correlation between  $CH_{CV}$  and the ratio ( $R^2 = 0.59$ ). In principle, when the  $CH_{CV}$  value exceeds 0.05, the tiller ratio increased dramatically, which suggests that the  $CH_{CV}$  is a good indicator for lodging assessment.  $\Delta PL$ ,  $\Delta CH_{max}$ , and  $\Delta CH_{mean}$  also proved useful ( $R^2 = 0.39$ , 0.51, and 0.34 respectively) however, noise from border plants and soil resulted in the underestimation or overestimation by these models and are expected to be minimized by the results indicate the usefulness of the evaluation methods, especially  $CH_{CV}$  to assess lodging in rice.

Because of the flexibility of data collecting, unmanned aerial vehicles (UAVs) are becoming more popular in agriculture. Plant breeders, insurance firms, and farmers may get extensive information on plant attributes quickly and at a cheap cost. Breeding experiments are difficult and time-consuming to monitor, necessitating a greater requirement for a speedier selection of better lines. When compared to previous methodologies, lodging quantification based on 3D canopy structure is substantially more independent of environmental circumstances, which greatly boosts the practicability. The proposed DSM approach has a great potential to assist in the rapid assessment of lodging. The model can also be applied in many developing regions, especially in Africa where the advancement of UAV remote sensing technology is still basic or lacking in some cases. However, the challenge remains with the model improvement to increase the estimation accuracy which needs redress.

## References

- Aasen, Helge, Andreas Burkart, Andreas Bolten, and Georg Bareth. 2015. "Generating 3D Hyperspectral Information with Lightweight UAV Snapshot Cameras for Vegetation Monitoring: From Camera Calibration to Quality Assurance." *ISPRS Journal of Photogrammetry and Remote Sensing* 108 (October): 245–59.
- Agrios, George. 2004. "Plant Pathology: Fifth Edition." *Plant Pathology: Fifth Edition* 9780080473789 (December): 1–922. <https://doi.org/10.1016/C2009-0-02037-6>.
- Al-wassai, Firouz Abdullah. 2013. "Satelite\_limitations." *Journal of Global Research in Computer Science* 4 (5): 51–59.
- Ampatzidis, Yiannis, Victor Partel, Bo Meyering, and Ute Albrecht. 2019. "Citrus Rootstock Evaluation Utilizing UAV-Based Remote Sensing and Artificial Intelligence." *Computers and Electronics in Agriculture* 164 (September): 104900.
- Anderson, Karen, and Kevin J. Gaston. 2013. "Lightweight Unmanned Aerial Vehicles Will Revolutionize Spatial Ecology." *Frontiers in Ecology and the Environment*. John Wiley & Sons, Ltd.
- Aoyama, Naomi, Genki Kobori, Masanori Okazaki, Takashi Motobayashi, and Masaharu Murakami. 2010. "Development of a Rational Sampling Method for Evaluation of Cd Concentration in Wheat ( *Triticum Aestivum* ) Grain and Soil." *World*, no. August: 3–5.
- Baltsavias, Emmanuel P., Etienne Favey, Andreas Bauder, Hermann Bosch, and Maria Pateraki. 2001. "Digital Surface Modelling by Airborne Laser Scanning and Digital Photogrammetry for Glacier Monitoring." *Photogrammetric Record* 17 (98): 243–73.
- Barrand, Nicholas E., Tavi Murray, Timothy D. James, Stuart L. Barr, and Jon P. Mills. 2009. "Optimizing Photogrammetric DEMs for Glacier Volume Change Assessment Using Laser-Scanning Derived Ground-Control Points." *Journal of Glaciology* 55 (189): 106–16.

- Bauer, Marvin, and Jan Cipra. 1973. "Identification of Agricultural Crops by Computer Processing of ERTS MSS Data." *LARS Technical Reports*, January.  
<https://docs.lib.purdue.edu/larstech/20>.
- Bendig, Juliane, Andreas Bolten, Simon Bennertz, Janis Broscheit, Silas Eichfuss, and Georg Bareth. 2014. "Estimating Biomass of Barley Using Crop Surface Models (CSMs) Derived from UAV-Based RGB Imaging." *Remote Sensing* 6 (11): 10395–412.
- Bendig, Juliane, Maximilian Willkomm, Nora Tilly, Martin Leon Gnyp, Simon Bennertz, Victoria I.S. Lenz-Wiedemann, Georg Bareth, Yuxin Miao, and Qiang Cao. 2015. "Very High Resolution Crop Surface Models (CSM) from UAV-Based Stereo Images for Rice Growth Monitoring in Northeast China." *Gis.Science - Die Zeitschrift Fur Geoinformatik*, no. 1: 1–9.
- Bendig, Juliane, Kang Yu, Helge Aasen, Andreas Bolten, Simon Bennertz, Janis Broscheit, Martin L. Gnyp, and Georg Bareth. 2015. "Combining UAV-Based Plant Height from Crop Surface Models, Visible, and Near Infrared Vegetation Indices for Biomass Monitoring in Barley." *International Journal of Applied Earth Observation and Geoinformation* 39: 79–87.
- Berge, H. F.M. Ten, T. M. Thiyagarajan, Qinghua Shi, M. C.S. Wopereis, H. Drenth, and M. J.W. Jansen. 1997. "Numerical Optimization of Nitrogen Application to Rice. Part I. Description of manage-N." *Field Crops Research* 51 (1–2): 29–42.
- Berry, P. M., M. Sterling, C. J. Baker, J. Spink, and D. L. Sparkes. 2003. "A Calibrated Model of Wheat Lodging Compared with Field Measurements." *Agricultural and Forest Meteorology* 119 (3–4): 167–80.
- Berry, P. M., M. Sterling, J. H. Spink, C. J. Baker, R. Sylvester-Bradley, S. J. Mooney, A. R. Tams, and A. R. Ennos. 2004. "Understanding and Reducing Lodging in Cereals." *Adv. Agron.* 84: 217–71.
- Bhattacharjee, Paramita, Rekha S. Singhal, and Pushpa R. Kulkarni. 2002. "Basmati Rice: A

- Review.” *International Journal of Food Science and Technology* 37 (1): 1–12.
- Boomsma, Christopher R., Judith B. Santini, Terry D. West, Jason C. Brewer, Lauren M. McIntyre, and Tony J. Vyn. 2010. “Maize Grain Yield Responses to Plant Height Variability Resulting from Crop Rotation and Tillage System in a Long-Term Experiment.” *Soil and Tillage Research* 106 (2): 227–40.
- Burkart, A., V. L. Hecht, T. Kraska, and U. Rascher. 2018. “Phenological Analysis of Unmanned Aerial Vehicle Based Time Series of Barley Imagery with High Temporal Resolution.” *Precision Agriculture* 19 (1): 134–46.
- Candiago, Sebastian, Fabio Remondino, Michaela De Giglio, Marco Dubbini, and Mario Gattelli. 2015. “Evaluating Multispectral Images and Vegetation Indices for Precision Farming Applications from UAV Images.” *Remote Sensing* 7 (4): 4026–47.
- Cen, Haiyan, Liang Wan, Jiangpeng Zhu, Yijian Li, Xiaoran Li, Yueming Zhu, Haiyong Weng, et al. 2019. “Dynamic Monitoring of Biomass of Rice under Different Nitrogen Treatments Using a Lightweight UAV with Dual Image-Frame Snapshot Cameras.” *Plant Methods* 15 (1): 32.
- Chauhan, Sugandh, Roshanak Darvishzadeh, Mirco Boschetti, Monica Pepe, and Andrew Nelson. 2019. “Remote Sensing-Based Crop Lodging Assessment: Current Status and Perspectives.” *ISPRS Journal of Photogrammetry and Remote Sensing* 151 (August 2018): 124–40.
- Christopher, John T., Mandy J. Christopher, Andrew K. Borrell, Susan Fletcher, and Karine Chenu. 2016. “Stay-Green Traits to Improve Wheat Adaptation in Well-Watered and Water-Limited Environments.” *Journal of Experimental Botany* 67 (17): 5159–72.
- Chu, Tianxing, Michael J. Starek, Michael J. Brewer, Seth C. Murray, and Luke S. Pruter. 2017. “Assessing Lodging Severity over an Experimental Maize (*Zea Mays* L.) Field Using UAS Images.” *Remote Sensing* 9 (9).

- . 2018. “Characterizing Canopy Height with UAS Structure-from-Motion Photogrammetry—Results Analysis of a Maize Field Trial with Respect to Multiple Factors.” *Remote Sensing Letters* 9 (8): 753–62.
- Cogliati, S., M. Rossini, T. Julitta, M. Meroni, A. Schickling, A. Burkart, F. Pinto, U. Rascher, and R. Colombo. 2015. “Continuous and Long-Term Measurements of Reflectance and Sun-Induced Chlorophyll Fluorescence by Using Novel Automated Field Spectroscopy Systems.” *Remote Sensing of Environment* 164: 270–81.
- Cosmas Mojulat, Welland, Mohd Rafii Yusop, Mohd Razi Ismail, Abdul Shukor Juraimi, Abdul Rahim Harun, Fahim Ahmed, Fatah Abro Tanweer, and Abdul Latif. 2017. “Analysis of Simple Sequence Repeat Markers Linked to Submergence Tolerance on Newly Developed Rice Lines Derived from MR263 × Swarna-Sub1 (Analisis Penanda Ulangan Jujukan Ringkas Terhadap Titisan Padi Baharu Dibangunkan Yang Toleransi Tenggelam Daripada Kacukan MR263 × Swarna-Sub1).” *Sains Malaysiana* 46 (4): 521–28.
- Dammer, Karl Heinz, and Gerhard Wartenberg. 2007. “Sensor-Based Weed Detection and Application of Variable Herbicide Rates in Real Time.” *Crop Protection* 26 (3): 270–77.
- Dan, Zhiwu, Jun Hu, Wei Zhou, Guoxin Yao, Renshan Zhu, Yingguo Zhu, and Wenchao Huang. 2016. “Metabolic Prediction of Important Agronomic Traits in Hybrid Rice (*Oryza Sativa* L.).” *Scientific Reports* 2016 6:16 (1): 1–9.
- Debell, L., K. Anderson, R. E. Brazier, N. King, and L. Jones. 2015. “Water Resource Management at Catchment Scales Using Lightweight Uavs: Current Capabilities and Future Perspectives.” *Journal of Unmanned Vehicle Systems*. Canadian Science Publishing.
- Delgado, Jorge A., Nicholas M. Short, Daniel P. Roberts, and Bruce Vandenberg. 2019. “Big Data Analysis for Sustainable Agriculture on a Geospatial Cloud Framework.” *Frontiers in Sustainable Food Systems* 3 (July): 54.

- Dessart, François J., Jesús Barreiro-Hurlé, and René Van Bavel. 2019. “Behavioural Factors Affecting the Adoption of Sustainable Farming Practices: A Policy-Oriented Review.” In *European Review of Agricultural Economics*, 46:417–71. Oxford University Press.
- Dhillon, Amandeep K., Neerja Sharma, Navkiran K. Dosanjh, Meenakshi Goyal, and Gulshan Mahajan. 2018. “Variation in the Nutritional Quality of Rice Straw and Grain in Response to Different Nitrogen Levels.” 1946–56.
- Donoghue, Daniel N.M., Peter J. Watt, Nicholas J. Cox, and Jimmy Wilson. 2007. “Remote Sensing of Species Mixtures in Conifer Plantations Using LiDAR Height and Intensity Data.” *Remote Sensing of Environment* 110 (4): 509–22.
- Du, Mengmeng, and Noboru Noguchi. 2017. “Monitoring of Wheat Growth Status and Mapping of Wheat Yield’s within-Field Spatial Variations Using Color Images Acquired from UAV-Camera System.” *Remote Sensing* 9 (3): 289.
- Duan, T., S. C. Chapman, Y. Guo, and B. Zheng. 2017. “Dynamic Monitoring of NDVI in Wheat Agronomy and Breeding Trials Using an Unmanned Aerial Vehicle.” *Field Crops Research* 210 (August): 71–80.
- Ehlert, Detlef, Rolf Adamek, and Hans Juergen Horn. 2009. “Laser Rangefinder-Based Measuring of Crop Biomass under Field Conditions.” *Precision Agriculture* 10 (5): 395–408.
- Fageria, N. K. 2007. *Yield Physiology of Rice*. *Journal of Plant Nutrition*. Vol. 30.
- Fang, Hongliang, Wenjuan Li, Shanshan Wei, and Chongya Jiang. 2014. “Seasonal Variation of Leaf Area Index (LAI) over Paddy Rice Fields in NE China: Intercomparison of Destructive Sampling, LAI-2200, Digital Hemispherical Photography (DHP), and AccuPAR Methods.” *Agricultural and Forest Meteorology* 198 (November): 126–41.
- Fischer, Mauro, Matthias Huss, Mario Kummert, and Martin Hoelzle. 2016. “Use of an Ultra-Long-Range Terrestrial Laser Scanner to Monitor the Mass Balance of Very Small Glaciers in the

Swiss Alps.” *The Cryosphere Discussions* 0: 1–27.

Foley, Jonathan A., Navin Ramankutty, Kate A. Brauman, Emily S. Cassidy, James S. Gerber, Matt Johnston, Nathaniel D. Mueller, et al. 2011. “Solutions for a Cultivated Planet.” *Nature* 2011 478:7369 478 (7369): 337–42.

Foulkes, M. John, Gustavo A. Slafer, William J. Davies, Pete M. Berry, Roger Sylvester-Bradley, Pierre Martre, Daniel F. Calderini, Simon Griffiths, and Matthew P. Reynolds. 2011. “Raising Yield Potential of Wheat. III. Optimizing Partitioning to Grain While Maintaining Lodging Resistance.” *J. Exp. Bot.* 62 (2): 469–86.

Freeman, Kyle W., Kefyalew Girma, Daryl B. Arnall, Robert W. Mullen, Kent L. Martin, Roger K. Teal, and William R. Raun. 2007. “By-Plant Prediction of Corn Forage Biomass and Nitrogen Uptake at Various Growth Stages Using Remote Sensing and Plant Height.” In *Agronomy Journal*, 99:530–36.

Furbank, Robert T., and Mark Tester. 2011. “Phenomics – Technologies to Relieve the Phenotyping Bottleneck.” *Trends in Plant Science* 16 (12): 635–44.

Geipel, Jakob, Johanna Link, and Wilhelm Claupein. 2014. “Combined Spectral and Spatial Modeling of Corn Yield Based on Aerial Images and Crop Surface Models Acquired with an Unmanned Aircraft System.” *Remote Sensing* 6 (11): 10335–55.

George, Eobin Alex, Gaurav Tiwari, R. N. Yadav, Edward Peters, and Srishti Sadana. 2013. “UAV Systems for Parameter Identification in Agriculture.” In *C2013 IEEE Global Humanitarian Technology Conference: South Asia Satellite, GHTC-SAS 2013*, 270–73.

Gil-Docampo, M. L., M. Arza-García, J. Ortiz-Sanz, S. Martínez-Rodríguez, J. L. Marcos-Robles, and L. F. Sánchez-Sastre. 2020. “Above-Ground Biomass Estimation of Arable Crops Using UAV-Based SfM Photogrammetry.” *Geocarto International* 35 (7): 687–99.

Godfray, H. Charles J., John R. Beddington, Ian R. Crute, Lawrence Haddad, David Lawrence,

- James F. Muir, Jules Pretty, Sherman Robinson, Sandy M. Thomas, and Camilla Toulmin. 2010. "Food Security: The Challenge of Feeding 9 Billion People." *Science* 327 (5967): 812–18.
- Gomiero, T., D. Pimentel, and M.G. Paoletti. 2011. "Environmental Impact of Different Agricultural Management Practices: Conventional vs. Organic Agriculture." *Crit. Rev. Plant Sci.* 30,: 95–124.
- Green, Rhys E., Stephen J. Cornell, Jörn P.W. Scharlemann, and Andrew Balmford. 2005. "Farming and the Fate of Wild Nature." *Science (New York, N.Y.)* 307 (5709): 550–55.
- Großkinsky, Dominik K., Jesper Svendsgaard, Svend Christensen, and Thomas Roitsch. 2015. "Plant Phenomics and the Need for Physiological Phenotyping across Scales to Narrow the Genotype-to-Phenotype Knowledge Gap." *Journal of Experimental Botany* 66 (18): 5429–40.
- Guo, Guancheng, Qiyu Wen, and Jingjuan Zhu. 2015. "The Impact of Aging Agricultural Labor Population on Farmland Output: From the Perspective of Farmer Preferences."
- Haboudane, Driss, John R. Miller, Elizabeth Pattey, Pablo J. Zarco-Tejada, and Ian B. Strachan. 2004. "Hyperspectral Vegetation Indices and Novel Algorithms for Predicting Green LAI of Crop Canopies: Modeling and Validation in the Context of Precision Agriculture." *Remote Sensing of Environment* 90 (3): 337–52.
- Hama, Akira, Kei Tanaka, Atsushi Mochizuki, Yasuo Tsuruoka, and Akihiko Kondoh. 2020. "Estimating the Protein Concentration in Rice Grain Using UAV Imagery Together with Agroclimatic Data." *Agronomy* 10 (3): 7–10.
- Han, Liang, Guijun Yang, Huayang Dai, Bo Xu, Hao Yang, Haikuan Feng, Zhenhai Li, and Xiaodong Yang. 2019. "Modeling Maize Above-Ground Biomass Based on Machine Learning Approaches Using UAV Remote-Sensing Data." *Plant Methods* 15 (1): 1–19.
- Han, Liang, Guijun Yang, Haikuan Feng, Chengquan Zhou, Hao Yang, Bo Xu, Zhenhai Li, and

- Xiaodong Yang. 2018. “Quantitative Identification of Maize Lodging-Causing Feature Factors Using Unmanned Aerial Vehicle Images and a Nomogram Computation.” *Remote Sensing* 2018, Vol. 10, Page 1528 10 (10): 1528.
- Han, Xiongze, J. Alex Thomasson, G. Cody Bagnall, N. Ace Pugh, David W. Horne, William L. Rooney, Jinha Jung, et al. 2018. “Measurement and Calibration of Plant-Height from Fixed-Wing UAV Images.” *Sensors* 18 (12): 4092.
- Hansen, P. M., and J. K. Schjoerring. 2003. “Reflectance Measurement of Canopy Biomass and Nitrogen Status in Wheat Crops Using Normalized Difference Vegetation Indices and Partial Least Squares Regression.” *Remote Sensing of Environment* 86 (4): 542–53.
- Hegarty-Craver, Meghan, Jason Polly, Margaret O’Neil, Noel Ujeneza, James Rineer, Robert H. Beach, Daniel Lapidus, and Dorota S. Temple. 2020. “Remote Crop Mapping at Scale: Using Satellite Imagery and UAV-Acquired Data as Ground Truth.” *Remote Sensing* 12 (12): 1984.
- Hoffmeister, Dirk, Andreas Bolten, Constanze Curdt, Guido Waldhoff, and Georg Bareth. 2009. “High-Resolution Crop Surface Models (CSM) and Crop Volume Models (CVM) on Field Level by Terrestrial Laser Scanning.” *Sixth International Symposium on Digital Earth: Models, Algorithms, and Virtual Reality* 7840 (Cvm): 78400E.
- Holman, Fenner H., Andrew B. Riche, Adam Michalski, March Castle, Martin J. Wooster, and Malcolm J. Hawkesford. 2016a. “High Throughput Field Phenotyping of Wheat Plant Height and Growth Rate in Field Plot Trials Using UAV Based Remote Sensing.” *Remote Sensing* 2016, Vol. 8, Page 1031 8 (12): 1031.
- Holman, Fenner, Andrew Riche, Adam Michalski, March Castle, Martin Wooster, and Malcolm Hawkesford. 2016. “High Throughput Field Phenotyping of Wheat Plant Height and Growth Rate in Field Plot Trials Using UAV Based Remote Sensing.” *Remote Sensing* 8 (12): 1031.
- Honkavaara, Eija, Heikki Saari, Jere Kaivosoja, Ilkka Pölönen, Teemu Hakala, Paula Litkey, Jussi

- Mäkynen, and Liisa Pesonen. 2013. “Processing and Assessment of Spectrometric, Stereoscopic Imagery Collected Using a Lightweight UAV Spectral Camera for Precision Agriculture.” *Remote Sensing* 5 (10): 5006–39.
- Hu, Pengcheng, Scott C. Chapman, Xuemin Wang, Andries Potgieter, Tao Duan, David Jordan, Yan Guo, and Bangyou Zheng. 2018. “Estimation of Plant Height Using a High Throughput Phenotyping Platform Based on Unmanned Aerial Vehicle and Self-Calibration: Example for Sorghum Breeding.” *European Journal of Agronomy* 95 (April): 24–32.
- Hu, Xueqian, Lin Sun, Xiaohe Gu, Qian Sun, Zhonghui Wei, Yuchun Pan, and Liping Chen. 2021. “Assessing the Self-Recovery Ability of Maize after Lodging Using UAV-LiDAR Data.” *Remote Sensing* 13 (12): 2270..
- Huang, Jianxi, Liyan Tian, Shunlin Liang, Hongyuan Ma, Inbal Becker-Reshef, Yanbo Huang, Wei Su, Xiaodong Zhang, Dehai Zhu, and Wenbin Wu. 2015. “Improving Winter Wheat Yield Estimation by Assimilation of the Leaf Area Index from Landsat TM and MODIS Data into the WOFOST Model.” *Agricultural and Forest Meteorology* 204 (May): 106–21.
- Hulme, Mark F., Juliet A. Vickery, Rhys E. Green, Ben Phalan, Dan E. Chamberlain, Derek E. Pomeroy, Dianah Nalwanga, et al. 2013. “Conserving the Birds of Uganda’s Banana-Coffee Arc: Land Sparing and Land Sharing Compared.” *Plos one* 8 (2): e54597.
- Hunt, E. Raymond, Michel Cavigelli, Craig S.T. Daughtry, James E. McMurtrey, and Charles L. Walthall. 2005. “Evaluation of Digital Photography from Model Aircraft for Remote Sensing of Crop Biomass and Nitrogen Status.” *Precision Agriculture* 2005 6:4 6 (4): 359–78.
- Iersel, Wimala van, Menno Straatsma, Elisabeth Addink, and Hans Middelkoop. 2018. “Monitoring Height and Greenness of Non-Woody Floodplain Vegetation with UAV Time Series.” *ISPRS Journal of Photogrammetry and Remote Sensing* 141 (July): 112–23.
- Inoue, Y, M Guérif, F Baret, A Skidmore, A Gitelson, M Schlerf, R Darvishzadeh, and A. Olivos.

2016. “Simple and Robust Methods for Remote Sensing of Canopy Chlorophyll Content: A Comparative Analysis of Hyperspectral Data for Different Types of Vegetation.” *Plant Cell Environ.* 39,: 2609–2623.
- Ishihara, Mitsunori, Yoshio Inoue, Keisuke Ono, Mariko Shimizu, and Shoji Matsuura. 2015. “The Impact of Sunlight Conditions on the Consistency of Vegetation Indices in Croplands- Effective Usage of Vegetation Indices from Continuous Ground-Based Spectral Measurements.” *Remote Sensing* 7 (10): 14079–98.
- Islam, M. Sirajul, Shaobing Peng, Romeo M. Visperas, Nelzo Ereful, M. Sultan Uddin Bhuiya, and A. W. Julfikar. 2007. “Lodging-Related Morphological Traits of Hybrid Rice in a Tropical Irrigated Ecosystem.” *Field Crops Research* 101 (2): 240–48.
- “Japan Meteorological Agency | Search Past Weather Data.” n.d. Accessed March 23, 2021. [http://www.data.jma.go.jp/obd/stats/etrn/view/nml\\_amd\\_ym.php?prec\\_no=44&block\\_no=1133&year=&month=&day=&view](http://www.data.jma.go.jp/obd/stats/etrn/view/nml_amd_ym.php?prec_no=44&block_no=1133&year=&month=&day=&view).
- Javernick, L., J. Brasington, and B. Caruso. 2014. “Modeling the Topography of Shallow Braided Rivers Using Structure-from-Motion Photogrammetry.” *Geomorphology* 213: 166–82.
- Jay, Sylvain, Gilles Rabatel, Xavier Hadoux, Daniel Moura, and Nathalie Gorretta. 2015. “In-Field Crop Row Phenotyping from 3D Modeling Performed Using Structure from Motion.” *Computers and Electronics in Agriculture* 110: 70–77.
- Jimenez-Berni, Jose A., David M. Deery, Pablo Rozas-Larraondo, Antony Tony G. Condon, Greg J. Rebetzke, Richard A. James, William D. Bovill, Robert T. Furbank, and Xavier R.R. Sirault. 2018. “High Throughput Determination of Plant Height, Ground Cover, and above-Ground Biomass in Wheat with LiDAR.” *Frontiers in Plant Science* 9 (February).
- Jin, Xiuliang, Shouyang Liu, Frédéric Baret, Matthieu Hemerlé, and Alexis Comar. 2017. “Estimates of Plant Density of Wheat Crops at Emergence from Very Low Altitude UAV

Imagery.” *Remote Sensing of Environment* 198 (September): 105–14.

- Kawamura, Kensuke, Hidetoshi Asai, Taisuke Yasuda, Phanthasin Khanthavong, Pheunphit Soisouvanh, and Sengthong Phongchanmixay. 2020. “Field Phenotyping of Plant Height in an Upland Rice Field in Laos Using Low-Cost Small Unmanned Aerial Vehicles (UAVs).” *Plant Production Science* 23 (4): 452–65.
- Koppe, Wolfgang, Martin L. Gnyp, Christoph Hütt, Yinkun Yao, Yuxin Miao, Xinping Chen, and Georg Bareth. 2012. “Rice Monitoring with Multi-Temporal and Dual-Polarimetric Terrasar-X Data.” *International Journal of Applied Earth Observation and Geoinformation* 21 (1): 568–76.
- Kuria, David N., Gunter Menz, Salome Misana, Emiliana Mwita, Hans-Peter Thamm, Miguel Alvarez, Neema Mogha, et al. 2014. “Seasonal Vegetation Changes in the Malinda Wetland Using Bi-Temporal, Multi-Sensor, Very High Resolution Remote Sensing Data Sets.” *Advances in Remote Sensing* 3 (1): 33–48.
- Laza, Ma Rebecca C., Shaobing Peng, Shigemi Akita, and Hitoshi Saka. 2015. “Contribution of Biomass Partitioning and Translocation to Grain Yield under Sub-Optimum Growing Conditions in Irrigated Rice.” 6 (1): 28–35.
- Lee, Kyu Jong, and Byun Woo Lee. 2013. “Estimation of Rice Growth and Nitrogen Nutrition Status Using Color Digital Camera Image Analysis.” *European Journal of Agronomy* 48 (July): 57–65.
- Lelong, Camille C.D., Philippe Burger, Guillaume Jubelin, Bruno Roux, Sylvain Labbé, and Frédéric Baret. 2008. “Assessment of Unmanned Aerial Vehicles Imagery for Quantitative Monitoring of Wheat Crop in Small Plots.” *Sensors 2008, Vol. 8, Pages 3557-3585* 8 (5): 3557–85.
- Li, Wang, Zheng Niu, Hanyue Chen, Dong Li, Mingquan Wu, and Wei Zhao. 2016. “Remote

Estimation of Canopy Height and Aboveground Biomass of Maize Using High-Resolution Stereo Images from a Low-Cost Unmanned Aerial Vehicle System.” *Ecological Indicators* 67 (August): 637–48.

Li, Wang, Zheng Niu, Shuai Gao, Ni Huang, and Hanyue Chen. 2014. “Correlating the Horizontal and Vertical Distribution of LiDAR Point Clouds with Components of Biomass in a *Picea Crassifolia* Forest.” *Forests* 2014, Vol. 5, Pages 1910-1930 5 (8): 1910–30.

Li, Wang, Zheng Niu, Ni Huang, Cheng Wang, Shuai Gao, and Chaoyang Wu. 2015. “Airborne LiDAR Technique for Estimating Biomass Components of Maize: A Case Study in Zhangye City, Northwest China.” *Ecological Indicators* 57 (June): 486–96.

Liang, S. 2004. *Quantitative Remote Sensing of Land Surfaces*. Wiley-Interscience, USA, DC.

Liu, Tao, Rui Li, Xiaochun Zhong, Min Jiang, Xiuliang Jin, Ping Zhou, Shengping Liu, Chengming Sun, and Wenshan Guo. 2018. “Estimates of Rice Lodging Using Indices Derived from UAV Visible and Thermal Infrared Images.” *Agricultural and Forest Meteorology* 252 (April): 144–54.

López-Lozano, Raúl, Frédéric Baret, Iñaki García de Cortázar-Atauri, Nadine Bertrand, and M. Auxiliadora Casterad. 2009. “Optimal Geometric Configuration and Algorithms for LAI Indirect Estimates under Row Canopies: The Case of Vineyards.” *Agricultural and Forest Meteorology* 149 (8): 1307–16.

Lopez-Sanchez, Juan M., J. David Ballester-Berman, Irena Hajnsek, and Irena Hajnsek. 2011. “First Results of Rice Monitoring Practices in Spain by Means of Time Series of TerraSAR-X Dual-Pol Images.” *IEEE Journal of Selected Topics in Applied Earth Observations and Remote Sensing* 4 (2): 412–22.

Lübberstedt, Thomas, Albrecht E. Melchinger, Chris C. Schön, H. Friedrich Utz, and Dietrich Klein. 1997. “QTL Mapping in Testcrosses of European Flint Lines of Maize: I. Comparison

- of Different Testers for Forage Yield Traits.” *Crop Science* 37 (3): 921–31.
- MacDonald, Robert B. 1983. “Summary of the History of the Development of Automated Remote Sensing for Agricultural Applications.” *IEEE Transactions on Geoscience and Remote Sensing* GE-22 (6): 473–82.
- Mackill, David J., and Gurdev S. Khush. 2018. “IR64: A High-Quality and High-Yielding Mega Variety.” *Rice*. Springer New York LLC.
- Maes, Wouter H., and Kathy Steppe. 2019. “Perspectives for Remote Sensing with Unmanned Aerial Vehicles in Precision Agriculture.” *Trends in Plant Science* 24 (2): 152–64.
- Maimaitijiang, Maitiniyazi, Abduwasit Ghulam, Paheding Sidike, Sean Hartling, Matthew Maimaitiyiming, Kyle Peterson, Ethan Shavers, et al. 2017. “Unmanned Aerial System (UAS)-Based Phenotyping of Soybean Using Multi-Sensor Data Fusion and Extreme Learning Machine.” *ISPRS Journal of Photogrammetry and Remote Sensing* 134 (December): 43–58.
- Matese, Alessandro, Piero Toscano, Salvatore Di Gennaro, Lorenzo Genesio, Francesco Vaccari, Jacopo Primicerio, Claudio Belli, Alessandro Zaldei, Roberto Bianconi, and Beniamino Gioli. 2015. “Intercomparison of UAV, Aircraft and Satellite Remote Sensing Platforms for Precision Viticulture.” *Remote Sensing* 7 (3): 2971–90.
- Matsumoto, Takashi, Jianzhong Wu, Hiroyuki Kanamori, Yuichi Katayose, Masaki Fujisawa, Nobukazu Namiki, Hiroshi Mizuno, et al. 2005. “The Map-Based Sequence of the Rice Genome.” *Nature* 436 (7052): 793–800.
- Metternicht, G. 2005. “Spatial Modeling in Natural Sciences and Engineering: Software Development and Implementation.” *The Photogrammetric Record* 20 (109): 92–93.
- Mora, André, Tiago M.A. Santos, Szymon Lukasik, João M.N. Silva, António J. Falcão, José M. Fonseca, and Rita A. Ribeiro. 2017. “Land Cover Classification from Multispectral Data Using Computational Intelligence Tools: A Comparative Study.” *Information 2017, Vol. 8, Page 147*

- Mulla, David J. 2013. "Twenty Five Years of Remote Sensing in Precision Agriculture: Key Advances and Remaining Knowledge Gaps." *Biosystems Engineering* 114 (4): 358–71. <https://doi.org/10.1016/J.BIOSYSTEMSENG.2012.08.009>.
- Murakami, Toshifumi, Mamiko Yui, and Koichi Amaha. 2012a. "Canopy Height Measurement by Photogrammetric Analysis of Aerial Images: Application to Buckwheat (*Fagopyrum Esculentum* Moench) Lodging Evaluation." *Computers and Electronics in Agriculture* 89 (November): 70–75. <https://doi.org/10.1016/J.COMPAG.2012.08.003>.
- Muthayya, Sumithra, Jonathan D. Sugimoto, Scott Montgomery, and Glen F. Maberly. 2014. "An Overview of Global Rice Production, Supply, Trade, and Consumption." *Annals of the New York Academy of Sciences* 1324 (1): 7–14.
- Næsset, Erik, Ole Martin Bollandsås, Terje Gobakken, Timothy G. Gregoire, and Göran Ståhl. 2013. "Model-Assisted Estimation of Change in Forest Biomass over an 11 Year Period in a Sample Survey Supported by Airborne LiDAR: A Case Study with Post-Stratification to Provide 'Activity Data.'" *Remote Sensing of Environment* 128 (January): 299–314.
- Njinju, Symon M., Hiroaki Samejima, Keisuke Katsura, Mayumi Kikuta, Joseph P. Gweyi-Onyango, John M. Kimani, Akira Yamauchi, and Daigo Makihara. 2018. "Grain Yield Responses of Lowland Rice Varieties to Increased Amount of Nitrogen Fertilizer under Tropical Highland Conditions in Central Kenya." *Plant Production Science* 21 (2): 59–70. <https://doi.org/10.1080/1343943X.2018.1436000>.
- Norberg, O. S., S. C. Mason, and S. R. Lowry. 1988. "Ethephon Influence on Harvestable Yield, Grain Quality, and Lodging of Corn." *Agronomy Journal* 80 (5): 768–72.
- Nouwakpo, Sayjro Kossi, Mark A. Weltz, and Kenneth McGwire. 2016. "Assessing the Performance of Structure-from-Motion Photogrammetry and Terrestrial LiDAR for Reconstructing Soil Surface Microtopography of Naturally Vegetated Plots." *Earth Surface*

*Processes and Landforms* 41 (3): 308–22.

- Okazaki, Masanori, and Shinji Saito. 1989. “Copper and Zinc Balance in Soils, Rice Plants and Aquatic Systems in an Area along the Fuchu Precipice Line, Tokyo, Japan.” *Water, Air, and Soil Pollution* 43 (3–4): 265–75.
- Papadavid, George. 2011. “Mapping Potato Crop Height and Leaf Area Index through Vegetation Indices Using Remote Sensing in Cyprus.” *Journal of Applied Remote Sensing* 5 (1): 053526.
- Patel, P., H.S. Srivastava, S. Panigrahy, and J.S. Parihar. 2006. “Comparative Evaluation of the Sensitivity of Multi-Polarized Multi-Frequency SAR Backscatter to Plant Density.” *Int. J. Remote Sens.* 27 (2),: 293–305.
- Pearcy, Robert W., and Daniel A. Sims. 1994. “Photosynthetic Acclimation to Changing Light Environments: Scaling from the Leaf to the Whole Plant.” *Exploitation of Environmental Heterogeneity by Plants*, 145–74.
- Peng, S, K G Cassman, S S Virmani, J Sheehy, and G S Khush. 1999. “Yield Potential Trends of Tropical Rice since the Release of IR8 and the Challenge of Increasing Rice Yield Potential,” 1552–59.
- Peng, Shaobing, and Gurdev S. Khush. 2003. “Four Decades of Breeding for Varietal Improvement of Irrigated Lowland Rice in the International Rice Research Institute.” *Plant Production Science*. Taylor & Francis.
- Peng, Shaobing, Gurdev S. Khush, Parminder Virk, Qiyuan Tang, and Yingbin Zou. 2008. “Progress in Ideotype Breeding to Increase Rice Yield Potential.” *Field Crops Research* 108 (1): 32–38.
- Phalan, Ben, Andrew Balmford, Rhys E. Green, and Jörn P.W. Scharlemann. 2011. “Minimising the Harm to Biodiversity of Producing More Food Globally.” *Food Policy* 36 (SUPPL. 1): S62–71.

- Phalan, Ben, Malvika Onial, Andrew Balmford, and Rhys E. Green. 2011. “Reconciling Food Production and Biodiversity Conservation: Land Sharing and Land Sparing Compared.” *Science (New York, N.Y.)* 333 (6047): 1289–91.
- Pierson, Elizabeth A., Richard N. Mack, and R. Alan Black. 1990. “The Effect of Shading on Photosynthesis, Growth, and Regrowth Following Defoliation for *Bromus Tectorum*.” *Oecologia* 84 (4): 534–43.
- Pingali P. 2006. *Westernization of Asian Diets and the Transformation of Food Systems: Implications for Research and Policy*. Food Polic.
- Pinthus, Moshe J. 1974. “Lodging in Wheat, Barley, and Oats: The Phenomenon, Its Causes, and Preventive Measures.” *Advances in Agronomy* 25 (C): 209–63.
- Plaza-Wuthrich, S., R. Blosch, A. Rindisbacher, G. Cannarozzi, and Z. Tadele. 2016. “Gibberellin Deficiency Confers Both Lodging and Drought Tolerance in Small Cereals.” *Front. Plant Sci.* 7, 643–649.
- Portz, G., J. P. Molin, and J. Jasper. 2012. “Active Crop Sensor to Detect Variability of Nitrogen Supply and Biomass on Sugarcane Fields.” *Precision Agriculture* 13 (1): 33–44.
- Quang Duy, P., Hirano, M., Sagawa, S., Kuroda, E. 2004. “Analysis of the Dry Matter Production Process Related to Yield and Yield Components of Rice Plants Grown under the Practice of Nitrogen-Free Basal Dressing Accompanied with Sparse Planting Density. Plant.” *Plant Prod. Sci.* (2), (7): 155–164.
- Rahman, M. M., D. W. Lamb, and J. N. Stanley. 2015. “The Impact of Solar Illumination Angle When Using Active Optical Sensing of NDVI to Infer FAPAR in a Pasture Canopy.” *Agricultural and Forest Meteorology* 202: 39–43.
- Rasmussen, Jesper, Georgios Ntakos, Jon Nielsen, Jesper Svendsgaard, Robert N. Poulsen, and Svend Christensen. 2016. “Are Vegetation Indices Derived from Consumer-Grade Cameras

- Mounted on UAVs Sufficiently Reliable for Assessing Experimental Plots?” *European Journal of Agronomy* 74 (March): 75–92.
- Ribbes, F., and T. Letoan. 1999. “Rice Field Mapping and Monitoring with Radarsat Data.” *International Journal of Remote Sensing* 20 (4): 745–65.
- Rock, G., J. B. Ries, and T. Udelhoven. 2012. “Sensitivity Analysis of Uav-Photogrammetry for creating Digital Elevation Models (DEM).” *ISPRS - International Archives of the Photogrammetry, Remote Sensing and Spatial Information Sciences XXXVIII-1/C22* (September): 69–73.
- Rueda-Ayala, Victor P., José M. Peña, Mats Höglind, José M. Bengochea-Guevara, and Dionisio Andújar. 2019. “Comparing UAV-Based Technologies and RGB-D Reconstruction Methods for Plant Height and Biomass Monitoring on Grass Ley.” *Sensors* 2019, Vol. 19, Page 535 19 (3): 535.
- Salas Fernandez, Maria G., Philip W. Bcraft, Yanhai Yin, and Thomas Lübberstedt. 2009. “From Dwarves to Giants? Plant Height Manipulation for Biomass Yield.” *Trends in Plant Science* 14 (8): 454–61.
- Sankaran, Sindhuja, Lav R. Khot, Carlos Zúñiga Espinoza, Sanaz Jarolmasjed, Vidyasagar R. Sathuvalli, George J. Vandemark, Phillip N. Miklas, et al. 2015. “Low-Altitude, High-Resolution Aerial Imaging Systems for Row and Field Crop Phenotyping: A Review.” *European Journal of Agronomy*. Elsevier.
- Schaepman, Michael E., Susan L. Ustin, Antonio J. Plaza, Thomas H. Painter, Jochem Verrelst, and Shunlin Liang. 2009. “Earth System Science Related Imaging Spectroscopy—An Assessment.” *Remote Sensing of Environment* 113 (SUPPL. 1): S123–37.
- Schellberg, Jürgen, Michael J. Hill, Roland Gerhards, Matthias Rothmund, and Matthias Braun. 2008. “Precision Agriculture on Grassland: Applications, Perspectives and Constraints.”

*European Journal of Agronomy* 29 (2–3): 59–71.

- Schirrmann, Michael, Antje Giebel, Franziska Gleiniger, Michael Pflanz, Jan Lentschke, and Karl-Heinz Heinz Dammer. 2016. “Monitoring Agronomic Parameters of Winter Wheat Crops with Low-Cost UAV Imagery.” *Remote Sensing* 8 (9): 706.
- Seelan, Santhosh K., Soizik Laguette, Grant M. Casady, and George A. Seielstad. 2003. “Remote Sensing Applications for Precision Agriculture: A Learning Community Approach.” *Remote Sensing of Environment* 88 (1–2): 157–69.
- Semchenko, Marina, and Kristjan Zobel. 2005. “The Effect of Breeding on Allometry and Phenotypic Plasticity in Four Varieties of Oat (*Avena Sativa* L.).” *Field Crops Research* 93 (2–3): 151–68.
- Setter, T. L., E. V. Laureles, and A. M. Mazaredo. 1997. “Lodging Reduces Yield of Rice by Self-Shading and Reductions in Canopy Photosynthesis.” *Field Crops Research* 49 (2–3): 95–106.
- Shanahan, J. F., N. R. Kitchen, W. R. Raun, and J. S. Schepers. 2008. “Responsive In-Season Nitrogen Management for Cereals.” *Computers and Electronics in Agriculture* 61 (1): 51–62.
- Sharma, L. K., H. Bu, D. W. Franzen, and A. Denton. 2016. “Use of Corn Height Measured with an Acoustic Sensor Improves Yield Estimation with Ground Based Active Optical Sensors.” *Computers and Electronics in Agriculture* 124 (June): 254–62.
- Shi, Yujie, Yuan Gao, Yu Wang, Danni Luo, Sizhou Chen, Zhaotang Ding, and Kai Fan. 2022. “Using Unmanned Aerial Vehicle-Based Multispectral Image Data to Monitor the Growth of Intercropping Crops in Tea Plantation.” *Frontiers in Plant Science* 13 (February): 1–14.
- Shu, Meiyang, Longfei Zhou, Xiaohu Gu, Yuntao Ma, Qian Sun, Guijun Yang, and Chengquan Zhou. 2020. “Monitoring of Maize Lodging Using Multi-Temporal Sentinel-1 SAR Data.” *Advances in Space Research* 65 (1): 470–80.
- Song, Libing, and Jiming Jin. 2020. “Effects of Sunshine Hours and Daily Maximum Temperature

- Declines and Cultivar Replacements on Maize Growth and Yields.” *Agronomy* 10 (12): 1862.
- Souza, Carlos Henrique Wachholz De, Rubens Augusto Camargo Lamparelli, Jansle Vieira Rocha, and Paulo Sergio Graziano Magalhães. 2017. “Height Estimation of Sugarcane Using an Unmanned Aerial System (UAS) Based on Structure from Motion (SfM) Point Clouds.” *International Journal of Remote Sensing* 38 (8–10): 2218–30.
- Stafford, John V. 2000. “Implementing Precision Agriculture in the 21st Century.” *Journal of Agricultural and Engineering Research* 76 (3): 267–75.
- Su, Zhongbin, Yue Wang, Qi Xu, Rui Gao, and Qingming Kong. 2022. “LodgeNet: Improved Rice Lodging Recognition Using Semantic Segmentation of UAV High-Resolution Remote Sensing Images.” *Computers and Electronics in Agriculture* 196 (May): 106873.
- Sulik, John J., and Dan S. Long. 2016. “Spectral Considerations for Modeling Yield of Canola.” *Remote Sensing of Environment* 184 (October): 161–74.
- Sullivan, Dana G., J. N. Shaw, and D. Rickman. 2005. “IKONOS Imagery to Estimate Surface Soil Property Variability in Two Alabama Physiographies.” *Soil Science Society of America Journal* 69 (6): 1789–98.
- Sun, Qian, Lin Sun, Meiyang Shu, Xiaohe Gu, Guijun Yang, and Longfei Zhou. 2019. “Monitoring Maize Lodging Grades via Unmanned Aerial Vehicle Multispectral Image.” *Plant Phenomics* 2019.
- Swain, Kishore C., Hemantha P.W. Jayasuriya, and Vilas M. Salokhe. 2007. “Suitability of Low-Altitude Remote Sensing Images for Estimating Nitrogen Treatment Variations in Rice Cropping for Precision Agriculture Adoption.” 1 (1): 013547.
- Tahar, Khairul Nizam, Anuar Ahmad, Wan Abdul, Aziz Wan, Mohd Akib, Wan Mohd, and Naim Wan Mohd. n.d. “Assessment on Ground Control Points in Unmanned Aerial System Image Processing for Slope Mapping Studies.” Accessed June 3, 2021.

<http://citeseerx.ist.psu.edu/viewdoc/summary?doi=10.1.1.301.7111>.

- Takai, Toshiyuki, Shoji Matsuura, Takahiro Nishio, Akihiro Ohsumi, Tatsuhiko Shiraiwa, and Takeshi Horie. 2006. "Rice Yield Potential Is Closely Related to Crop Growth Rate during Late Reproductive Period." *Field Crops Research* 96 (2–3): 328–35.
- Takeda, T., H. Oguma, F. Ishihama, and Takenaka A. 2010. "Estimation of Vegetation Height in the Watarase Wetland from Digital Aerial Photographs." *J. Agric. Meteorol.*, 66 (4): 237–44.
- Tammaing, A., C. Hugenholtz, B. Eaton, and M. Lapointe. 2015. "Hyperspatial Remote Sensing of Channel Reach Morphology and Hydraulic Fish Habitat Using an Unmanned Aerial Vehicle (UAV): A First Assessment in the Context of River Research and Management." *River Research and Applications* 31 (3): 379–91.
- Tang, Yunchao, Mingyou Chen, Chenglin Wang, Lufeng Luo, Jinhui Li, Guoping Lian, and Xiangjun Zou. 2020. "Recognition and Localization Methods for Vision-Based Fruit Picking Robots: A Review." *Frontiers in Plant Science*. Frontiers Media S.A.
- Tatsumi, Kenichi, Yoshiki Kuwabara, and Takashi Motobayashi. 2019. "Monthly Variability in the Photosynthetic Capacities, Leaf Mass per Area and Leaf Nitrogen Contents of Rice (*Oryza Sativa* L.) Plants and Their Correlations." *Journal of Agricultural Meteorology* 75 (2): 111–19.
- Tilly, Nora, Dirk Hoffmeister, Qiang Cao, Shanyu Huang, Victoria Lenz-Wiedemann, Yuxin Miao, and Georg Bareth. 2014. "Multitemporal Crop Surface Models: Accurate Plant Height Measurement and Biomass Estimation with Terrestrial Laser Scanning in Paddy Rice." *Journal of Applied Remote Sensing* 8 (1): 083671.
- Tilman, D., C. Balzer, J. Hill, and B. L. Befort. 2011. "Global Food Demand and the Sustainable Intensification of Agriculture." *Proceedings of the National Academy of Sciences* 108 (50): 20260–64.
- Torres-Sánchez, J, J M Peña, A I De Castro, and F López-Granados. 2014. "Multi-Temporal

Mapping of the Vegetation Fraction in Early-Season Wheat Fields Using Images from UAV.” *Comput Electron Agric.* 2014; 103: 104–13.

Tscharntke, Teja, Yann Clough, Thomas C. Wanger, Louise Jackson, Iris Motzke, Ivette Perfecto, John Vandermeer, and Anthony Whitbread. 2012. “Global Food Security, Biodiversity Conservation and the Future of Agricultural Intensification.” *Biological Conservation* 151 (1): 53–59.

Tsouros, Dimosthenis C., Stamatia Bibi, and Panagiotis G. Sarigiannidis. 2019. “A Review on UAV-Based Applications for Precision Agriculture.” *Information (Switzerland)* 10 (11).

Verger, Alexandre, Nathalie Vigneau, Corentin Chéron, Jean Marc Gilliot, Alexis Comar, and Frédéric Baret. 2014. “Green Area Index from an Unmanned Aerial System over Wheat and Rapeseed Crops.” *Remote Sensing of Environment* 152 (September): 654–64.

Verhoeven, Geert. 2011. “Taking Computer Vision Aloft - Archaeological Three-Dimensional Reconstructions from Aerial Photographs with Photoscan.” *Archaeological Prospection*. John Wiley & Sons, Ltd.

Verhoeven, Geert, and Frank Vermeulen. 2016. “Engaging with the Canopy—Multi-Dimensional Vegetation Mark Visualisation Using Archived Aerial Images.” *Remote Sensing* 8 (9): 752.

Wan, Liang, Haiyan Cen, Jiangpeng Zhu, Jiafei Zhang, Yueming Zhu, Dawei Sun, Xiaoyue Du, et al. 2020. “Grain Yield Prediction of Rice Using Multi-Temporal UAV-Based RGB and Multispectral Images and Model Transfer – a Case Study of Small Farmlands in the South of China.” *Agricultural and Forest Meteorology* 291 (June): 108096.

Wang, Cheng, Sheng Nie, Xiaohuan Xi, Shezhou Luo, Xiaofeng Sun, Jixian Zhang, Xiangguo Lin, Nicolas Baghdadi, Richard Gloaguen, and Prasad S Thenkabail. 2016. “Estimating the Biomass of Maize with Hyperspectral and LiDAR Data.” *Remote Sensing 2017, Vol. 9, Page 11* 9 (1): 11.

- Wang, Yanyu, Ke Zhang, Chunlan Tang, Qiang Cao, Yongchao Tian, Yan Zhu, Weixing Cao, and Xiaojun Liu. 2019. "Estimation of Rice Growth Parameters Based on Linear Mixed-Effect Model Using Multispectral Images from Fixed-Wing Unmanned Aerial Vehicles." *Remote Sensing* 2019, Vol. 11, Page 1371 11 (11): 1371.
- Watanabe, Hirozumi, My Hoang Tra Nguyen, Komany Souphasay, Son Hong Vu, Thai Khanh Phong, Julien Tournebize, and Satoru Ishihara. 2007. "Effect of Water Management Practice on Pesticide Behavior in Paddy Water." *Agricultural Water Management* 88 (1–3): 132–40.
- Watanabe, Kakeru, Wei Guo, Keigo Arai, Hideki Takanashi, Hiromi Kajiya-Kanegae, Masaaki Kobayashi, Kentaro Yano, et al. 2017a. "High-Throughput Phenotyping of Sorghum Plant Height Using an Unmanned Aerial Vehicle and Its Application to Genomic Prediction Modeling." *Frontiers in Plant Science* 8 (March): 421.
- Weiss, M., F. Jacob, and G. Duveiller. 2020. "Remote Sensing for Agricultural Applications: A Meta-Review." *Remote Sensing of Environment* 236 (November 2019): 111402.
- Wilke, N., B. Siegmann, F. Frimpong, O. Muller, L. Klingbeil, and U. Rascher. 2019. "Quantifying Lodging Percentage, Lodging Development and Lodging Severity Using a Uav-Based Canopy Height Model." In *International Archives of the Photogrammetry, Remote Sensing and Spatial Information Sciences - ISPRS Archives*, 42:649–55. International Society for Photogrammetry and Remote Sensing.
- Wilke, Norman, Bastian Siegmann, Lasse Klingbeil, Andreas Burkart, Thorsten Kraska, Onno Muller, Anna van Doorn, Sascha Heinemann, and Uwe Rascher. 2019. "Quantifying Lodging Percentage and Lodging Severity Using a UAV-Based Canopy Height Model Combined with an Objective Threshold Approach." *Remote Sensing* 11 (5): 515.
- Willkomm, M., A. Bolten, and G. Bareth. 2016a. "Non-Destructive Monitoring of Rice by Hyperspectral in-Field Spectrometry and UAV-Based Remote Sensing: Case Study of Field-

- Grown Rice in North Rhine-Westphalia, Germany.” *International Archives of the Photogrammetry, Remote Sensing and Spatial Information Sciences - ISPRS Archives 2016-Janua* (July): 1071–77.
- Willkomm, M, A Bolten, and G Bareth. 2016b. “Non-Destructive Monitoring of Rice by Hyperspectral in-Field Spectometry and UAV-Based Remote Sensing; Case Study of Field-Grown Rice in North Rhine-Westphalia, Germany.” *The International Archives of the Photogrammetry, Remote Sensing and Spatial Information Sciences XLI-B1*,: 12–19.
- Wu, Jindong, Dong Wang, and Marvin E. Bauer. 2007. “Assessing Broadband Vegetation Indices and QuickBird Data in Estimating Leaf Area Index of Corn and Potato Canopies.” *Field Crops Research* 102 (1): 33–42.
- Wu, W., and B.L. Ma. 2004. “A New Method for Assessing Plant Lodging and the Impact of Management Options on Lodging in Canola Crop Production.” *Sci. Rep.* 6, 31890.
- Wu, Wei, and Bao Luo Ma. 2016. “A New Method for Assessing Plant Lodging and the Impact of Management Options on Lodging in Canola Crop Production.” *Scientific Reports 2016 6:1 6* (1): 1–17.
- Xu, Yanan, Iskander M. Ibrahim, and Patricia J. Harvey. 2016. “The Influence of Photoperiod and Light Intensity on the Growth and Photosynthesis of *Dunaliella Salina* (Chlorophyta) CCAP 19/30.” *Plant Physiology and Biochemistry* 106 (September): 305–15.
- Yamaguchi, Tomoaki, Yukie Tanaka, Yuto Imachi, Megumi Yamashita, and Keisuke Katsura. 2020. “Feasibility of Combining Deep Learning and RGB Images Obtained by Unmanned Aerial Vehicle for Leaf Area Index Estimation in Rice.” *Remote Sensing* 13 (1): 84.
- Yang, Ming Der, Kai Siang Huang, Yi Hsuan Kuo, Hui Ping Tsai, and Liang Mao Lin. 2017. “Spatial and Spectral Hybrid Image Classification for Rice Lodging Assessment through UAV Imagery.” *Remote Sensing* 9 (6).

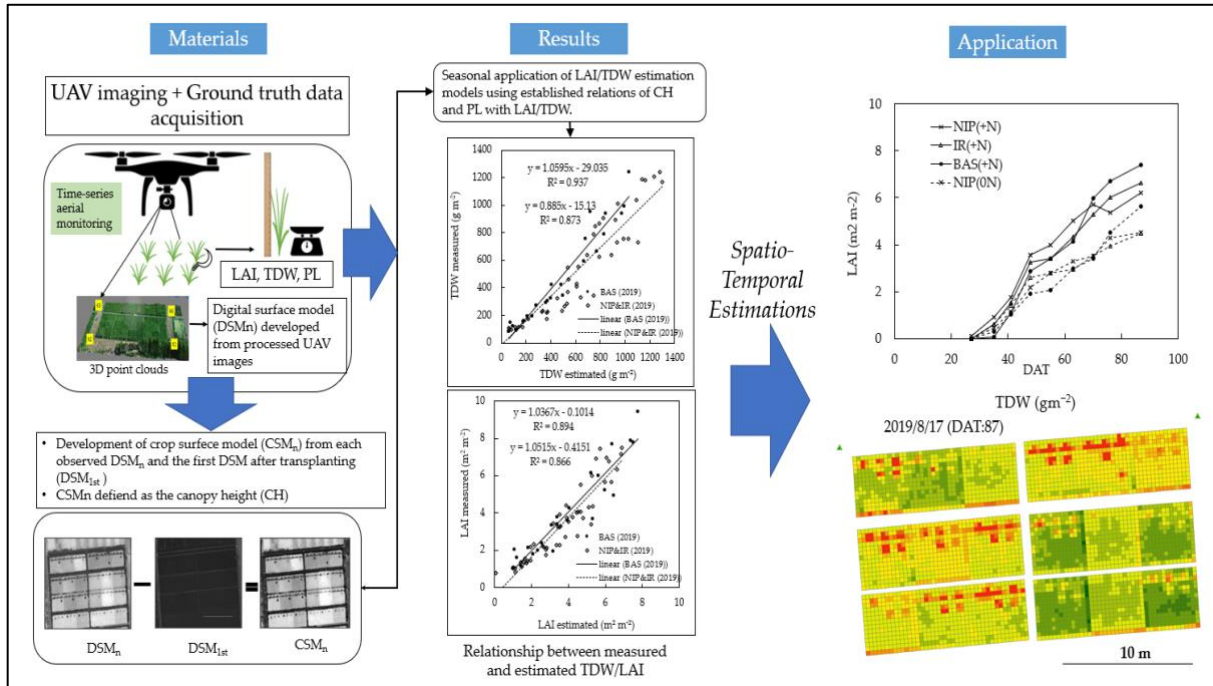
- Yoshida, Hiroe, and Takeshi Horie. 2010. “A Model for Simulating Plant N Accumulation, Growth and Yield of Diverse Rice Genotypes Grown under Different Soil and Climatic Conditions.” *Field Crops Research* 117 (1): 122–30.
- Yoshida, Hiroe, Takeshi Horie, Keisuke Katsura, and Tatsuhiko Shiraiwa. 2007. “A Model Explaining Genotypic and Environmental Variation in Leaf Area Development of Rice Based on Biomass Growth and Leaf N Accumulation.” *Field Crops Research* 102 (3): 228–38.
- Yoshida Souichi. 1981. *Fundamentals of Rice Crop Science*. Los Banos, Philippines: International Rice Research Institute.
- Yuan, Joshua S., Kelly H. Tiller, Hani Al-Ahmad, Nathan R. Stewart, and C. Neal Stewart. 2008. “Plants to Power: Bioenergy to Fuel the Future.” *Trends in Plant Science* 13 (8): 421–29.
- Yuan L. 2014. *Development of Hybrid Rice to Ensure Food Security*. 2nd ed. Rice Sci.
- Yukie, Tanaka, Keisuke Katsura, and Megumi Yamashita. 2020. “Verification of Image Processing Methods Using Digital Cameras for Rice Growth Diagnosis.” *J. Japan Soc. Photogramm. Remote Sens.* 2020, 59,: 248–258.
- Zarco-Tejada, P. J., V. González-Dugo, and J. A.J. Berni. 2012. “Fluorescence, Temperature and Narrow-Band Indices Acquired from a UAV Platform for Water Stress Detection Using a Micro-Hyperspectral Imager and a Thermal Camera.” *Remote Sensing of Environment* 117 (February): 322–37.
- Zeng, Linglin, Guozhang Peng, Ran Meng, Jianguo Man, Weibo Li, Binyuan Xu, Zhengang Lv, and Rui Sun. 2021. “Wheat Yield Prediction Based on Unmanned Aerial Vehicles-Collected Red–Green–Blue Imagery.” *Remote Sensing* 13 (15): 1–19.
- Zhang, Chunhua, and John M. Kovacs. 2012a. “The Application of Small Unmanned Aerial Systems for Precision Agriculture: A Review.” *Precision Agriculture* 13 (6): 693–712.
- Zhang, Huifang, Yi Sun, Li Chang, Yu Qin, Jianjun Chen, Yan Qin, Jiaying Du, Shuhua Yi, and

- Yingli Wang. 2018. "Estimation of Grassland Canopy Height and Aboveground Biomass at the Quadrat Scale Using Unmanned Aerial Vehicle." *Remote Sensing* 2018, Vol. 10, Page 851
- Zhang Ke, Osamu Tsuji, Masato Kimura, Toshimi Muneoka, And Kenichi Hoshiyama. 2020. "Monitoring of Crop Plant Height Based on DSM Data Obtained by Small Unmanned Vehicle Considering the Difference of Plant Shapes." *International Journal of Environmental and Rural Development* 11 (1): 133–39.
- Zhang, Naiqian, Maohua Wang, and Ning Wang. 2002. "Precision Agriculture—a Worldwide Overview." *Computers and Electronics in Agriculture* 36 (2–3): 113–32.
- Zhang, Tianyi, Yao Huang, and Xiaoguang Yang. 2013. "Climate Warming over the Past Three Decades Has Shortened Rice Growth Duration in China and Cultivar Shifts Have Further Accelerated the Process for Late Rice." *Global Change Biology* 19 (2): 563–70.
- Zhou, X., H. B. Zheng, X. Q. Xu, J. Y. He, X. K. Ge, X. Yao, T. Cheng, Y. Zhu, W. X. Cao, and Y. C. Tian. 2017. "Predicting Grain Yield in Rice Using Multi-Temporal Vegetation Indices from UAV-Based Multispectral and Digital Imagery." *ISPRS Journal of Photogrammetry and Remote Sensing* 130: 246–55.

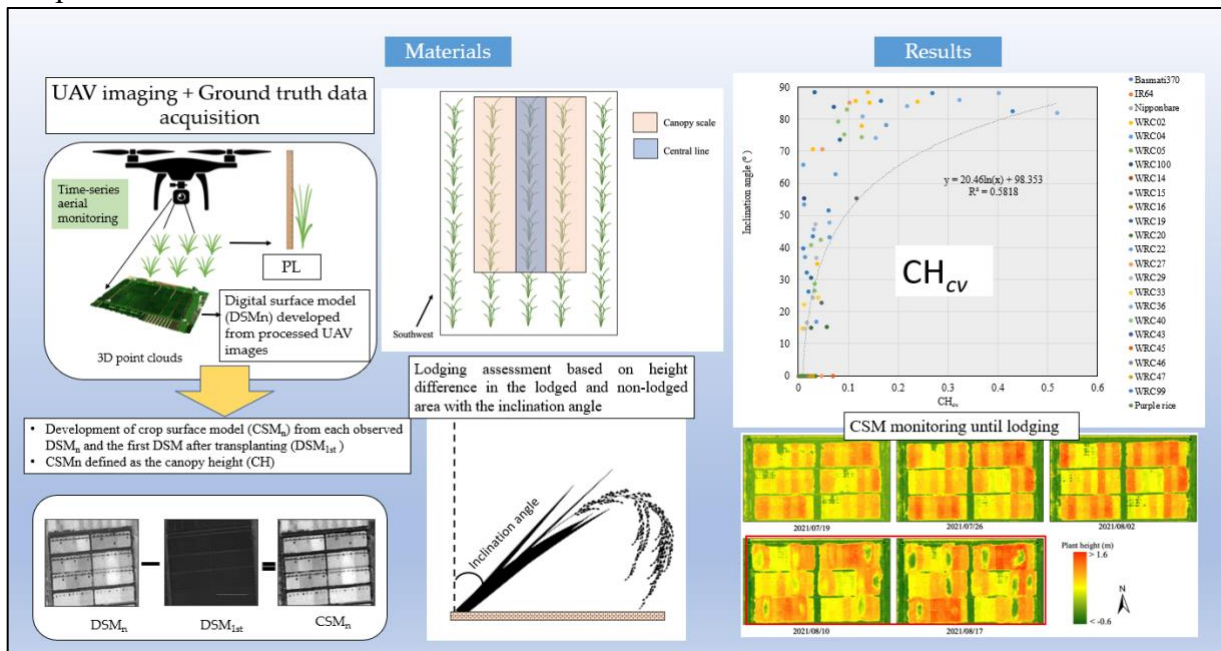
## Appendix

Graphical abstracts

Chapters two and three



## Chapter 4



## Publications

学位論文を構成する論文・著書（学位論文審査要件を満たすもの）

**Peprah, C. O.**, Yamashita, M., Yamaguchi, T., Sekino, R., Takano, K., Katsura, K. Spatio-temporal Estimation of Biomass Growth in Rice Using Canopy Surface Model by Unmanned Aerial Vehicle Images. *Remote Sensing*, 13 (12), 2388, 2021 June.

その他の論文・著書

Appiah, K. S., **Peprah, C. O.**, Mardani, H. K., Omari, R. A., Kpabitey, S., Amoatey, C. A., Onwona-Agyeman, S., Oikawa, Y., Katsura, K., Fujii, Y. Medicinal plants used in the Ejisu-Juaben Municipality, Southern Ghana: An ethnobotanical study. *Medicines*, 6, 1, 2018, December.